Lake Tegel: Hydrodynamics, pharmaceutical micro-pollutants and management strategies

Dissertation
zur Erlangung des akademischen Grades
doctor rerum naturalium (Dr. rer. nat.)

im Fach Geographie
eingereicht an der Mathematisch-Naturwissenschaftlichen Fakultät
der Humboldt-Universität zu Berlin

von Dipl.-Ing. Sebastian Schimmelpfennig

Präsident: Prof. Dr. Jan-Hendrik Olbertz
Dekan: Prof. Dr. Elmar Kulke
Gutachter: Prof. Dr. Gunnar Nützmann
Prof. Dr. Tobias Krüger
Dr. habil. Bertram Boehrer

Tag der Verteidigung: 15.12.2015

Acknowledgements

Most of all I would like to thank my supervisors Gunnar Nützmann, Georgiy Kirillin and Christof Engelhardt who were the initiators of this project. Without their support, suggestions, and professional advices, this work never would have been possible. Special thanks go to Georgiy and Christof for giving me the opportunity to participate in the adventures on ice-covered lakes in Finland and Germany.

Many thanks go to my co-advisor, Uwe Dünnbier, who organized the analysis of micro-pollutants in the laboratory of Berliner Wasserbetriebe, and helped me with all chemical questions. In particular, I would like to thank Inke Schauser for introducing me to Lake Tegel and providing numerical results of her model.

Special thanks go to Alexander Sperlich for deep discussions, proofreading, and assistance with CTD measurements. Many thanks go to Sascha Block, for helping me to drill 46 holes into Lake Tegel's ice cover for subsequently CTD measurements during an 8-hour walk over the lake.

Especially, I thank Antje Scheuritzel for proofreading the manuscript and linguistic-logical fine-tuning. Many thanks go to Andrea Hoyer for discussions about interpolation and wind averaging, and to Sonja Baumgart for support on the wind model ENVI-MET.

Additionally, this thesis benefited from the comments of Andreas Matzinger, Katharina Gabriel, Andreas Kleeberg, Gesche Grützmacher, Andreas Brand and Thomas Mehner. I thank all reviewers for the comments and suggestions, which considerably helped to improve the presentation of my results.

Furthermore, I would like to thank the North-German Supercomputing Alliance (HLRN) for providing considerably computational resources. I thank the Berliner Wasserbetriebe (BWB), Senatsverwaltung Berlin (SenGUV, SenStadtUm), Umweltbundesamt (UBA), Wasser- und Schifffahrtsamt (WSA), and Deutscher Wetterdienst (DWD) for the convenient provision of data. This study was funded by the Leibniz Association within the Project "PAKT 2008 – Pharmaceutical active compounds in the aquatic environment".

Finally, I wish to thank Nina Odzinieks for her essential support on figure editing and text layout, and in addition for her unlimited encouragement.

Kurzfassung

Ziele dieser Dissertation sind die Aufklärung der Strömungsverhältnisse und Untersuchungen zum Verhalten von Arzneimittelrückständen im Tegeler See, die Entwicklung eines Simulationsmodells für Szenarioberechnungen sowie die Ableitung neuer Bewirtschaftungskonzepte unter Zuhilfenahme der gewonnenen Erkenntnisse und Modellergebnisse.

Das zweidimensionale Strömungsmodell 2D-POM kann die Mischungsverhältnisse der beiden Zuflüsse zum Tegeler See, insbesondere den Einstrom der Oberhavel, ausreichend genau abbilden. Der Oberhaveleinstrom ist sowohl windinduziert als auch vom Abfluss der Oberhavel abhängig. Der Wind wirkt je nach Windrichtung verstärkend oder abschwächend auf den Oberhaveleinstrom.

Der Tegeler See weist im Vergleich zu anderen Oberflächengewässern, die als Trinkwasserressource dienen, die höchsten bisher berichteten Gehalte an Arzneimittelrückständen auf. Die räumliche Verteilung von Carbamazepin (CBZ) und Sulfamethoxazol (SMX) wird hauptsächlich durch die Verdünnung mit Oberhavelwasser bestimmt. Nur ein geringer Teil des CBZ (40 %) wird im Tegeler See eliminiert. Für SMX konnte keine Elimination festgestellt werden. Im Gegensatz dazu wird Diclofenac (DCF) im Oberflächenwasser photolytisch abgebaut (50 % in den Wintermonaten, mehr als 95 % im Sommer). Die Konzentrationen von DCF im Tegeler See zeigen deshalb eine hohe saisonale Variabilität.

Durch Simulation von sieben Bewirtschaftungsszenarien wurde untersucht, ob mithilfe der existierenden Seeleitung und Phosphateliminierungsanlage die Konzentrationen der Arzneimittelrückstände im Tegeler See verringert werden können, ohne die erfolgreiche Seerestaurierung zu gefährden. In keinem Szenario konnten die Gehalte an Arzneimittelrückständen und Phosphor gleichzeitig auf einem akzeptablen Niveau gehalten werden. Aus diesem Grund sind ergänzende Maßnahmen notwendig, z.B. eine zusätzliche Spurenstoffentfernung im Zulauf des Sees oder eine weitere Phosphorreduzierung in der Oberhavel.

Abstract

This cumulative thesis aims at (i) understanding the hydrodynamic characteristics of Lake Tegel, (ii) examining the occurrence and fate of pharmaceutical micro-pollutants in the lake, (iii) developing a modeling tool for scenario prediction, and (iv) utilizing the above findings and applying the above modeling tool to create new management strategies for Lake Tegel.

The free-surface two-dimensional circulation model 2D-POM serves as an adequate tool for representing the intrusion of River Havel and the mixing intensity of both inflows, as validated by measured data. The calculations indicated that the intrusion of River Havel into Lake Tegel fluctuates with river discharge and wind, both of which can amplify or neutralize the other.

Compared to other surface waters also used as drinking water resources, Lake Tegel seams to feature the highest ever reported pharmaceutical concentrations worldwide. The spatial distribution of carbamazepine (CBZ) and sulfamethoxazole (SMX) in the lake was shown to be primarily affected by dilution with water from River Havel rather than by degradation within the lake. By contrast, concentrations of diclofenac (DCL) are affected by both dilution and photodegradation. DCF showed the strongest elimination of all three pharmaceuticals and revealed significant seasonality with 50% elimination in winter and more than 95% in summer. Elimination of CBZ was 40%, while SMX did not degrade at determinable rates.

Seven different management scenarios were tested to answer the question of whether the existing lake pipeline could be used to reduce the amount of pharmaceuticals in Lake Tegel without deteriorating the current phosphorus level. No scenario provided a strategy optimal for both pharmaceuticals and phosphorus. Consequently, additional efforts need to be made, such as supplementary pharmaceutical treatment of the inflow originating from the wastewater treatment plant, or phosphorus reduction in the River Havel catchment.

Contents

1 Introduction

The contamination of freshwater ecosystems by anthropogenic pollutants has long been an important topic in environmental science. Significant improvements in chemical analytics combined with a steady increase in the use of industrial and domestic chemicals have made the problem of organic micro-pollutants a high research priority (Schwarzenbach et al., 2006). Organic micro-pollutants include industrial and household chemicals, pharmaceuticals, personal care products and their residues which can be analyzed at nanogram to low microgram-per-liter levels. Pharmaceutical micro-pollutants in particular are subject to intense scrutiny in terms of human and ecological toxicology. Still, the available knowledge on their sources, occurrence, fate, additive and chronic effects, and treatment opportunities remains insufficient for the demands of appropriate risk assessment (Kümmerer, 2009).

The multiple use of urban freshwater bodies as drinking water resources, receiving waters for treated wastewater, inland waterways, and recreational sites tends to pose severe challenges to a sustainable water management. Lake Tegel, located in the German capital of Berlin, is a prime example of such an intensively used freshwater ecosystem within a partially closed urban water cycle (Ziegler, 2001).

Within the framework of this cumulative thesis, Lake Tegel is examined with a view to three major topics – hydrodynamics, pharmaceutical micro-pollutants, and management strategies – detailed below. The thesis aims at (i) understanding the hydrodynamic characteristics of Lake Tegel, (ii) examining the occurrence and fate of pharmaceutical micro-pollutants in the lake, (iii) developing a modeling tool for scenario prediction, and (iv) utilizing the above findings and applying the above modeling tool to create new management strategies for Lake Tegel.

1.1 Hydrodynamics of Lake Tegel

Limnological research is based on an examination and understanding of both general and site-specific hydrodynamics. Chapter 2 presents the particular hydrodynamics of Lake Tegel. These include a complex bathymetry, numerous islands, density stratification, temporary ice cover, in- and outlets in close proximity to one another, and a pipeline underneath the lake bottom used for shore-to-shore water transfer. River intrusion and the mixing intensity of water masses are examined in order to distinguish the influence of wind and of river discharge on currents and mass transport in the lake. To this end, the two-dimensional version of the Princeton Ocean Model (POM), a hydrodynamic circulation model with high spatial resolution and dynamic wind forcing, was used. Further information on the model application is contained in Appendix I.

The dimictic Lake Tegel shows seasonal density stratification which can not be reproduced by a two-dimensional circulation model. Against this background, Section 2.3.1 discusses the validity of the 2D approach taken in this thesis. The approach is validated by the measured data in Sections 2.3.2 and 4.3.2. Any application of three-dimensional circulation models failed due to computational limitations caused by the pressure gradient error (PGE) as described in Appendix II.

The findings of this thesis are supported by monitoring data on, e.g., electrical conductivity and the concentration of pharmaceuticals. Their interpretation is backed by graphical presentations, which necessitated 2D spatial interpolation of the measured data. To avoid poor interpolation across islands, Dijkstra's path-finding algorithm was applied (Dijkstra, 1959), as described in Appendix III.

1.2 Pharmaceutical micro-pollutants in Lake Tegel

Since Lake Tegel receives treated wastewater from a municipal wastewater treatment plant (WWTP), it contains many pharmaceutical micro-pollutants. Chapter 3 presents the spatial distribution, elimination rates, and seasonal patterns of three pharmaceuticals in Lake Tegel: carbamazepine (CBZ), diclofenac (DCL), and sulfamethoxazole (SMX). All three substances were chosen because the German Federal Environment Agency (UBA), recognizing the potential threat they pose to aquatic life, proposed specific environmental quality standards (EQS) for them. CBZ, DCL and SMX are also useful indicator substances for elimination processes in natural surface waters (Jekel et al., 2015). Additional information on the concentration of other micro-pollutants in Lake Tegel derived from the same samples is provided in Appendix IV.

1.3 Management strategies for Lake Tegel

Lake Tegel is controlled by two main inflows: While inflow #1 (River Havel) is heavily phosphorus-laden, inflow #2 is an artificial confluence that includes discharge from a municipal WWTP characterized by high levels of both phosphorus and pharmaceuticals. To reduce the phosphorus load to the lake, a phosphorus elimination plant (PEP) was erected at inflow #2. In addition, the two inflows are short-circuited by a pipeline that transfers part of the water of inflow #1 to the PEP before eventually releasing it into inflow #2. Both the pipeline and the PEP have contributed to a continuous reduction in the total phosphorus concentration of Lake Tegel over the past 25 years, contributing to the lake's successful restoration. (Heinzmann and Chorus, 1994; Schauser and Chorus, 2009)

Chapter 4 investigates the question of whether the existing lake pipeline may also be used to reduce the amount of pharmaceuticals in Lake Tegel originating from inflow #2, by either diluting it with water from River Havel, by diverting part of inflow #2 around the

lake, or by a combination of both these strategies. Seven different management scenarios are tested by way of hydrodynamic model simulations over a period of 16 years using the two-dimensional version of the Princeton Ocean Model (POM).

2 Effects of wind-driven circulation on river intrusion in Lake Tegel: modeling study with projection on transport of pollutants.

Sebastian Schimmelpfennig[a], Georgiy Kirillin[a], Christof Engelhardt[a], Gunnar Nützmann[a]

Environmental Fluid Mechanics 2012, 12, 321-339

Prediction of mixing intensity of water masses in riverine Lake Tegel (Berlin, Germany) can be used to trace the fate of pollutants that enter the lake through several inflows. Because the contributions of each inflow have not yet been quantified and because the lake features complex bathymetry and numerous islands, a hydrodynamic circulation model with high spatial resolution and dynamic wind forcing is useful. We applied the two-dimensional version of the Princeton Ocean Model (POM) to separate the influences of wind and river discharge on the currents and mass transport in Lake Tegel. For model validation, we compared the simulation results with one year of electrical conductivity data, which was used as a conservative tracer to distinguish between water from the River Havel and water supplied by a smaller second inflow. Calculation of currents alone is insufficient to investigate water exchanges between rivers and lakes, especially when several islands create multiple pathways for river intrusion. Therefore, mass transport simulations are applied. Our calculations based on archetypical scenarios indicate that the proportion of (polluted) water from the River Havel in the main basin of Lake Tegel fluctuates with river discharge and wind, which either amplify or neutralize each other.

[a] Leibniz-Institute of Freshwater Ecology and Inland Fisheries, Department of Ecohydrology, Müggelseedamm 310, D-12587 Berlin, Germany

2.1 Introduction

Understanding the mixing behavior of water entering lakes via river inflows is valuable to many environmental studies because river waters may be sources of contaminants, nutrients, or invasive biological species, thus affecting the lake water quality (Okely et al., 2010; Rueda and MacIntyre, 2010). The fate of inflow water is determined by several factors, including lake morphometry, stratification, locations and strengths of inflows, winds, and differences in density between the inflow and the lake water (Imberger and Hamblin, 1982).

Numerous studies have examined mixing driven by the density difference between the inflow and the water of a stratified lake. Balanced by the buoyancy force, river inflows either penetrate into a lake as plunging intrusions (Alavian et al., 1992; Carmack et al., 1986; Rueda and MacIntyre, 2010; Stevens et al., 1995) or remain as a buoyant plume at the lake surface (Carmack et al., 1979; Vincent et al., 1991) if the inflowing water is less dense than the lake water.

In shallow, non-stratified lakes, the temperature-driven buoyancy difference is typically of minor importance; inflow waters are rapidly mixed throughout the lake water column by winds and nighttime convection. Under these conditions, several factors determine the retention of inflow waters in the lake, including the inflow discharge, the relative positions of in- and outflows, the lake morphometry, and the prevailing wind directions and speeds. For example, if the in- and outlets are located relatively close to each other, the inflow can short-circuit (at least temporarily) to the next outlet (Englert and Stewart, 1983; Vincent et al., 1991). Wind distribution across the lake plays a crucial role in the formation of such short-circuits, and combined with lake morphometry, it may control the distribution of river waters across the lake (Rueda et al., 2005). Hence, in non-stratified lakes, inflow dynamics is highly variable spatially as well as temporally due to complex interplay of several hydrodynamic factors, which make the resulting circulation pattern largely specific to a certain lake.

In this study, we estimate the roles of these factors in the fate of inflows in Lake Tegel, an important drinking water resource for the German capital, Berlin. This lake serves approximately 0.8 million people with bank-filtered water (Möller and Burgschweiger, 2008). It is distinguished by a complicated hydrological regime, being affected by two inflows carrying different pollutant loads (Fig. 2.1). The first inflow is the River Havel, which flows through the southwestern part of the lake and undergoes serious nutrient loading due to agriculture in the catchment area. The second inflow, located in the northeastern part of the lake, is connected to an upstream wastewater treatment plant and contaminates the lake with trace pollutants remaining in the treated wastewater. The in-

and outlets of the River Havel are located close to each other and are separated from the main lake basin by several islands. The water level of the River Havel is regulated by a lock situated 2 km downstream of the lake's outflow. The second inflow is regulated by a pipeline located under the lake's bottom and connecting a point near the outlet of the River Havel to the second inlet. The phosphorus-contaminated Havel water is pumped through the pipeline to a phosphorus elimination plant (PEP) and is released after treatment to the second inflow. The PEP reduces the phosphorus concentration of the second inflow but not the concentration of trace pollutants (Reemtsma et al., 2010).

An estimate of lake-river mixing is useful to understand the retention time of nutrients and trace pollutants in the lake water and to efficiently apply regulatory measures. Thus, Lake Tegel has become a subject of continuous limnological research. However, most of this research has been devoted to chemical and biological properties (Heinzmann and Chorus, 1994; Ripl et al., 1993), and the hydrodynamics of the lake have not yet been thoroughly investigated. An observational study (Franke, 1998) of the water exchange between the River Havel and Lake Tegel was unable to quantify the water exchange rates between the river and the main basin of the lake due to the high spatial and temporal variability of the current patterns and technical limitations of the measurements. A two-dimensional hydrodynamic model (Lindenschmidt and Fröhlich, 2000) has been applied to Lake Tegel, but this model was driven by in- and outflow alone and did not consider wind forcing, nor varying water level. An empirical box model has also been developed to quantify the water exchange between the River Havel and the main basin of the lake by fitting model parameters to tracer concentrations (Schauser and Chorus, 2009). This model is able to simulate the water composition of the main basin with a monthly resolution. However, the mechanisms governing the distribution of inflow waters across the lake remain unresolved, and the contributions of wind and river discharge as drivers of mixing are unknown. Numerical modeling of lake hydrodynamics is a reliable tool to investigate these effects (Laborde et al., 2010; Okely et al., 2010). Below, we apply a two-dimensional hydrodynamic circulation model including conservative tracer transport to Lake Tegel. We verify the two-dimensional approach by comparing the modeled tracer distribution against measurements of electrical conductivity, a natural tracer of the inflow waters. Using different wind pattern and river discharge scenarios, we identify the conditions that lead to the short-circuiting of the inflow and those that lead to the maximum river intrusion into the lake.

2.2 Methods

2.2.1 Study site

Lake Tegel is a small, shallow lake (length 4 km, maximum depth 16 m, mean depth 6 m) located in northwestern Berlin (52°34'N, 13°15'E) (Fig. 2.1). The two inflows differ in discharge and chemical concentrations. The River Havel has a mean annual flow (MAF) of 13 $m^3 s^{-1}$, a mean monthly maximum flow (MMX) of 35.3 $m^3 s^{-1}$, and a mean monthly minimum flow (MMN) of 3.35 $m^3 s^{-1}$. The smaller second inflow (MAF 2.4 $m^3 s^{-1}$) is a confluence of a lake pipeline, the stream Tegeler Fließ, and the Nordgraben canal. Approximately 70–90 % of the water in the Nordgraben canal is treated wastewater from a municipal wastewater treatment plant (WWTP). The water from the pipeline, stream and canal, is treated together in a phosphorus elimination plant (PEP) (Heinzmann et al., 1991). Therefore, the phosphorus content is lower in the second inflow (0.02 mg L^{-1} total P) than in the first inflow (0.12 mg L^{-1} total P). However, the concentrations of substances originating from the wastewater are higher in the second inflow than in the first inflow. Therefore, electrical conductivity differs between the two inflows: κ_{25} = 890 µS cm^{-1} for the second inflow and 520 µS cm^{-1} for the River Havel.

The lake pipeline pumps water from a point near the outflow of Lake Tegel to the PEP to increase the second inflow and decrease the phosphorus load to Lake Tegel, mainly during the summer. During the winter, the lake pipeline occasionally pumps water in the opposite direction if the total discharge of the stream and the canal exceeds the capacity of the PEP or if the PEP is out of service because of maintenance. During the last decade, the mean annual flow (MAF) of the pipeline was 0.65 $m^3 s^{-1}$.

Lake Tegel has one main outflow (located 1 km from the first inflow) with a downstream lock that regulates the discharge of the River Havel and consequently the water level of the lake. Additional outflows are the lake pipeline (temporarily) and the almost stagnant Berlin-Spandau ship canal (MAF 0.07 $m^3 s^{-1}$).

More than one hundred drinking water wells are installed along the east and west shore and on two islands. These wells extract water from the lake via bank filtration (Fig. 1). Additionally, some water is taken directly from the lake and used for artificial groundwater recharge. The mean annual water extraction rate from Lake Tegel by these waterworks is 1.16 $m^3 s^{-1}$, calculated with a bank-filtration-to-groundwater ratio of 7:3 for all shore-parallel well galleries (Wiese, 2007).

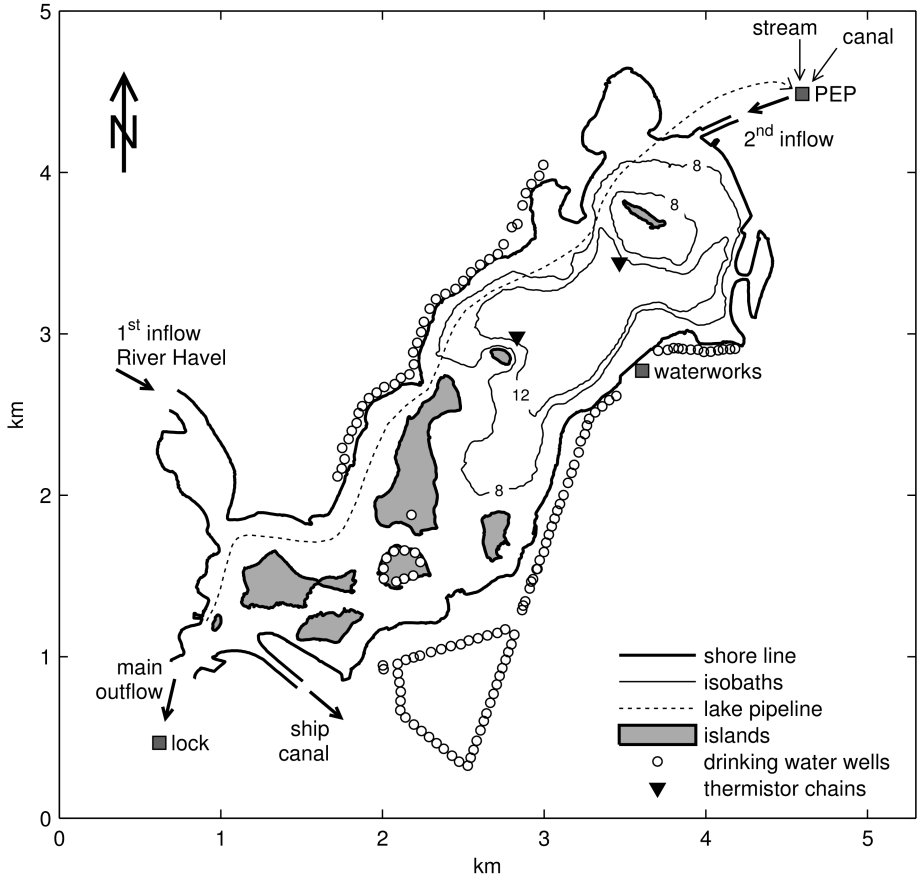

Fig. 2.1 Map of Lake Tegel (Berlin, Germany) with locations of in- and outflows, phosphorus elimination plant (PEP) and measuring devices

2.2.2 Hydrodynamic model

To simulate the circulation and pollutant transport in Lake Tegel, we applied the Princeton Ocean Model (POM) (Blumberg and Mellor, 1987) in two-dimensional mode onto a curvilinear horizontal grid (200x60, mesh size 10–150 m, barotropic time step 0.3 s). Horizontal eddy viscosity was modeled by the Smagorinsky diffusivity (Smagorinsky, 1963) with a non-dimensional coefficient $C = 0.2$. Bottom friction was parameterized according to Nikuradse's law (Nikuradse, 1933) with a roughness length of $z_0 = 1$ cm. Horizontal advection of the tracer was calculated using the Smolarkiewicz iterative upstream scheme (Smolarkiewicz, 1984) (number of iterations 2, smoothing parameter 0.5). Horizontal diffusion of the tracer was assumed to be a constant fraction of eddy viscosity (subgrid-scale turbulent Schmidt number $Sc = 5$). The lateral open boundary conditions (inflows and outflows) were implemented as flow conditions (velocity was set, and elevation was calculated from neighboring cells). The normal component of velocity at open boundaries was set to the flow rate divided by the cross-sectional area. The tangential component was set to zero. Wind stress was parameterized by a constant drag coefficient $C_{10} = 0.0026$. Wind direction was assumed to be constant over the lake surface. To account

for variations in wind speed due to lee effects behind trees on the shore and islands, we calculated the fetch length for each grid cell as a function of wind direction and set the wind stress to zero over a length of 6 times the height of the surrounding trees (15 m). Over an additional distance of 7 times the height, the wind stress grew linearly to its full value (Ottesen Hansen, 1978).

The extraction of water by the waterworks was simulated as homogeneous outflow over all grid cells with a water depth of less than 6 m. Infiltration into groundwater generally takes place only in the shallow parts of the lake because the flow through the sediment in deeper areas is hampered by a thick mud layer and anaerobic clogging (Wiese and Nützmann, 2009).

We neglected precipitation and evaporation because they have minor influences compared to the other inflows and outflows. They roughly balance each other on an annual scale: 630 mm yr^{-1} mean precipitation, 718 mm yr^{-1} mean evaporation (DVWK, 1996).

2.2.2.1 Data for model forcing and validation

Hourly wind speed and direction data (measured 10 m above the surface) were obtained from the Tegel Airport (4 km from Lake Tegel). West winds prevail in the Tegel region, with one main direction (270° ± 25°, relative abundance of 23 %) and three minor peaks at other directions (E, SE and SW) (Fig. 2.2a). Wind direction shows no seasonal pattern but exhibits high temporal variability at a scale of hours to days (Fig. 2.2b).

The flow rates of the PEP effluent, lake pipeline and waterworks pumping were available at a daily resolution. The flow rate of the main outflow (the River Havel) was calculated at the downstream lock (2 km from Lake Tegel) based on the discharge over two weirs (calibrated formula, temporal resolution 15 min), the lock-chamber through-flow (daily resolution) and three minor bypasses assumed to have constant discharge. We derived the flow rate of the River Havel inflow from the water balance over the whole study site, including water level variations (temporal resolution 15 min). Subsequently, all lateral boundary conditions were low-pass filtered (with a window width of 8 h) to avoid numerical instabilities.

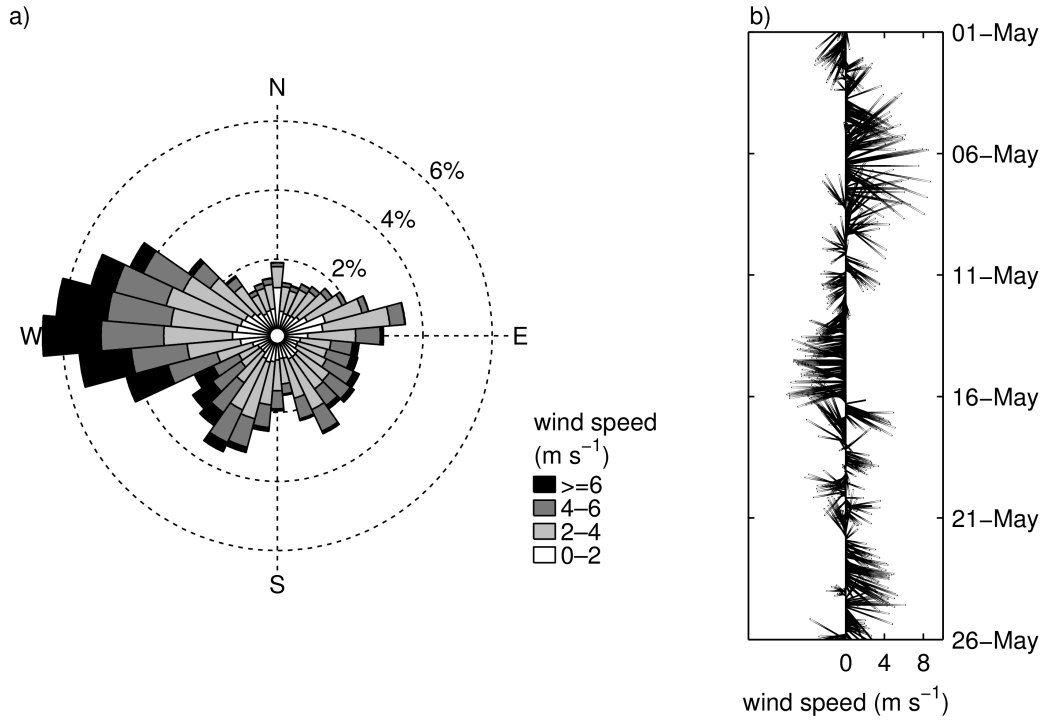

Fig. 2.2 Wind data from Tegel Airport (4 km distance to Lake Tegel) measured 10 m above surface, raw data provided in hourly resolution, a) wind rose 2000–2009, b) stick plot of hourly wind vectors, May 2009

In addition to obtaining long-term hydrological data, we collected a yearlong series of water temperature and conductivity observations during 2009/2010. Conductivity, temperature, and depth (CTD)-profiles were taken at 40 to 50 different locations spread over the whole study site on 12 different days using an XR-420 CTD-profiler (RBR Ltd., Canada). The CTD data of four days (14 Jun 09, 17 Sep 09, 17 Nov 09, 01 Dec 09) is presented in this chapter (see Appendix V for all sampling data). The raw conductivity C was normalized to a reference temperature of 25°C: $\kappa_{25} = C / (1 + \alpha_{25} \cdot (T - 25°C))$, $\alpha_{25} = 0.02$ (Boehrer and Schultze, 2008). Vertically integrated values were used to interpolate horizontal distributions. To avoid poor interpolation across islands, which common algorithms (e.g., kriging) could not accommodate, we developed a combination of Dijkstra's path-finding algorithm (Dijkstra, 1959) and simple inverse distance weighting. The resulting algorithm uses the real distances ("around" the islands) instead of the shortest distances ("through" the islands). This algorithm was used for the two-dimensional spatial interpolation of measured conductivity profiles (Appendix III). Additionally, vertical profiles of electrical conductivity at the deepest point of the lake with a temporal resolution of 14 days were provided by local authorities. Water temperature was measured from May 2009 through April 2010 using two moored thermistor chains (see Fig. 2.1 for locations). Each chain consisted of seven thermistor loggers (TR-1050, RBR Ltd., Canada) with a distance between sensors of 1.3 m and a temporal resolution of 10 s.

Two pressure sensors (TDR-2050, RBR Ltd.) were added to the thermistor chains to measure water level fluctuations with a temporal resolution of 20 s. Water density was derived from temperature and electrical conductivity using a formula given by Bührer and Ambühl (1975): $\rho = \rho(T,\kappa_{20}) = a_1 + 10^{-3}\cdot(a_2T^3 + a_3T^2 + a_4T) + a_5\kappa_{20}$, where a_i = [999.8429; 0.059385; −8.56272; 65.4891; 6.7 x 10^{-4}]. To obtain κ_{20}, the raw conductivity C was normalized to a reference temperature of 20°C: $\kappa_{20} = C / (1 + \alpha_{20}\cdot(T-20°C))$, where α_{20} = 0.02226. The value of α_{20} was fitted to C-T curves from laboratory experiments with water samples from Lake Tegel, according to Boehrer and Schultze (2008).

2.2.2.2 Validation procedure

To validate the model, we used electrical conductivity as an easily measurable, naturally conservative tracer. This choice was justified by the strong difference in salt concentration between the two inflows (520 vs. 890 µS cm^{-1}) and the absence of other significant salt sources or sinks within the lake. Consequently, the electrical conductivity distribution across the lake should reflect the actual circulation pattern and mixing regime.

To compare the measured data with the model results, we ran a simulation with time-variable boundary conditions (wind, inflow discharges, inflow concentrations and water level) from May to December 2009. We compared the simulated electrical conductivities with the measured values on four particular days (14-Jun, 17-Sep, 17-Nov, 01-Dez) and with the fortnightly measurements from the middle of the main basin. Following Rueda and Schladow (2003), we used the I_1 and I_2 error norms to measure deviance:

$$I_1 = \frac{1}{n}\sum_{i=1}^{n}\left|c_i^{obs} - c_i^{sim}\right| \Big/ \frac{1}{n}\sum_{i=1}^{n}\left|c_i^{obs}\right| \tag{2.1}$$

$$I_2 = \sqrt{\frac{1}{n}\sum_{i=1}^{n}\left(c_i^{obs} - c_i^{sim}\right)^2} \Big/ \sqrt{\frac{1}{n}\sum_{i=1}^{n}\left(c_i^{obs}\right)^2} \tag{2.2}$$

$$I_3 = \sqrt{\frac{1}{n}\sum_{i=1}^{n}\left(c_i^{obs} - c_i^{sim}\right)^2} \Big/ \sqrt{\frac{1}{n}\sum_{i=1}^{n}\left(c_i^{obs} - \bar{c}_m^{obs}\right)^2} \tag{2.3}$$

where c_i^{obs} is the observed electrical conductivity at a given location and time, c_i^{sim} is the corresponding simulated value, n is the number of values compared, and c_m^{obs} is the mean of observed data. The I_1 error norm (Eq. 2.1) equals the mean absolute error divided by the mean of the observations, which Mayer and Butler recommend for model validation (Mayer and Butler, 1993). The I_2 error norm (Eq. 2.2) equals the root mean square error (RMSE) divided by the root mean square of the observed data (RMS_{obs}). Both error norms are often used to compare results from hydrodynamic models with observed data (Gross et al., 1999; Hodges et al., 2000; Laborde et al., 2010; Morillo et al., 2008; Morillo et al.,

2009; Rueda and Schladow, 2003). The I_3 error norm (Eq. 2.3) equals the RMSE divided by the standard deviation of the observed data, furthermore, I_3 equals I_2 of our model divided by the I_2-value of a uniform conductivity model, i.e. I_3 is a measure of how much better our model reproduces the observed data compared to a simple zero-order model. Additionally, we calculated the widely used coefficient of determination R^2 for the linear regression between observed and simulated values.

2.2.2.3 Model scenarios

Because the forces that drive circulation are highly non-stationary, it is difficult to separate different influences based on real wind/inflow data. The hydrodynamic model facilitates the simulation of steady-state conditions, providing a way to quantify the individual influences of the river discharge and wind on the flow field and mixing. We use the model in a "quasi-stationary" approach by applying it in 27 scenarios by combining 3 characteristic discharge parameters of the River Havel (mean monthly minimum flow (MMN), mean annual flow (MAF) and mean monthly maximum flow (MMX)) with 9 different wind vectors (8 wind directions from 45° to 360° with a 45° interval and a wind speed of 3.5 m s^{-1}; and without wind forcing). All other boundary conditions were set to their mean annual values as described in Section 2.2.1. The simulation continued until the flow field achieved a steady state (3-8 days spin-up time).

To interpret the simulated scenarios, we first analyzed the simulated flow fields. This analysis provided an overview of the general circulation patterns (e.g., clockwise or anti-clockwise flow) as a function of wind direction and river discharge (Fig. 2.3a). Additionally, using the simulated horizontal velocities, we derived flow rates at a specific cross-section representing the "river-lake boundary" and calculated the overall intrusion flow rate Q_i as the sum of cross-sectional flow rates directed from west to east (i.e., to the main lake basin) (Fig. 2.3b). Because the islands divide the connection between the river and the main basin into several pathways, the intrusion flow rate Q_i is only a rough estimator of the transfer rate between the River Havel and Lake Tegel. In particular, Q_i does not account for back-mixing (recirculation) and dispersion in the island-rich area between the river-lake boundary and the main basin. To obtain an alternative overall estimator including these effects, we applied the hydrodynamic model complemented by the mass transport of a conservative tracer. We virtually marked the River Havel water by setting the concentration in the first inflow to one and that in the second inflow to zero. The initial concentration in the lake was set to zero, and the simulation continued until the virtual concentrations in the lake achieved a steady state (about 400 days of real time, 30 h of computing time). The resulting mean concentration of the tracer in the main basin was

subsequently used as an asymptotic estimator of the river water fraction in Lake Tegel, labeled as f_H (Fig. 2.4).

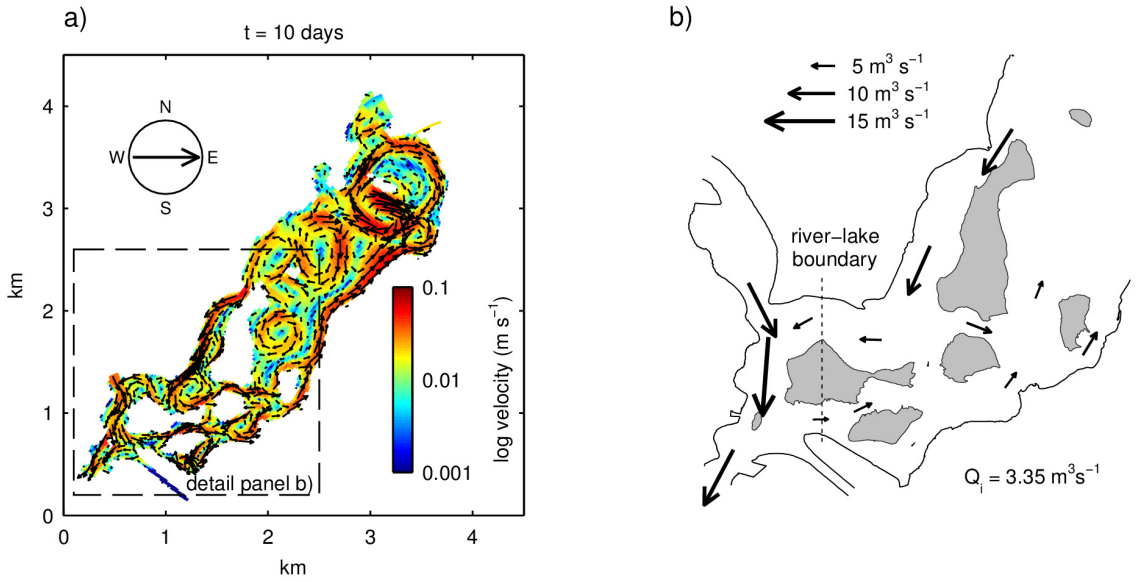

Fig. 2.3 First step of model interpretation - the flow field:
a) simulated currents after 10 days with steady-state boundary conditions: Q_{Havel} = 13 m^3 s^{-1} (MAF), wind direction 270°; arrows represent velocities
b) circulation pattern between the islands (detail view, same run as panel a); arrows represent cross-sectional flow rates; intrusion flow rate of River Havel water Q_i is derived from the flow field crossing the river-lake boundary (dashed line)

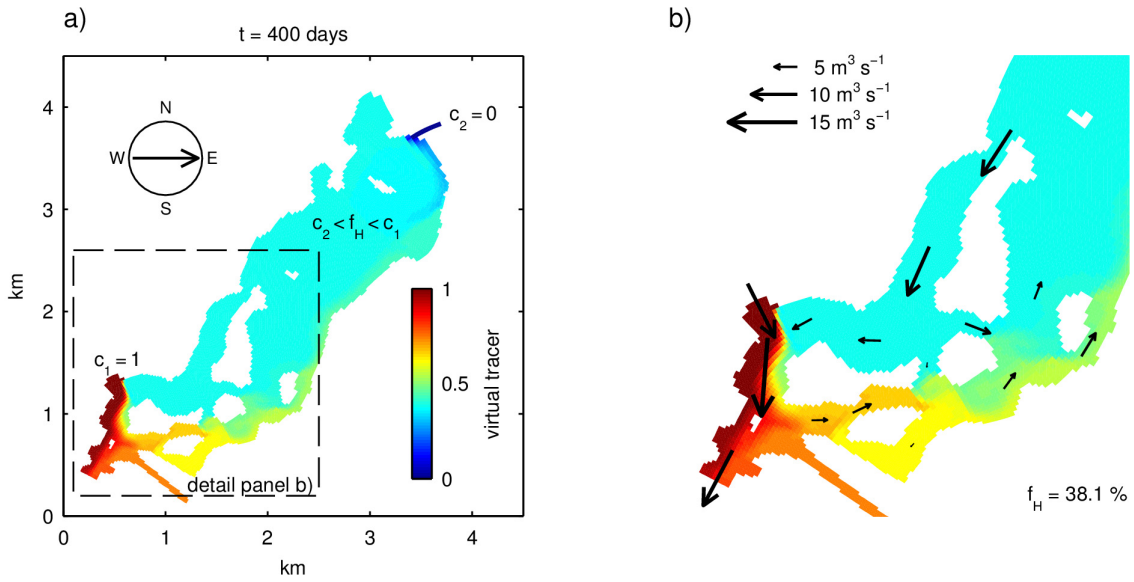

Fig. 2.4 Second step of model interpretation - the tracer transport:
a) simulated concentration of virtual tracer after 400 days with steady-state boundary conditions: Q_{Havel} = 13 m^3 s^{-1} (MAF), wind direction 270°
b) detailed view between the islands (same run as panel a), arrows represent cross-sectional flow rates; f_H is the mean concentration of virtual tracer in the main basin and represents the averaged water fraction of River Havel in Lake Tegel

2.3 Results

2.3.1 Density stratification: 2009–2010 CTD data

The seasonal stratification pattern in Lake Tegel was typical for temperate dimictic lakes. (Fig. 2.5). The surface-bottom temperature difference of 6–8°C at the peak of stratification in July-August was small compared to typical values in lakes of the region (15–20°C) indicating strong vertical mixing. The thermocline was located between 6 and 10 m depth from May to September, i.e. the depth of the surface mixed layer was comparable to or larger than the mean lake depth throughout the entire summer stratification period. The lake was completely mixed from October until January. From January until the end of March 2010, the lake was covered by ice and had inverse stratification under the ice (this rather long ice-covered period resulted from the exceptionally cold winter of 2009–2010).

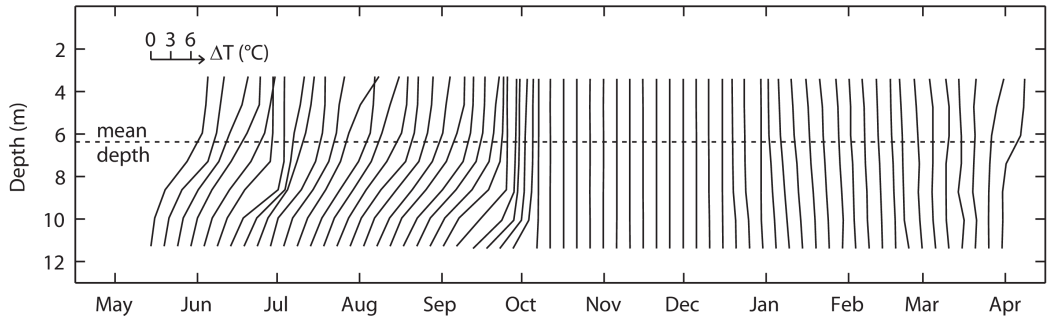

Fig. 2.5 Evolution of measured vertical temperature profiles of Lake Tegel from May 2009 to April 2010. Due to statutory requirements, the minimum water depth of the thermistor chain is 2.85 m.

The inflowing water from the River Havel remained less dense than the lake water throughout the year (Fig. 2.6). One reason for this pattern is that river waters equilibrate faster with air temperature than lake water and thus are more buoyant during the warming period (e.g., in spring) and during the winter at temperatures below 4°C. The possible development of negative buoyancy in autumn, when the river waters are colder than the lake, is prevented by slightly higher salt concentrations in Lake Tegel due to the increased contribution of salinity to density differences at lower water temperatures. As a consequence, the always less dense river water will always remain in the vertically mixed epilimnion when entering the lake. Therefore, the river intrusion can be idealized by a horizontally two-dimensional problem.

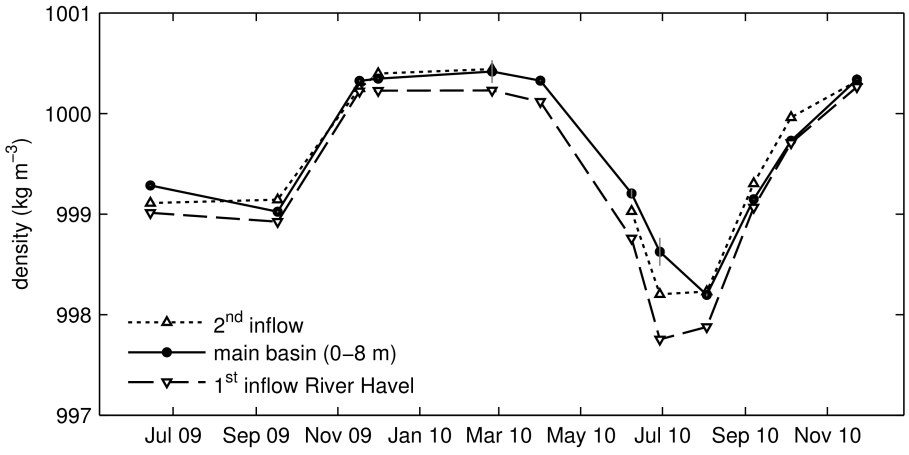

Fig. 2.6 Time series of density derived from temperature and electrical conductivity probes for both inflows (before entering the lake, $n = 1$) and for the main basin of Lake Tegel (epilimnion, average of the upper 8 m, $n = 1–7$, gray vertical lines are standard deviation error bars)

The water of the second inflow is less dense during the warming period and denser during the cooling period than the upper 8-m layer of Lake Tegel (Fig. 2.6). In summer, the contribution of the higher salt content in the second inflow to its density is negligible compared to the contribution of temperature. During the cooling period, however, the salt

and temperature differences both increase the density of the second inflow. When the water from the second inflow is less dense than the lake water, it is horizontally mixed by wind. When the water from the second inflow is denser than the lake water (e.g., in autumn), it is mixed by lake circulation (cf. Fig. 2.5). In both cases, the water from the second inflow is rapidly mixed with the lake water, unless the lake is ice-covered. In the last case, the water sinks and fills the hypolimnion.

Hence, we suggested both lake-river density difference and the seasonal temperature stratification, while not negligible, play a minor role in the horizontal circulation in Lake Tegel compared to the large-scale wind/river interchange dynamics. The advantage of neglecting the stratification effects consists in reducing of the modeling task to a two-dimensional shallow-water problem. We further estimated the validity of the two-dimensional approach by testing the model against data on the electrical conductivity distribution in the lake.

2.3.2 Model validation

The horizontal distribution of electrical conductivity predicted by the hydrodynamic model (simulation run with dynamic boundary conditions) agrees well with the measured data. Fig. 2.7 shows the situation for one of the four sampling days (other days see Appendix I).

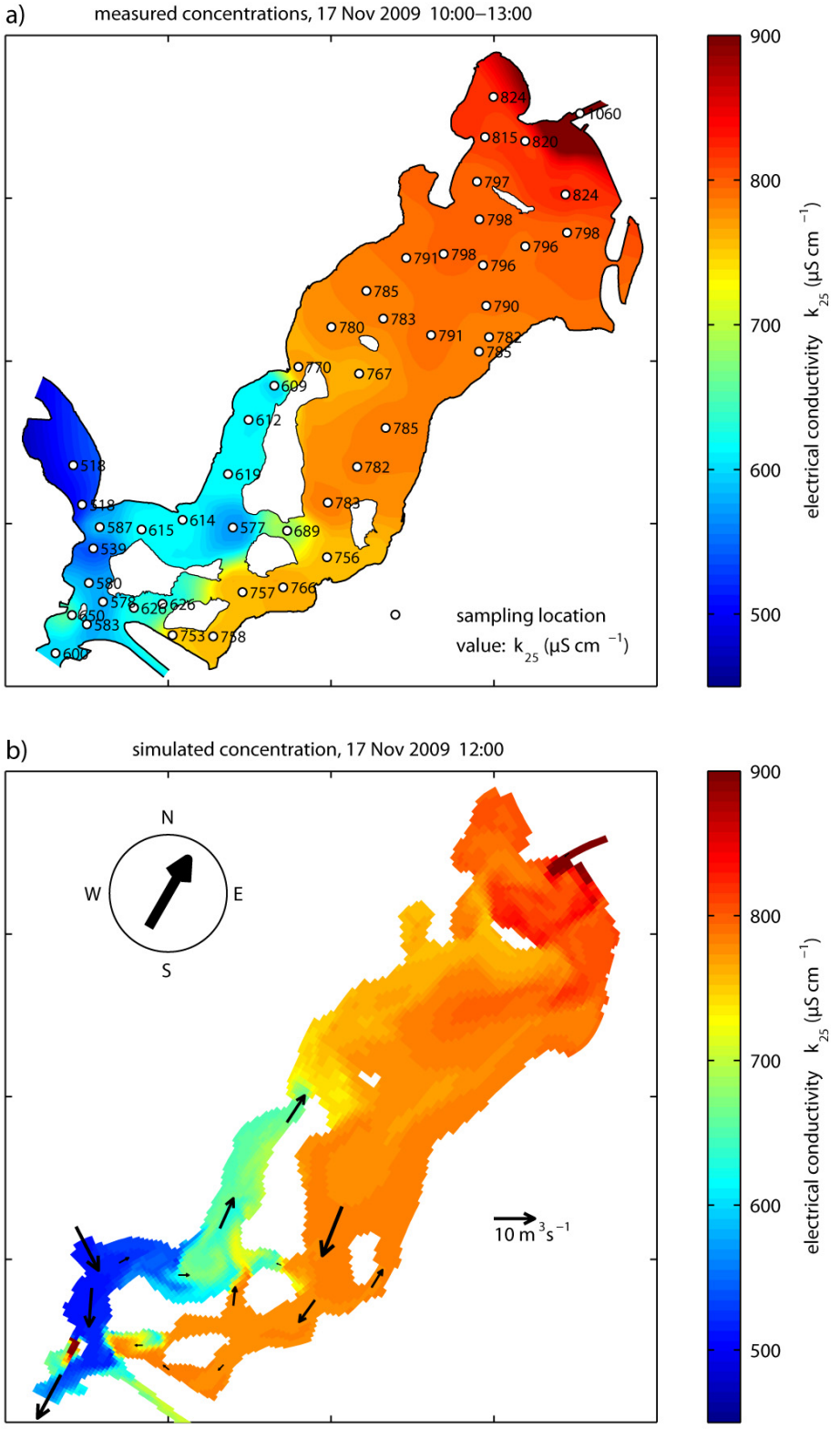

Fig. 2.7 Measured a) and simulated b) electrical conductivity on 17 Nov 2009; the colored contour plot in panel a) is spatial interpolated from vertically integrated measured values (white circles) with a combination of Dijkstra's path-finding algorithm and inverse distance weighting

The error norms I_1 and I_2 are comparable with the results of previously published modeling studies (Table 2.1). The coefficient of determination R^2 is 0.76. The I_3 error norm is 0.54, i.e. the hydrodynamic model reproduces the observed data approximately two times better than a simple zero-order model, which assumes a constant conductivity value over all space and time.

Table 2.1 Error norms I_1 and I_2 for validation of model results from this and other studies

I1	*I2*	compared quantity	study site, reference
0.040	0.061	electrical conductivity	Lake Tegel, this study
0.031	no value	salinity	San Francisco Bay (Gross et al., 1999)
0.125	0.164	temperature	Lake Kinneret (Hodges et al., 2000)
0.022	0.028	temperature	Clear Lake (Rueda and Schladow, 2003)
0.044	0.053	temperature	Coeur d'Alene Lake (Morillo et al., 2008)
0.034	0.054	temperature	Lake Como (Morillo et al., 2009)
0.057	0.063	temperature	Lake Como (Laborde et al., 2010)

Direct comparison of the observed and predicted conductivities (Fig. 2.8) for the entire simulation period suggests that the model slightly underestimates horizontal mixing (the simulated values are lower than the observed values at low absolute concentrations and higher at high absolute concentrations). However, this trend cannot be verified because the remaining residuals between the predicted and observed values are too small to distinguish between other effects, such as insufficient data for the boundary conditions or the neglected stratification in summer.

To investigate the effect of neglecting stratification, we repeated all scenario simulations with truncated bathymetry (max. depth 8 m, roughness length of truncated cells $z_0 = 1$ mm). We compared the river intrusion flow rate Q_i from the original and truncated scenarios (Fig. A 7, Appendix I). The differences are small and, consequently, substantiate our approach to simulate the river intrusion with a 2D-model and neglecting stratification.

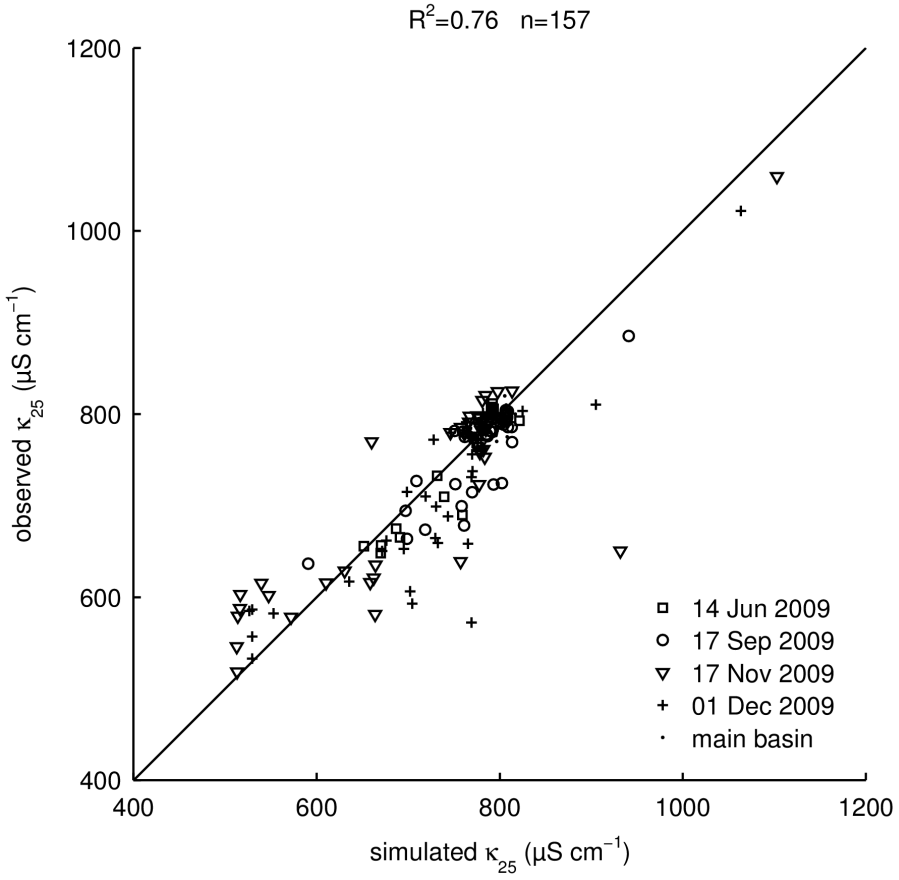

Fig. 2.8 Scatter plot of observed versus simulated data of electrical conductivity from May to December 2009, solid line represents equality

2.3.3 Simulations: flow field

The first 3 of the 27 simulated scenarios were forced by the River Havel discharge alone, with the wind speed set to zero (Fig. 2.9). In the case of low discharge (MMN), no water from the River Havel entered the lake ($Q_i = 0$), and no circulation was established around the islands. However, in the case of medium or high discharge, the River Havel inflow was split into two parts. The main part left the lake directly to the south, while approximately 10 % of the River Havel inflow entered the main basin of Lake Tegel via the northern passage and returned via the southern passage, creating a clockwise-like circulation around the islands.

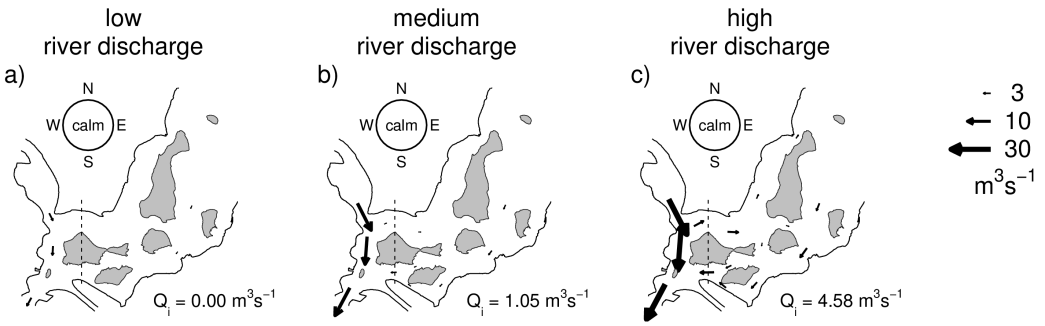

Fig. 2.9 Exclusive influence of river discharge;
simulated circulation patterns of calm scenarios for three discharges of River Havel: a) 3.35 $m^3\ s^{-1}$ MMN; b) 13 $m^3\ s^{-1}$ MAF; c) 35.3 $m^3\ s^{-1}$ MMX; Q_i is the intrusion flow rate of water from river basin through the boundary (dashed line); arrows represent cross-sectional flow rates

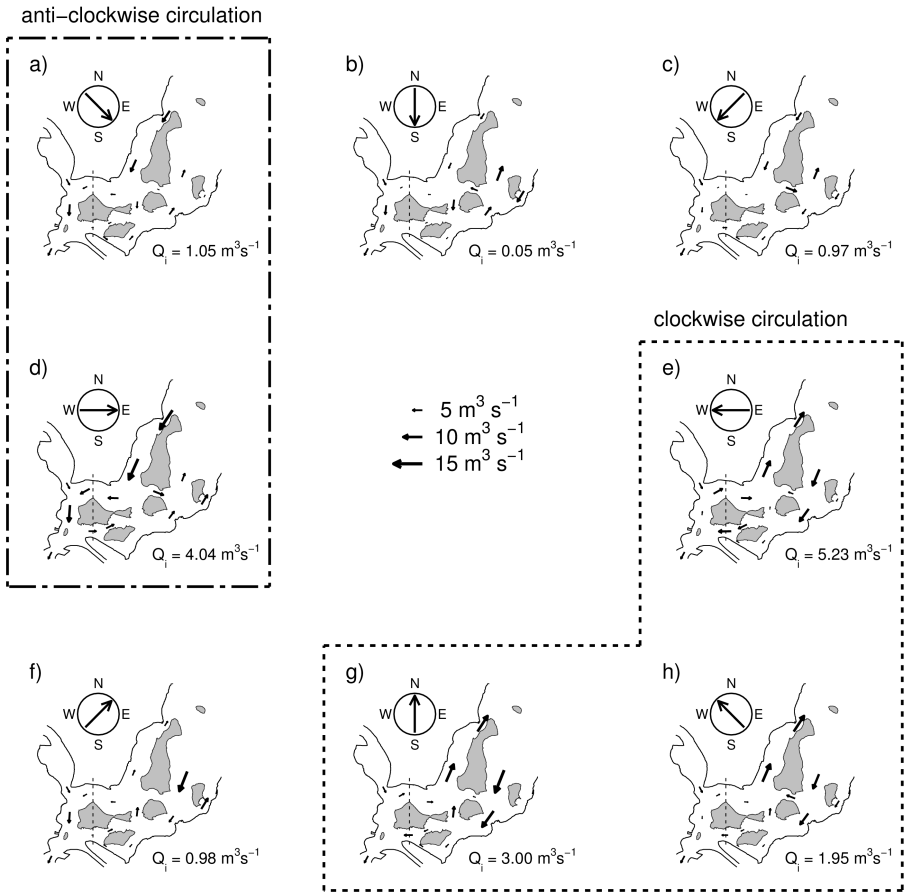

Fig. 2.10 Exclusive influence of wind;
circulation patterns of scenarios for 8 different wind directions with constant wind speed (3.5 m s^{-1}) and low river discharge (3.35 $m^3\ s^{-1}$, MMN); the panels are arranged in a way, that the position represents the direction from which the wind blows; Q_i is the intrusion flow rate of water from river basin through the boundary (dashed line); arrows represent cross-sectional flow rates

To show the exclusive influence of wind without interfering with river discharge, it would be useful to run wind-driven scenarios with zero river discharge. However, setting the discharge of River Havel to zero would imply an artificial no-flow boundary condition, i.e. a solid boundary at the river inlet, which might generate unrealistic currents. Therefore, we used the mean monthly minimum flow (MMN) of 3.35 $m^3 s^{-1}$ instead of zero discharge as a background for the wind-only scenarios (Fig. 2.10). This assumption did not affect the resulting circulation patterns, since the MMN-only scenario above (Fig. 2.9a) demonstrated zero river intrusion into the lake.

The eight scenarios corresponding to eight wind directions could be classified into three groups (Fig. 2.10): (i) winds creating clockwise circulations (directions in the southeastern quadrant, panels e, g and h); (ii) winds creating anti-clockwise circulations (west and northwest winds, panels a and d); and (iii) winds creating no distinguished circulation patterns (remaining panels). North winds, which coincide roughly with the direction of river flow (panel b), generate several small gyres around the islands at the river-lake boundary, resulting in nearly zero river-lake exchange. If the wind blows from the northeast, along the main axis of the lake, two larger gyres (clockwise and anti-clockwise) are established around the islands, also short-circuiting the river flow (panel c). A similar situation occurs if the wind blows from the opposite direction (southwest, panel f), but with the opposite directions of gyre circulation.

The west and east wind scenarios produce the maximum intrusion flow rates among all wind directions and are the most probable wind directions over the lake (Fig. 2.2). In combination with the maximum river discharge, they create two cases of "maximum forcing", representing the combined effects of the wind and river discharge (Fig. 2.11). The intrusion flow rate Q_i of the west-wind/high-discharge scenario is significantly lower than those of both the calm/high-discharge scenario and the west-wind/low-discharge scenario (cf. Fig. 2.9c, Fig. 2.10d and Fig. 2.11a). Thus, the effects of west winds and high river discharge balance each other because they generate circulations in opposite directions. As a result, almost no intrusion takes place despite the high river flow rate. In turn, east winds and high river discharge together intensify the intrusion flow rate (Fig. 2.11b) because both driving forces generate clockwise circulations, which amplify each other (compare Fig. 2.9c and Fig. 2.10e).

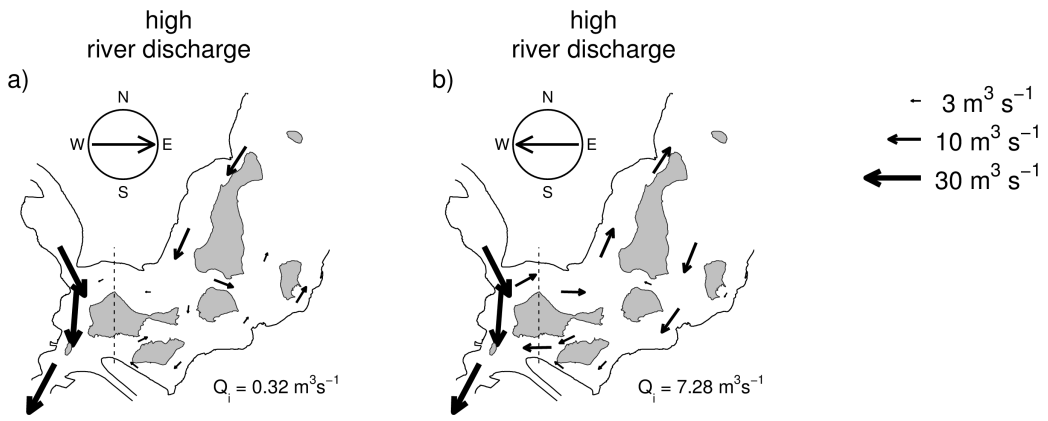

Fig. 2.11 Combined influence of wind and river discharge;
circulation patterns of the a) west and b) east wind direction with high river discharge (35.3 $m^3 s^{-1}$, MMX) and constant wind speed (3.5 $m s^{-1}$); Q_i is the intrusion flow rate of water from river basin through the boundary (dashed line); arrows represent cross-sectional flow rates

2.3.4 Simulations: tracer transport

Whereas the flow field simulations provide a picture of the advection of river water into the lake, the virtual tracer transport indicates the combined effects of advection, diffusion and back-mixing on the river-lake exchange (Fig. 2.12). The calm/low-discharge scenario (Fig. 2.12a) shows almost no virtual tracer in the main basin of Lake Tegel, in agreement with the zero intrusion flow rate (Fig. 2.9a). The calm scenarios with mean and high river discharge (Fig. 2.12b and Fig. 2.12c) show increasing penetration of tracer into the main basin with increasing river discharge. We have to consider that the calm scenarios are highly idealized, because there are no long calm periods at Lake Tegel. Analysis of wind data from 1994 to 2010 shows that the longest yearly calm period (wind speed less then 0.3 m/s) takes typically 7h (maximum 20h). Therefore, the simulated tracer accumulation in the southwestern part of the lake will probably not occur in reality. This is supported by electrical conductivity measurements, which show that the main basin of Lake Tegel was always well mixed horizontally at the four sampling days (e.g. Fig. 2.7). Nevertheless, the calm scenarios are useful as a reference for comparison with wind scenarios.

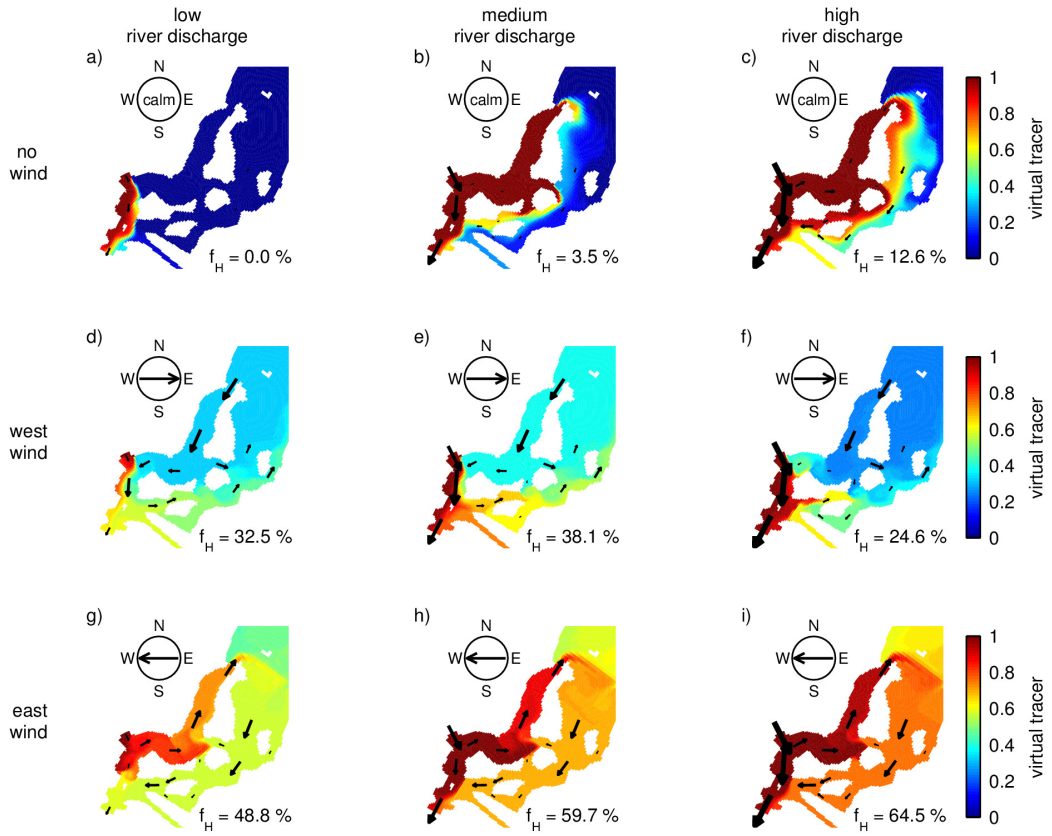

Fig. 2.12 Simulated concentrations of virtual tracer after reaching steady-state; River Havel discharge 3.35 $m^3 s^{-1}$ (MMN, left column), 13 $m^3 s^{-1}$ (MAF, middle column), 35.3 $m^3 s^{-1}$ (MMX, right column); no wind forcing (first row), west wind (second row), east wind (third row); concentration of virtual tracer in first inflow equals one and in second inflow equals zero; f_H is the mean concentration of virtual tracer in the main basin and represents the averaged water fraction of River Havel in Lake Tegel; arrows represent cross-sectional flow rates

The two wind-driven low-discharge scenarios (Fig. 2.12d and Fig. 2.12g) show that west and east winds increase the fraction of water from the River Havel in the main basin to approximately one third (32.5 %) and almost one half (48.8 %), respectively. The virtual tracer value is lower for west winds because the intrusion flow rate is lower for west winds than for east winds (Fig. 2.10d and Fig. 2.10e) and because the anti-clockwise background circulation around the islands results in more back-mixing of outflowing water back into the main basin, diluting the intrusion of River Havel water. For east winds, less back-mixing occurs because the outflowing water from the main basin leaves the lake primarily via the southern passage, traveling directly to the main outflow.

Increasing river discharge results in different trends of virtual tracer evolution in the main basin depending on the wind direction (Fig. 2.13). For west winds, the fraction of River Havel water in the lake first increases with increasing river discharge (up to the medium level MAF Fig. 2.12e). However, a further increase of the discharge up to the high MMX level causes the tracer concentration to decline to 24.6 % (Fig. 2.12f and Fig. 2.13). This

effect is a consequence of interference between the contrary circulations generated by west winds and high river discharge. For east winds, the fraction of River Havel water in the main basin increases monotonically with increasing river discharge (Fig. 2.12g-i and Fig. 2.13), in agreement with the intensification of the flow rate due to the superposition of similar clockwise circulations generated by east winds and high river discharge.

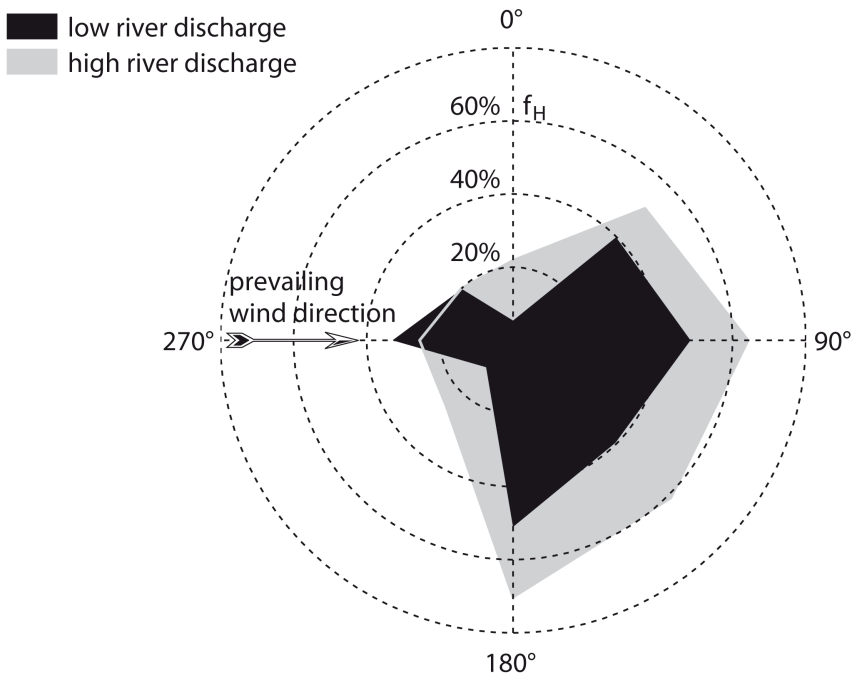

Fig. 2.13 Averaged water fraction of River Havel in main basin of Lake Tegel (f_H) versus wind direction for low and high discharge scenarios

2.3.5 Comparison with expectations

In agreement with the results of Lindenschmidt and Fröhlich (2000), who simulated the intrusion of the River Havel using a steady circulation model driven by inflow only, our model simulations demonstrate an increasing intrusion of river water into Lake Tegel with increasing river discharge in the absence of wind, as expected. However, the wind-driven effects introduce high complexity into the circulation pattern. An initial expectation might be that the intrusion of the River Havel should be intensified by western wind components and weakened by eastern wind components because the in- and outlets of the River Havel are located close to each other along the western shore of Lake Tegel. In contrast, both zonal wind directions (west and east) increase the simulated river intrusion by intensifying the water circulation around the islands. The amount of river water penetrating into the main basin of the lake depends strongly on the direction of circulation. The intrusion resulting from east winds (clockwise circulation) is larger than that resulting from west

winds (anti-clockwise circulation), apparently due to two reasons. First, for a given wind speed, clockwise circulation (east winds) results in higher flow rates than anti-clockwise circulation (west winds) due to the interaction between lake morphometry and wind. Second, clockwise circulation advects water from the river inlet directly into the main lake basin (via the northern passage), whereas anti-clockwise circulation first mixes the river water with lake water and then transports it to the main basin (via the southern passage), resulting in more back-mixing of lake water and greater dilution of river water.

The combined effect of the wind and river discharge on the fraction of River Havel water in the main basin of Lake Tegel (f_H) is non-linear and depends primarily on the direction of the resulting circulation (Fig. 2.12 and Fig. 2.13). Because the River Havel discharge alone creates a clockwise-like circulation around the islands, similar to that created by east winds, the intrusion is generally amplified under east wind conditions. For west winds, the intrusion rate increases with increasing river discharge from low to moderate values. At high discharge values, however, the intensity of the clockwise circulation driven by the river discharge becomes comparable to that of the anti-clockwise wind-driven circulation. Thus, the circulation effects of the wind and river discharge balance each other, and the intrusion rate drops significantly. This rather surprising result suggests that a stronger overall river flow would result in less river-lake mixing because west winds prevail locally over the lake.

2.4 Discussion

(1) Instead of examining the influence of episodic physical forcing on the lake-river interactions, our model simulations are focused on the complexity of possible interactions between the lake and entering inflows forced by archetypical wind scenarios. Compared to typical situations in stratified lakes (Carmack et al., 1979; Laborde et al., 2010; Morillo et al., 2008; Okely et al., 2010; Rueda and Schladow, 2003), the effects of lake stratification and of the river-lake density difference are of minor importance for the inflow intrusion into Lake Tegel. Nevertheless, the combined effects of the river discharge, wind direction and lake morphometry result in highly variable intrusion rates.

(2) To quantify the influences of the river discharge and wind, we calculated the intrusion flow rate Q_i (derived from the flow field only) and the average fraction of River Havel water in the main basin of Lake Tegel f_H (derived from flow field and mass transport simulations). Although f_H is preferable to Q_i because it includes additional effects, such as back-mixing and dispersion, that Q_i does not account for, it is inapplicable to calm scenarios and has a higher computational cost than Q_i. Nevertheless, f_H is the key value assessing the individual influences of wind and river discharge. Calculation of currents alone is insufficient to obtain satisfactory results. In this case, where several islands create

multiple pathways for water exchange between river and lake, a mass transport simulation is more representative.

(3) Due to the close proximity of the in- and outlet of the River Havel in Lake Tegel and complex morphometry including a number of islands, the wind force, especially its direction, plays a determining role in the river intrusion. By contrast to the west winds prevailing over the lake, the infrequent east wind events intensify the intrusion from 38 % to 60 %. This wind effect is not conditioned by superposition of the wind vector and the direction of the inflow. Indeed, the east wind might be expected to lock the eastward river inflow. Instead, the clockwise circulation created by the east wind entrains the river water into the main basin of the lake, whereas the anticlockwise circulation driven by the west winds accelerates the transport from the river inlet to the outlet. Therefore, the frequency of the disturbance of the predominant anticlockwise circulation is of crucial importance for the amount of river water entering the lake and, consequently, for nutrient loading.

(4) To obtain conclusions of long time effects of management measures, e.g. different lake pipe operations, our model can be used in future studies with small adaptations. We have shown that the amount of river intrusion depends strongly on wind direction. However, wind direction changes very quickly. Therefore, it is difficult to select an appropriate wind scenario which represents the typical annual wind forcing at Lake Tegel. Obviously, averaging wind data over a long period is not reasonable, because one single wind vector derived from any given averaging method does not contain enough information to represent the typical annual wind forcing. However, there is a need to find a method that will combine all available information of wind and river discharge to obtain one f_H value representing the typical annual situation in Lake Tegel. To achieve this objective, we propose two approaches for future studies: (i) hydrodynamic simulations with static boundary conditions and separated mass transport under several scenarios with differing winds and river discharge levels, followed by calculation of the weighted mean of f_H with respect to the relative frequency of occurrence of specific wind directions, wind speeds and river discharge levels; (ii) hydrodynamic simulations forced by dynamic boundary conditions, including mass transport over a long period (long enough to contain all relevant wind and discharge conditions in their natural frequencies of occurrence), followed by averaging of the resulting f_H time series over the whole period.

(5) Following future trends may be outlined in the prospective development of Lake Tegel: (i) the nutrient load of the River Havel will decrease due to improvements in wastewater treatment and agricultural management; (ii) the discharge of the River Havel will decrease due to declining precipitation in the Berlin/Brandenburg area as a result of climate change (Jacob and Gerstengarbe, 2005); and (iii) the prevailing wind direction may change from

west to east. The first two trends are well supported, while the third is rather speculative. Global climate model simulations predict stronger west winds in winter and stronger east winds in summer in Central Europe (van Ulden and van Oldenborgh, 2006); however, we cannot predict how the local wind regime in the Tegel region will be affected. Following conclusions may be drawn from our modeling results superimposed over these envisaged trends: (i) if the nutrient load of the River Havel drops below a specific threshold, the lake management scheme should probably be changed in the distant future. The present goal of minimizing the intrusion of river water will reverse to maximizing river intrusion so as to dilute the concentrations of trace pollutants originating from the second inflow. However, this reversal will not occur in the next decade; lake management will deal with pollutants in both inflows at the same time. (ii) The declining discharge of the River Havel will reduce its intrusion and, consequently, result in the decreasing role of the river water in the nutrient loading. (iii) The latter effect may be, however, compensated by a future shift of wind regime toward east winds because the river intrusion is greater under east winds than under west winds, which presently predominate.

2.5 Conclusion

We successfully applied a two-dimensional numerical model to separate the influences of wind and river discharge on the currents and mass transport in Lake Tegel. Our calculations indicate that the proportion of (polluted) water from the River Havel in the main basin of Lake Tegel fluctuates with river discharge and wind, which either amplify or neutralize each other. Our finding can be used to understand the retention time of nutrients and trace pollutants in the lake water and to efficiently apply regulatory measures.

3 Fate of pharmaceutical micro-pollutants in Lake Tegel (Berlin, Germany): spatial distribution, elimination rates, and seasonal patterns

Sebastian Schimmelpfennig[a], Georgiy Kirillin[a], Christof Engelhardt[a], Gunnar Nützmann[a,b], Uwe Dünnbier[c]

Environmental Science & Technology, submitted

Lake Tegel located in the city area of Berlin, Germany is of importance for drinking water supply and recreation, and experiences anthropogenic load by micro-pollutants from a municipal wastewater treatment plant. This study presents seasonal estimations of the micro-pollutants' fate and elimination rates concentrating on the three pharmaceuticals: carbamazepine (CBZ), diclofenac (DCL) and sulfamethoxazole (SMX). Lake Tegel is the natural drinking water resource with the highest so far reported pharmaceutical concentrations worldwide. Measured mean total loads to the lake were 260 g d^{-1} (CBZ), 180 g d^{-1} (DCL) and 60 g d^{-1} (SMX). Monthly mass balances of the four major in- and outflows result in substance-specific zero-order elimination rates characteristic for Lake Tegel. Diclofenac showed the strongest elimination and revealed a significant seasonality with 50 % elimination in winter, and 95 % and more in summer. Elimination of carbamazepine was 40 %, Sulfamethoxazole did not degrade at determinable rates. In summer a pseudo 1st-order elimination rate for diclofenac (0.058 d^{-1}, half-life 12 days) was calculated from horizontal concentration gradient. Apart from presenting the current state of pharmaceuticals pollution in Lake Tegel, results demonstrate the importance of lake-specific mechanisms, such as inflow-outflow balances and seasonal density stratification for the transport of micro-pollutants.

[a] Leibniz-Institute of Freshwater Ecology and Inland Fisheries, Department of Ecohydrology, Müggelseedamm 310, D-12587 Berlin, Germany
[b] Humboldt-University of Berlin, Department of Geography, Unter den Linden 6, D-10099 Berlin, Germany
[c] Berlin Water Company, Department of Laboratories, PO Box 310180, 10631 Berlin, Germany

3.1 Introduction

In the past decades, pharmaceuticals in the aquatic environment have risen to an relevant topic, due to the risk of harmful effects to ecosystem and drinking water production (Kümmerer, 2009; Schwarzenbach et al., 2006). Especially, polar and persistent substances which are released from wastewater treatment plants (WWTP) into receiving waters without reasonable dilution are able to exceed environmental quality standards in surface waters and may hamper the production of drinking water (Heberer, 2002; Jekel et al., 2013). To obtain a sustainable management of water quality, the spatial and temporal distribution as well as degradation rates of pharmaceuticals in surface waters are crucial.

The occurrence of pharmaceuticals has been investigated worldwide in several rivers, lakes and reservoirs (Benotti et al., 2009; Kleywegt et al., 2011; Roig, 2010). However, the spatial and temporal resolution of sampling data is often sparse, because comprehensive screening measurements are cost intensive, especially in large rivers and lakes (e.g. rivers Rhine, Pearl; lakes Michigan, Constance, Geneva) (Blair et al., 2013; Ferguson et al., 2013; Hoerger et al., 2014; Huang et al., 2011; Morasch et al., 2010; Moschet et al., 2013; ter Laak et al., 2010). Therefore, the assessment may be restricted by unknown dilution factors (Morasch et al., 2010), by varying composition of WWTP effluent (Lewandowski et al., 2011), has to be supported by predictions based on sales data (Moschet et al., 2013; Oosterhuis et al., 2013; ter Laak et al., 2010), or is highly dependent on the selection of degradation rates generated by laboratory studies, which may vary by orders of magnitude (Tixier et al., 2003). In some cases the fate of a specific substance remains unknown, e.g. carbamazepine in Lake Michigan (Blair et al., 2013).

Three studies investigated pharmaceuticals in Vidy Bay of Lake Geneva with high temporal and spatial resolution over several months (more than 200 samples) (Bonvin et al., 2011; Hoerger et al., 2014; Morasch et al., 2010). One difficulty to derive degradation rates was the unknown dilution caused by water exchange between Vidy Bay and the other parts of Lake Geneva. The authors used three different methods to overcome this challenge: Morasch et al. (2010) applied a simple mixing model parameterized by water residence time. Bonvin et al. (2011) normalized the data to concentrations of gabapentine, which was assumed to be a conservative tracer in surface waters. Hoerger et al. (2014) used substance specific background concentrations measured at locations well outside Vidy Bay.

There are several river studies which elucidate elimination rates of pharmaceuticals by mass balancing a river stretch, often with a high temporal resolution but short duration of several weeks (Kunkel and Radke, 2012; Lin et al., 2006; Radke et al., 2010). We know

only one lake study (Buser et al., 1998) which executes mass balancing in- and outflows of a lake to obtain degradation rates (diclofenac in Lake Greifensee).

This study investigates the spatial distribution and elimination of the three pharmaceuticals carbamazepine (CBZ), diclofenac (DCL) and sulfamethoxazole (SMX) with high sampling resolution in the shallow dimictic Lake Tegel (Germany) and all its major in- and outflows. Lake Tegel is an important drinking water resource for approximately 0.8 million inhabitants of Berlin, which underlines the relevance of our findings for a sustainable water quality management.

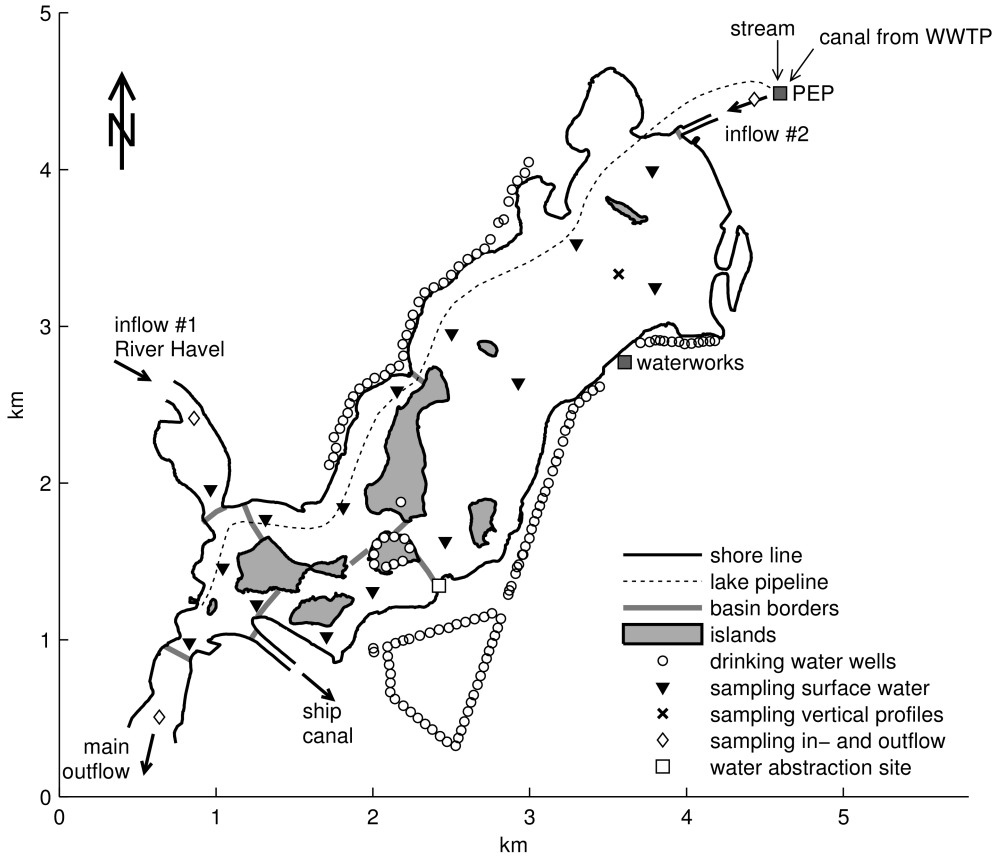

Fig. 3.1 Map of Lake Tegel (Berlin, Germany) with locations of inflows, outflows, phosphorus elimination plant (PEP) and water sampling.

3.2 Methods

3.2.1 Study site

Lake Tegel is a small (surface area 4.2 x 10^6 m^2), shallow (mean depth 6.4 m) lake located in northwestern Berlin (52°34'N, 13°15'E) affected by two inflows, which differ in

discharge and chemical concentrations. The bigger inflow #1, River Havel, contains more phosphorus and less pharmaceuticals then the smaller inflow #2, which carries high amounts of treated wastewater from a municipal wastewater treatment plant (WWTP). Additional features are a phosphorus elimination plant (PEP) at inflow #2, a lake pipeline, 131 drinking water wells along the shores, and a water abstraction site used for artificial groundwater recharge (Fig. 3.1). Further details on the study site have been described previously (Section 2.2.1).

3.2.2 Sampling and chemical analysis

96 water samples for pharmaceutical analysis were taken between April 2009 and April 2010. The inflows and the outflow were sampled monthly. Inflow #2 was monitored at the effluent of the PEP by a 24 h mixing sample. Inflow #1 and the outflow were sampled by equally mixing the water from four different subsamples taken at points 2 m deep, distributed equally over the cross section of River Havel (Fig. 3.1). Additionally, surface water samples were taken at 15 locations within Lake Tegel on two days (June 2009 and April 2010) at a depth of 0.5 m. At the deepest point of the lake, vertical profiles were obtained by sampling water from eight different depths (every 2 m) during the stratified period (May, July and September) and from three different depths (0.5, 7, 14 m) during the circulating period (November and February). All water samples were collected in glass bottles and were not filtered prior to analysis.

Chemical analysis of pharmaceuticals was described previously (Section 4.2.2). The limits of quantification are 0.02 µg L^{-1} (CBZ), 0.01 µg L^{-1} (DCF) and 0.03 µg L^{-1} (SMX).

3.2.3 Mass balancing of pharmaceuticals (zero-order elimination rates)

We use mass balancing as a black-box approach to obtain substance-specific zero-order elimination rates characteristic for Lake Tegel. The elimination of each pharmaceutical is calculated from balancing all four relevant in- and outgoing mass flows (Fig. 3.2), which are derived from flow rates and concentrations.

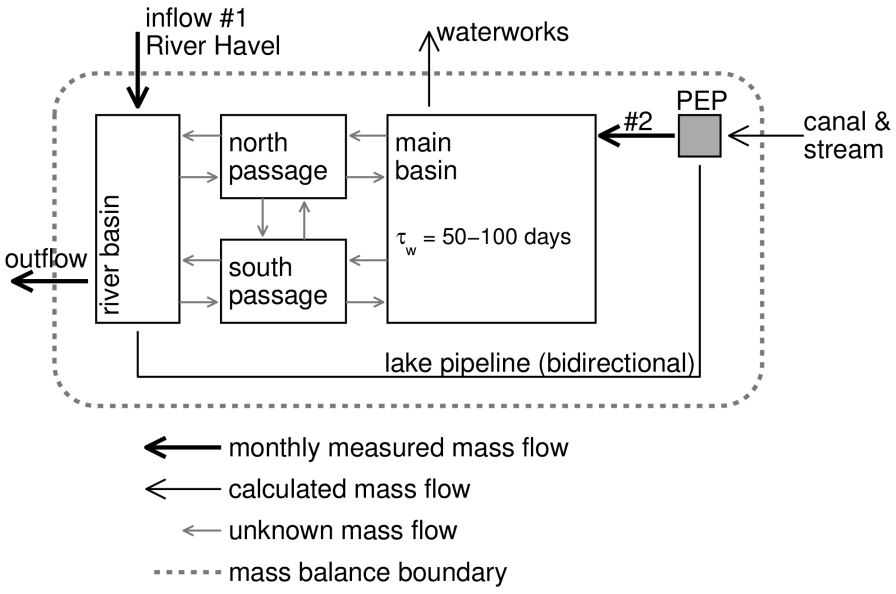

Fig. 3.2 Mass balance scheme of pharmaceuticals in Lake Tegel. τ_w is water residence time calculated from hydrodynamic model results.

The flow rates of the PEP effluent (inflow #2), lake pipeline, waterworks pumping and main outflow were available at a daily resolution. We derived the flow rate of inflow #1 (River Havel) from the water balance over the whole study site, including water level variations.

The pharmaceuticals' mass flows (inflow #1, inflow #2 and outflow) are derived from mean monthly flow rates and pharmaceuticals' concentration of monthly water samples (labeled as monthly measured mass flows in Fig. 3.2). Mass flow caused by waterworks is calculated from mean monthly water extraction rates (bank filtration and direct extraction for artificial groundwater recharge) and concentrations at outflow. Mass flow from canal & stream originated from WWTP is calculated from mass flows of inflow #2 and lake pipeline. Miehe (2010) found no elimination of CBZ, DCF or SMX during treatment in the PEP.

3.2.4 Calculating 1st-order elimination rates from horizontal distribution

In the case that the mass balancing of in- and outflows (black-box approach) results in very high (near 100%) elimination rates, it is possible to derive 1st-order elimination rates from measured concentration gradients within Lake Tegel. Therefore, we simplify the complex and dynamic mass transport in Lake Tegel to a very basic plug-flow approach under the following assumptions: (i) The horizontal concentration gradients which are measured at one day are characteristic for a longer period (stationarity); (ii) elimination is proportional to concentration (1st-order sink); (iii) mass transport is reduced to 1D advection (no

dispersion) from inflow #2 to outflow with an effective velocity of $v_e = L / \tau_w$, where L is the length of Lake Tegel's main basin and τ_w is the water residence time during the sampling period. Water residence time τ_w is calculated from hydrodynamic model results as described previously (Section 4.2.6).

Due to this simplification, the governing equation of mass transport is reduced to 1D steady-state advection with a 1st-order sink: $0 = - v_e \cdot (dc/dx) - \mu \cdot c$, where μ is the elimination rate which is used to calculate half-lives of pharmaceuticals: $t_{1/2} = \mu^{-1} \cdot ln\ 2$.

As an indicator of goodness of fit between the plug-flow model and the measured data we calculated Pearson's coefficient of correlations (r) and model efficiency (EF) following Mayer and Butler (1993): $EF = 1-(RMSE/STD_{obs})^2$. EF compares the root mean square error (RMSE) with the standard deviation of the observed data (STD_{obs}).

3.3 Results

3.3.1 Mass balances (zero-order elimination rates)

The sampling of in- and outflows confirms that the pharmaceutical load of Lake Tegel is caused solely from inflow #2. The load from River Havel is approximately 10 % for CBZ and insignificant (in most cases below LOQ) for DCF and SMX (Fig. 3.3). The mean total loads to Lake Tegel are 260, 180 and 60 g d^{-1} for CBZ, DCF and SMX, respectively. DCF shows a significant seasonal variation with low mass flows in summer and high loads in winter, whereas, the mass flows of the other two substances are less variable during the year.

Three of the 12 outflow samplings became compromised by short-circuit from inflow #2 caused by lake pipeline operation and are therefore not suitable for mass balancing and calculation of lake specific elimination rates. Finally, nine monthly balances are available to calculate zero-order elimination rates of pharmaceuticals (Fig. 3.4). CBZ and DCF show significant eliminaton in Lake Tegel, whereas, an elimination of SMX could not be deduced from the data. In the case of SMX, three monthly mass balances result in a 'negative elimination' (Apr, Aug, Oct), i.e. the calculated outgoing mass flows are higher than the incoming mass flows. Only DCF shows seasonal variation of elimination from 50 % in winter up to 95 % and more in summer.

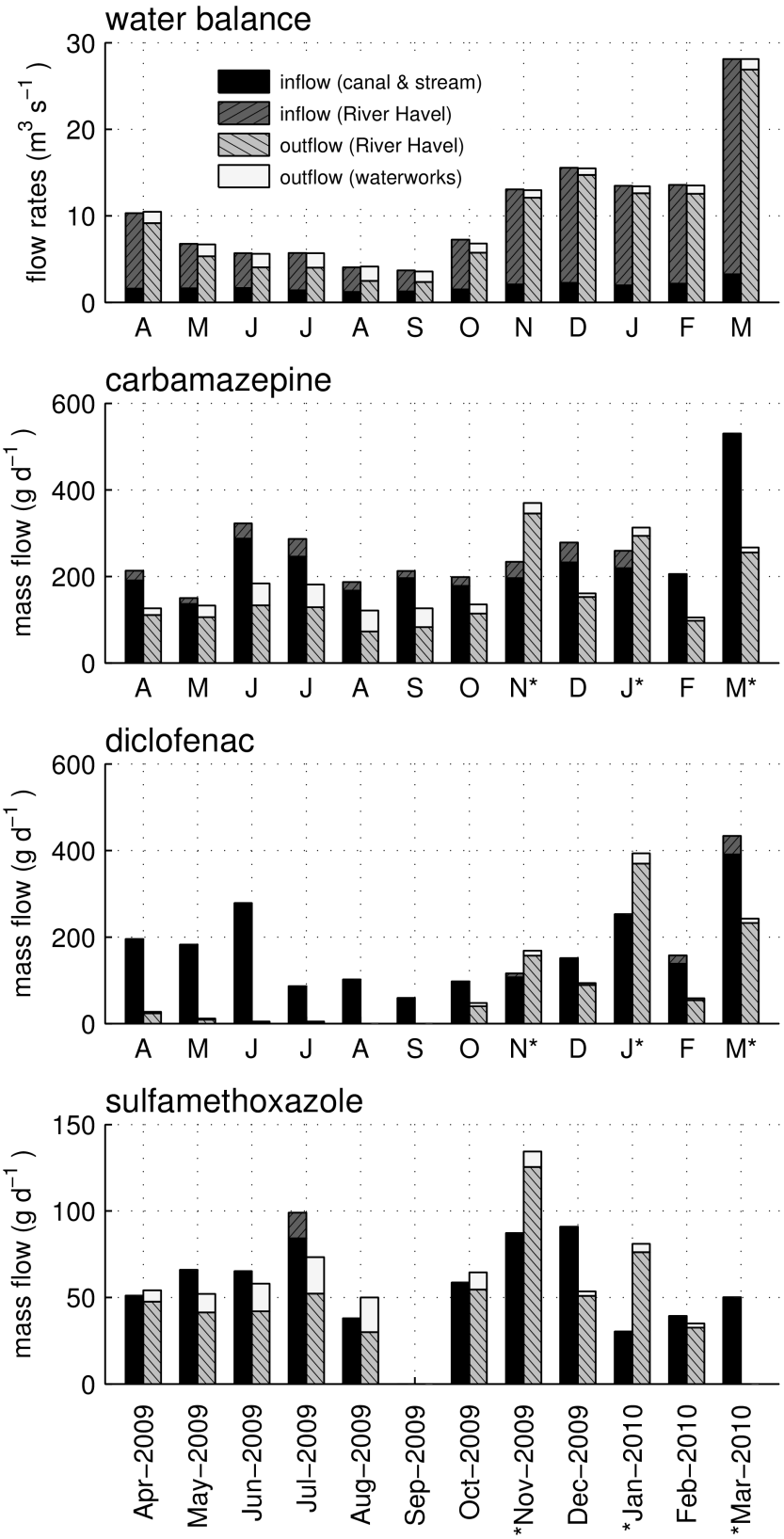

Fig. 3.3 Monthly balances of water and mass flow of pharmaceuticals in Lake Tegel, inflows (black & dark gray), outflows (light gray & white). * compromised outflow (River Havel) samplings by short-circuit from inflow #2 caused by lake pipeline operation.

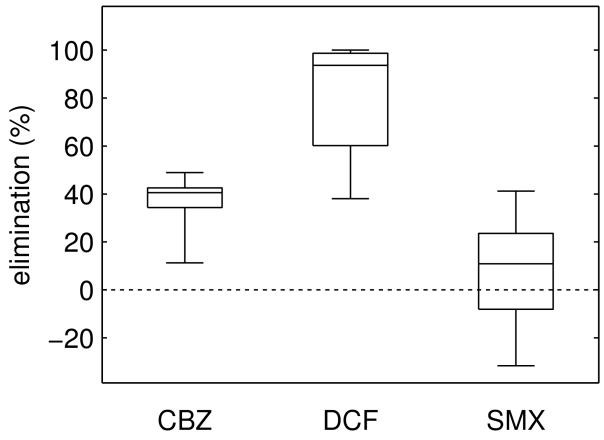

Fig. 3.4 Zero-order elimination rates of pharmaceuticals in Lake Tegel calculated from monthly mass balances (n = 9). Boxes represent 25th percentile, median and 75th percentile. The whiskers are determined by min and max values.

3.3.2 Horizontal distribution (1st-order elimination rates)

The horizontal distribution of pharmaceuticals shows similar patterns but at different concentration levels (Fig. 3.5). CBZ and SMX are more concentrated at the summer sampling date in June than at spring in April. In contrast, DCF shows the opposite relation: lower concentrations are observed in summer than in spring.

The general distribution pattern, except of DCF in summer, is similar to the measured distribution of electrical conductivity, a tracer for discharge from the municipal WWTP upstream of inflow #2 (Fig. 2.7a, p. 30). That general pattern is characterized by low concentrations in the river basin and northern passage due to river intrusion and a nearly well mixed (due to wind-driven circulation) main basin with higher concentrations.

In contrast, the summer sampling of DCF deviates from that general distribution pattern. In the main basin it shows a strong negative concentration gradient from inflow #2 to the islands. In reference to the previous Section 3.2.4, after reducing the horizontal distributed measurements to one dimension (dashed line in Fig. 3.5) and fitting the data to the simplified 1D transport equation parameterized only by the length of Lake Tegel's main basin (L = 2.800 m) and water residence time (τ_w = 51.5 d, mean of ± 25 days around 23 Jun 2009) it becomes possible to calculate the 1st-order elimination rate of diclofenac (μ = 0.058 d^{-1}) and a corresponding half-life ($t_{1/2}$ = 12 days, r = 0.99, EF = 0.94, Fig. A 36).

All of the five other horizontal distributions do not show a strong directed concentration gradient in the main basin. The calculated half-lives are higher than the water residence time and the data fits to model very poorly (r = 0.6−0.7, EF = 0.3−0.5). Consequentially, these data sets are not suitable to obtain reliable 1st-order elimination rates (Fig. A 36 and Fig. A 37).

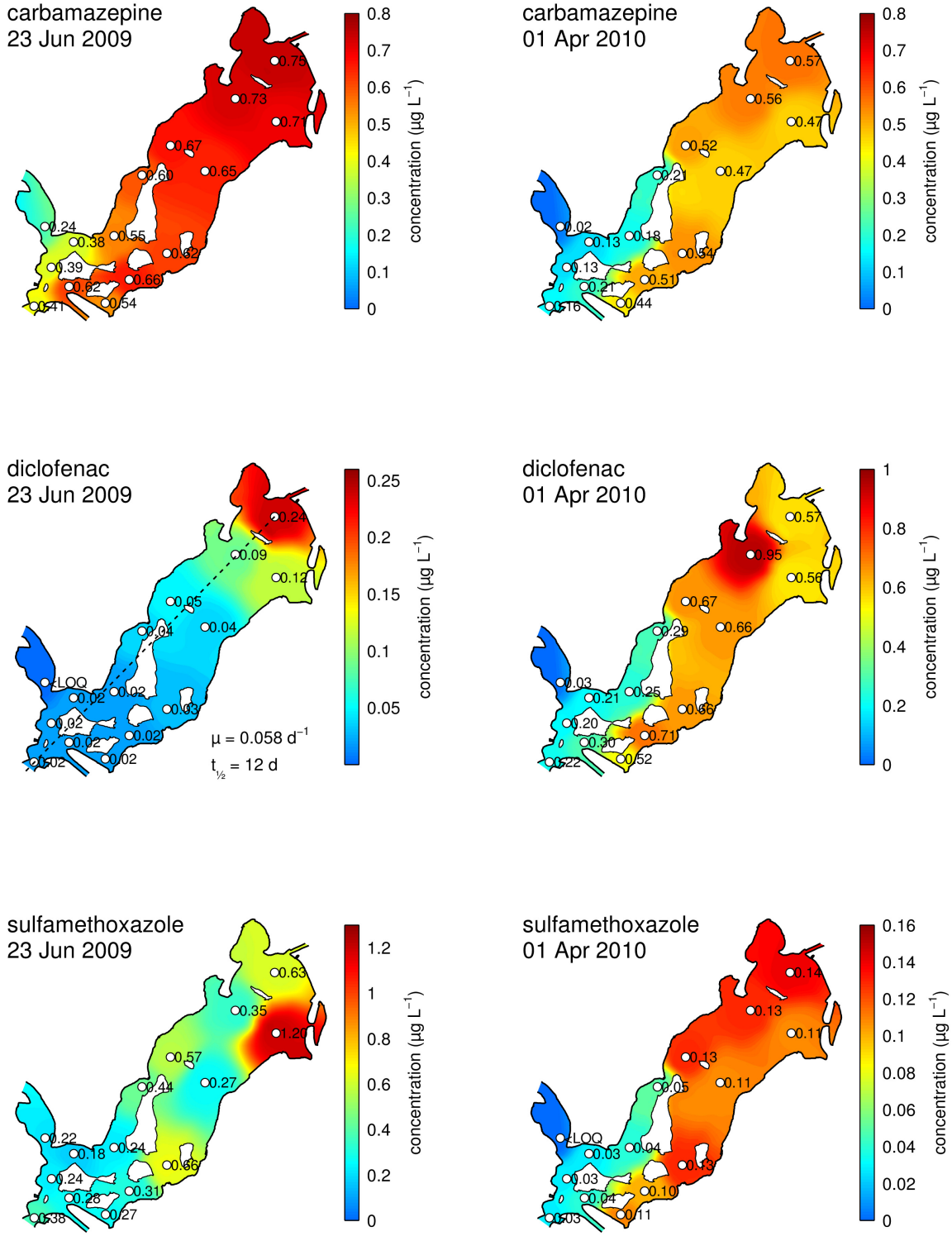

Fig. 3.5 Horizontal distribution of pharmaceuticals in summer (left) and spring (right); the contour plots are spatial interpolated from measured values (white circles) with a combination of Dijkstra's path-finding algorithm and inverse distance weighting; values below level of quantification (LOQ) are displayed as zero.

3.3.3 Vertical distribution

The vertical distribution of pharmaceuticals is affected by a temperature-derived density stratification of the dimictic Lake Tegel (Fig. 3.6a). The thickness of the epilimnion at the sampling days was 6 m (May), 4 m (Jul) and 8 m (Sep). The lake was vertically mixed in November and inversely stratified in February under a 28 cm ice cover.

Although, the lake was stratified between May and September, there is no vertical concentration gradient of CBZ and SMX (Fig. 3.6b, d). In contrast, DCF shows significant vertical gradients with low concentrations in the epilimnion and up to three times higher values in the hypolimnion (Fig. 3.6c).

As expected, during overturn in autumn all three pharmaceuticals shows no vertical gradient. During the inverse stratified period, all pollutants tend to have lower concentrations near the top beneath the ice cover.

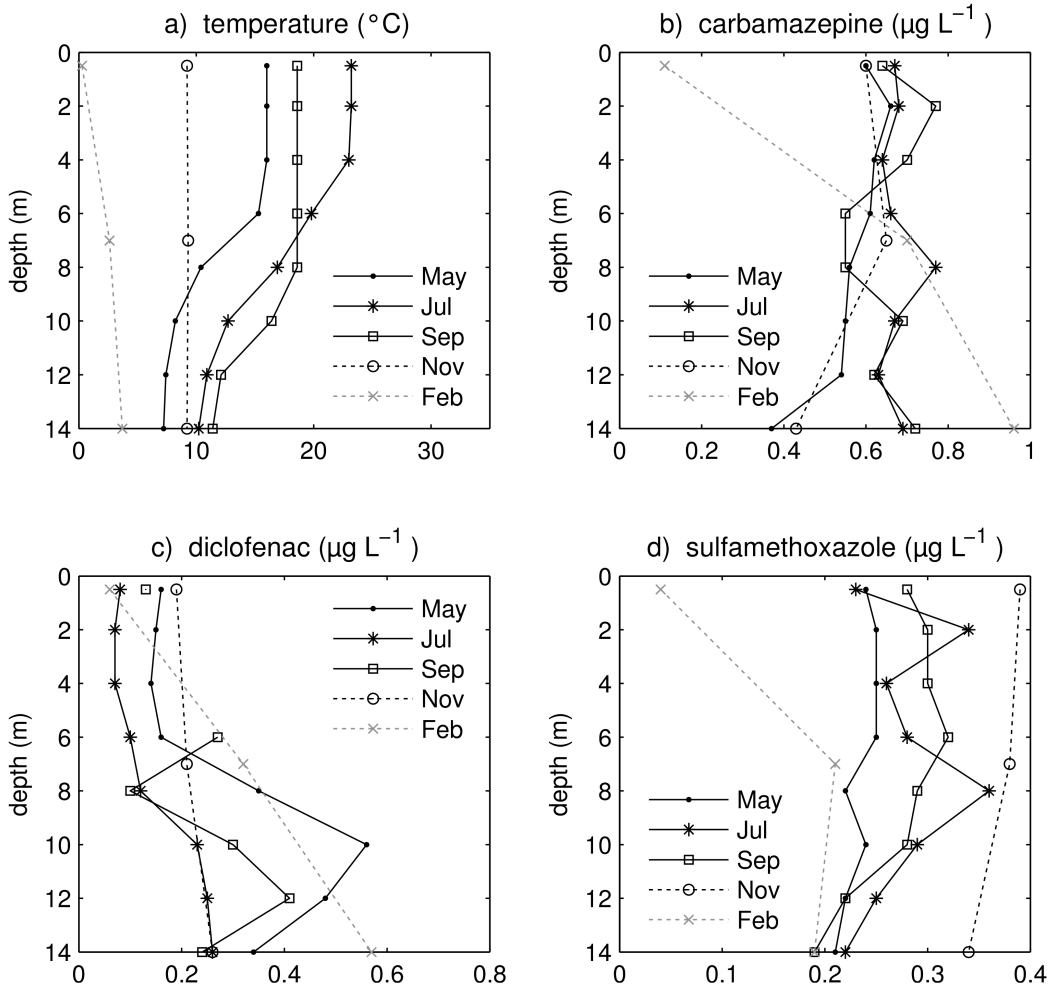

Fig. 3.6 Vertical distribution of water temperature (a) and pharmaceuticals (b–d) in Lake Tegel, 2009–2010, sampling in February beneath 28 cm ice cover.

3.4 Discussion

The reported mean concentrations of CBZ, DCF and SMX in North American surface waters (rivers, lakes and reservoirs) which are used for drinking water production are generally not much higher than 0.1 µg L^{-1} (Benotti et al., 2009; Blair et al., 2013; Ferguson et al., 2013; Kleywegt et al., 2011; Park et al., 2014; Roig, 2010; Snyder and Benotti, 2010; Zhang et al., 2008). Even in the highly wastewater-impacted estuary Jamaica Bay, New York City, the concentrations of CBZ and SMX do not exceed this limit (Benotti and Brownawell, 2007). In European surface waters the observed concentrations are in the same range or higher (Roig, 2010). The highest amounts have been reported from Germany and occur in small rivers downstream of WWTP effluent discharges (Heberer, 2002; Kunkel and Radke, 2012; Lewandowski et al., 2011). The concentrations of CBZ, DCF and SMX in large rivers, e.g. River Rhine (ter Laak et al., 2010), and large lakes, e.g. Lake Constance (Moschet et al., 2013), Lake Geneva (Hoerger et al., 2014; Morasch et al., 2010), Lake Greifensee (Tixier et al., 2003), Lake Chaohu (Tang et al., 2015) are also generally lower than 0.1 µg L^{-1}, with one exception of CBZ in Lake Geneva (0.4 µg L^{-1}) due to activities of pharmaceutical industries in the catchment (Bonvin et al., 2011).

In contrast, the concentrations of CBZ, DCF and SMX in Lake Tegel (this study) are approximately one order of magnitude higher than reported in other lakes. The reason becomes obvious, if one compares the total loads into the lakes with water residence time and lake volume (Table 3.1). In the case of Vidy Bay, which has the same volume as Lake Tegel, the daily loads and the water residence time are lower, i.e. less input and higher dilution. In the case of Lake Greifensee the water residence time is up to 8 times higher than in Lake Tegel, however this is overcompensated by the 10 times lower daily loads and 6 times higher volume. In the case of Lake Constance, the daily loads are up to three times and water residence time up to 30 times higher than in Lake Tegel, however this is overcompensated by the 1,830 times higher volume.

To the authors' knowledge, Lake Tegel is the natural drinking water resource with the highest so far reported pharmaceutical concentrations worldwide.

Table 3.1 Average daily loads of pharmaceuticals into different lakes compared to water residence time and lake volume

CBZ ($g\ d^{-1}$)	DCF ($g\ d^{-1}$)	SMX ($g\ d^{-1}$)	water residence time τ_w (d)	volume ($10^6\ m^3$)	study site, reference
260	180	60	50–100	26	Lake Tegel, this study
192	86	9	4	26	Vidy Bay, Lake Geneva (Morasch et al., 2010)
29	19		408	151	Lake Greifensee (Tixier et al., 2003)
320	520	180	1 570	47 600	Lake Constance (Moschet et al., 2013)

3.4.1 Elimination of carbamazepine

CBZ is poorly or not removed by WWTPs (Miehe, 2010; Zhang et al., 2008) and is often considered as persistent in natural waters (Löffler et al., 2005; Tixier et al., 2003), and used as a conservative tracer at study sites with short water residence time (Kunkel and Radke, 2012). However, the category persistent is relative and does not mean, that CBZ is not degradable, but degradation will be slow and therefore difficult to measure in surface waters. Tixier et al. (2003) determined a low degradation rate of CBZ in the epilimnion of Lake Greifensee (< 0.01 d^{-1}, i.e. half-life > 70 d) calculated from 1D vertical mixing model and measured vertical concentration profiles within three months of the stratified period (τ_w of epilimnion 116 d). We determined a median of 40 % elimination of CBZ in Lake Tegel derived by monthly mass balancing in- and outflows within one year. The corresponding half-life can be estimated to be in the same range or higher than the water residence time of Lake Tegel (> 50–100 d), which agrees with the findings of Lake Greifensee (> 70 d).

Laboratory studies showed that elimination of CBZ is mainly driven by indirect photolysis, which is enhanced by dissolved organic matter (DOM) (Lam and Mabury, 2005). Compared to natural waters, the observed half-lives in artificial setups are in the same order of magnitude (> 100 d (Andreozzi et al., 2003), 82±11 d (Lam et al., 2004)).

3.4.2 Elimination of diclofenac

Diclofenac's biodegradability is slow or non-existing (Vieno and Sillanpää, 2014) and it is not removed in Berlin's WWTPs (Miehe, 2010). However, several studies have shown fast photodegradation (Andreozzi et al., 2003; Bartels and von Tumpling, 2007; Buser et al.,

1998; Kunkel and Radke, 2012; Packer et al., 2003; Poiger et al., 2001; Tixier et al., 2003). In contrast to CBZ, the reported half-lives of DCF from laboratory studies, field experiments and natural waters vary in a wide range from minutes to days. The rate of photodegradation depends on several parameters (e.g. latitude, season, cloud cover) and water specific conditions (e.g. reflection, transmission and absorption of light, DOM content, water depth, vertical mixing, circulation). Therefore, the rate-limiting process varied and the scale-up from laboratory to natural waters becomes difficult. Poiger et al. (2001) successfully demonstrated the prediction of DCF concentrations in Lake Greifensee from photolysis rates obtained from natural sunlight experiments with the help of radiation measurements, a model of light intension and attenuation, and a 1D lake model whose vertical mixing parameters were obtained from monthly measured temperature profiles.

Two river studies determined elimination rates of DCF by mass balancing in- and outflows. In the shallow river Gründlach 41–69 % of DCF was eliminated in a 12.5 km long stretch (τ_w = 12–18 h, average water depth 15 cm, July) (Kunkel and Radke, 2012). Whereas, in the river Roter Main no elimination of DCF was observed in a 13.6 km long stretch (τ_w = 6–30 h, average water depth 1 m, Aug–Sep) (Radke et al., 2010). In Lake Greifensee (τ_w = 110–408 d) more than 90 % of DCF is degraded, with half-lives of 8 d during stratification in summer (Buser et al., 1998; Tixier et al., 2003) and 30 d during mixed lake situation in winter (Buser et al., 1998). We determined an elimination of DCF in Lake Tegel of more then 95 % in summer (half-life 12 d in epilimnion), which agreed with the findings of Lake Greifensee. In winter the elimination of DCF in Lake Tegel decreases to approximately 50 %.

3.4.3 Elimination of sulfamethoxazole

SMX is removed by Berlin's WWTPs in a range of 41–48 % (Miehe, 2010). However, for attenuation in surface waters photodegradation is assumed to be more important then biodegradation (Lam et al., 2004). Laboratory studies reported one order of magnitude faster photodegradation of SMX compared to CBZ (Andreozzi et al., 2003; Lam and Mabury, 2005). In agreement with the laboratory results, the field study at river Gründlach refers to 25–26 % elimination of SMX, whereas CBZ was assumed to be a conservative tracer (Kunkel and Radke, 2012). Furthermore, a field microcosm study reported half-lives in similar relation: 19±1.2 d for SMX and 82±11 d for CBZ (Lam et al., 2004).

In Lake Tegel, we found a contrary situation with no determinable elimination of SMX compared to 40 % elimination of CBZ. There are several possible explanations for this results: (i) an unknown external or internal source of SMX, e.g. combined sewer discharge or photolytic back-transformation (Bonvin et al., 2013); (ii) poor analyte stability in the 24 h combined samples at inflow #2 compared to the other samples, which are all grab

samples; (iii) too scarce sampling compared to the higher variability of SMX concentrations in the WWTP effluent. The first and second explanation can not be disproved by data and are under investigation; however we assess the data deficiency, explanation (iii), as most likely.

The question, if other organic substances affect the photodegradation of SMX is still under discussion. Andreozzi et al. (2003) reported that humic acids acts as photosensitizer, whereas Lam and Mabury (2005) constitute that DOM do not enhance degradation of SMX. In addition, Bonvin et al. (2013) observed a photolytic back-transformation of SMX from the human metabolite 4-nitroso-SMX, however, only of low environmental relevance because of the relatively high photolability of SMX.

3.4.4 Seasonal and spatial variation of pharmaceutical concentration in Lake Tegel

Horizontal and vertical distributions show, that concentrations of CBZ and SMX in Lake Tegel are mainly affected by dilution with less contaminated water of River Havel (intrusion of inflow #1 and operation of the lake pipeline), rather than degradation within the lake. In contrast, concentrations of DCL are affected by both dilution and photodegradation, which results in a seasonal and spatial variation of DCL in Lake Tegel. The vertical concentration profiles of DCL are similar to the measurements in Lake Greifensee (Poiger et al., 2001; Tixier et al., 2003), with the exception that the absolute concentrations in Lake Tegel are 20–40 times higher.

As described in a previous study (Section 2.3.1) the water of the pharmaceutical laden inflow #2 is less dense during the warming period when the lake is stratified and denser during winter compared to the upper 8-m layer of Lake Tegel, in contrast to the river intrusion from inflow #1, which is always less dense. If the lake is ice-covered, the water from inflow #2 sinks and fills the hypolimnion until the end of winter stratification (Fig. A 27, p. 118). As a result, in summer inflow #2 is mixed only within the epilimnion and the hypolimnion contains water from last winter inflow. The fraction of inflow #2 within the summer hypolimnion depends on the duration of previous ice-covered period and mixing-period between winter and summer stratification. After a weak winter with short or no ice cover, the pharmaceutical concentrations in the summer hypolimnion are assumed to be lower, due to higher dilution and flushing. Therefore, the interannual variations might be higher than supposed in small dimictic lakes with a mean water residence time not much longer than one season. However this can not be proven by this study and has to be investigated in further research.

Consequently, there are two amplifying processes which explain the vertical concentration profiles of DCL in Lake Tegel: (i) in summer the incoming mass flow of DCL is lower

than in winter and only mixed within the epilimnion, whereas the hypolimnion contains water affected by the higher incoming mass flow of the previous winter; (ii) the higher photodegradation of DCL in summer acts only in the epilimnion.

Nevertheless, the overall relevance of stratification on pharmaceutical concentrations in the shallow Lake Tegel is not as important as in deeper lakes, because the epilimnion (0−8 m) generally captures 77% of the lake volume and the hypolimnion (8−16 m) represents only 23%.

As reported in a previous study (Section 4.3.1), the concentrations of all three pharmaceuticals in Lake Tegel are above the proposed German environmental quality standards (EQS). A recommendation for periodic monitoring of pharmaceuticals with respect to EQS assessment is easy in the case of CBZ and SMX due to their low vertical and seasonal variation. Consequently, we suggest an analysis of the epilimnion every two months, e.g. at one point in the middle of the lake. In the case of DCL we suggest at least a monthly sampling of the main basin's epilimnion and inflow #2, to obtain the concentration range. If this data is not sufficient to decide whether the EQS of DCL is met or not, additional sampling of vertical and horizontal profiles will be necessary.

4 Seeking a compromise between pharmaceutical pollution and phosphorus load: management strategies for Lake Tegel, Berlin

Sebastian Schimmelpfennig[a], Georgiy Kirillin[a], Christof Engelhardt[a], Gunnar Nützmann[a], Uwe Dünnbier[b]

Water Research 2012, 46(13), 4153-4163

Lake Tegel (Berlin, Germany) is controlled by two main inflows: inflow #1 (River Havel) is heavily phosphorus-laden, whereas inflow #2 is an artificial confluence that includes discharge from a municipal wastewater treatment plant distinguished by high levels of phosphorus and pharmaceuticals. To reduce the phosphorus load on the lake, a phosphorus elimination plant (PEP) is situated at inflow #2. Moreover, the two inflows are short-circuited by a pipeline that transfers part of the inflow #1 water to the PEP and finally releases it into inflow #2. The pipeline and the PEP have contributed to a continuous reduction in the total phosphorus concentration of Lake Tegel in the past 25 years. We investigate the question of whether the existing lake pipeline can also be used to reduce the amount of pharmaceuticals in Lake Tegel originating from inflow #2 by dilution with water from River Havel, by diverting part of inflow #2 around the lake, or by a combination of both strategies. The circulation pattern of Lake Tegel is complicated by complex bathymetry and numerous islands and is therefore highly sensitive to winds. We tested seven different management scenarios by hydrodynamic modeling for a period of 16 years with the two-dimensional version of the Princeton Ocean Model (POM). None of the scenarios provided a strategy optimal for both pharmaceuticals and phosphorus. Nonetheless, compound regimes, such as alternating the pipe flow direction or adding another pipeline, allowed the most abundant pharmaceutical (carbamazepine) to be reduced while maintaining the current phosphorus level. This study demonstrates the ability of immediate lake regulation measures to maintain water quality. In the case of Lake Tegel, the pipeline can be fully effective with regard to pharmaceuticals only in combination with additional efforts such as advanced pharmaceutical treatment of wastewater and/or phosphorus reduction in the River Havel catchment.

[a] Leibniz-Institute of Freshwater Ecology and Inland Fisheries, Department of Ecohydrology, Müggelseedamm 310, D-12587 Berlin, Germany
[b] Berlin Water Company, Department of Laboratories, PO Box 310180, 10631 Berlin, Germany

4.1 Introduction

The contamination of freshwater systems by industrial and domestic compounds is increasing worldwide. Among the major anthropogenic pollutants in large urban agglomerations are phosphorus and pharmaceutically active compounds from treated wastewater (Nützmann et al., 2011). In the case of phosphorus, its sources, fate and relevant environmental processes are well understood, whereas existing knowledge on pollution by pharmaceuticals is insufficient for effective risk management (Kümmerer, 2009). A framework was set by the European Medicines Agency, who published an environmental risk assessment guideline for human pharmaceuticals (EMEA, 2006) based on the relation of the predicted environmental concentration (PEC) to the predicted no-effect-concentration (PNEC).

The reduction of pharmaceuticals in the environment is motivated by environmental hygiene rather than human toxicological risks, which seem to be negligible (Kümmerer, 2009). Hence, any measure must be assessed according to its net environmental benefit before being implemented. Wenzel et al. (2008) investigated the environmental impacts of three different advanced wastewater treatments (sand filtration, ozonation and membrane bioreactors) and compared them to the benefit of avoiding emissions for nine selected micro-pollutants within a life cycle assessment (LCA). The authors found the impacts and benefits to be of the same order of magnitude. This example demonstrates the need for further research on alternatives to advanced wastewater treatment for reducing the concentration of pharmaceuticals in open waters.

A large amount of recent studies is dedicated to the fate of pharmaceuticals in the aquatic environments and their potential effects on the ecosystems (Corcoran et al., 2010; Jones et al., 2001). Transport modeling is used for assessment of pharmaceuticals propagation and development of appropriate reduction strategies on the regional scales (Ort et al., 2009). The phosphorus-related management strategies have longer history for both for wastewater (Tchobanoglous et al., 2003) and natural open waters (Marsden, 1989). Regulation measures with regard to both pollutants are especially critical for enclosed water bodies—lakes and reservoirs—located in large megalopolises and used simultaneously as drinking water sources, recreational sites and reservoirs for treated wastewater. Their complex hydrodynamics represents an additional difficulty for development of adequate regulation measures.

Using Lake Tegel located in the German capitol Berlin as a natural example, we applied a deterministic circulation model to assess efficiency of water regime regulation scenarios for reduction of pharmaceuticals load from the wastewater plant and phosphorus load from the inflow of the River Havel. The hydrodynamics of Lake Tegel have been previously

investigated by applying a two-dimensional hydrodynamic circulation model including conservative tracer transport (Chapter 2). In the present study, we use the same two-dimensional approach to evaluate different operation strategies for the regulation system including a pipeline connecting the river inflow with the outlet of the wastewater plant and a phosphorus elimination plant.

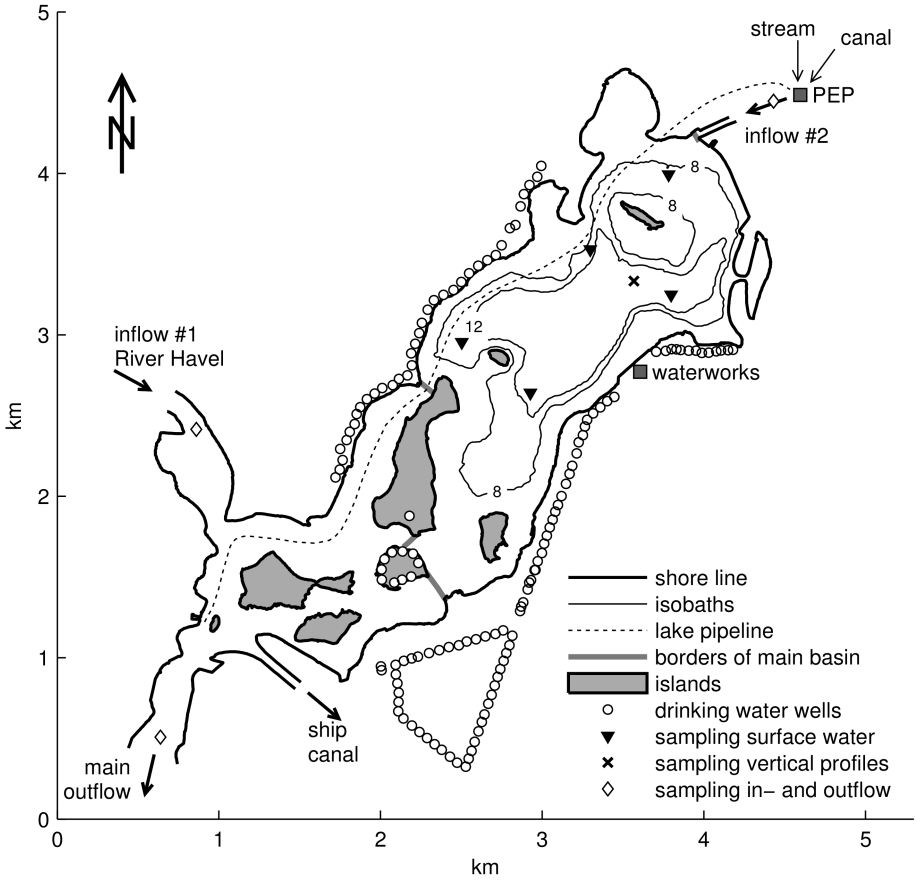

Fig. 4.1 Map of Lake Tegel (Berlin, Germany) with locations of inflows, outflows, phosphorus elimination plant (PEP) and water sampling

4.2 Methods

4.2.1 Study site

Lake Tegel is a small, shallow lake (length 4 km, maximum depth 16 m, mean depth 6 m, residence time of main basin 50–100 days) located in northwestern Berlin (52°34'N, 13°15'E) (Fig. 4.1) affected by two inflows. The inflow #1, River Havel, has a mean annual flow (MAF) of 13 $m^3 s^{-1}$. The mean monthly flow ranges from 3 to 40 $m^3 s^{-1}$. The smaller inflow #2 (MAF 2.4 $m^3 s^{-1}$) is a confluence of a lake pipeline, the stream Tegeler Fließ, and the Nordgraben canal. Approximately 70–90% of the water in the Nordgraben canal is treated wastewater from a municipal wastewater treatment plant. The water from

the pipeline, stream and canal is treated together in a phosphorus elimination plant (PEP) by coagulation/flocculation, sedimentation and dual-media filtration (Heinzmann et al., 1991). The PEP and lake pipeline went into operation in 1985. The lake pipeline pumps water from a point near the outflow of Lake Tegel to the PEP to increase the discharge of inflow #2 and decrease the phosphorus load to Lake Tegel, mainly during the summer. During the winter, the lake pipeline occasionally pumps water in the opposite direction if the total discharge of the stream and the canal exceeds the capacity of the PEP or if the PEP is out of service because of maintenance.

Lake Tegel has one main outflow (located 1 km inflow #1) with a downstream lock that regulates the discharge of the River Havel and consequently the water level of the lake. An additional outflow is the almost stagnant Berlin-Spandau ship canal (MAF 0.07 $m^3 s^{-1}$).

More than one hundred drinking water wells are installed along the east and west shores and on two islands. These wells extract water from the lake via bank filtration (Fig. 4.1). Additionally, some water is taken directly from the lake and used for artificial groundwater recharge. The mean annual water extraction rate from Lake Tegel by these waterworks is 1.16 $m^3 s^{-1}$, as calculated with a bank-filtration-to-groundwater ratio of 7:3 for all shore-parallel well galleries (Wiese and Nützmann, 2009).

4.2.2 Sampling and chemical analysis

Water samples for pharmaceutical analysis were taken from April 2009 until April 2010. The inflows and outflow were sampled monthly. Inflow #2 was sampled at the effluent of the PEP by a 24 h mixing probe. Inflow #1 and the outflow were sampled by equally mixing the water from four different subsamples taken at points 2 m deep distributed equally over the cross section of River Havel. Surface water samples were taken on two days (June 2009 and April 2010) at a depth of 0.5 m (see Fig. 4.1 for locations). At the deepest point of the lake, vertical profiles were estimated by sampling water from eight different depths (every 2 m) during the stratified period (May, July and September) and from three different depths (0.5, 7,14 m) during the circulating period (November and February). All water samples were collected in glass bottles and were not filtered before analysis.

Chemical analysis for pharmaceuticals was performed at the laboratory of the Berlin Water Company. The anti-epileptic drug carbamazepine was analyzed with automated solid-phase extraction (SPE), liquid chromatographic separation (LC), and tandem mass spectrometric detection (MS/MS). The method is described in detail by Zühlke et al. (2004). The painkiller and anti-inflammatory drug diclofenac was analyzed with SPE and HPLC-MS/MS according to German standard methods (DIN 38407-35). The antibiotic

sulfamethoxazole was analyzed with SPE and HPLC-MS/MS via the method of Richter et al. (2007) with small adaptations: The electrospray ionization operated in positive mode. One transition (m/z 254 to 156) was used for quantification and another transition (m/z 254 to 92) for proof of identity of the target.

The limits of quantification are 0.02 µg L^{-1} for carbamazepine, 0.01 µg L^{-1} for diclofenac and 0.03 µg L^{-1} for sulfamethoxazole.

Data regarding total phosphorus concentrations in the PEP effluent (daily resolution) were provided by Berlin Water Company (BWB). The phosphorus data for the River Havel and Lake Tegel (monthly resolution) were provided by the Senate of Berlin (SenGUV) and the Federal Environment Agency (UBA). Data regarding chloride concentrations (weekly to monthly resolution) were provided by BWB and SenGUV.

4.2.3 Hydrodynamic model

To simulate circulation and pollutant transport in Lake Tegel, we applied the Princeton Ocean Model (POM) (Blumberg and Mellor, 1987) in the two-dimensional mode on a curvilinear horizontal grid (200x60, mesh size 10–150 m); details are described in Section 2.2.2. A small model adaptation including simple parallelization was made to calculate long-time scenarios (16 years) with high temporal resolution (time step, 0.8 s) and transient wind and boundary conditions. The calculation time for one scenario was 4 days on an Intel Xeon 3 GHz 8 core processor.

The model was previously validated for an 8-month period in 2009 against measured electrical conductivity data (Section 2.3.2). To validate the model for the 16-year period 1995–2010, we used chloride data measured in both inflows as boundary conditions and compared the simulated concentrations in the main basin with measured values. We calculated model efficiency (EF) following Mayer and Butler (1993) as an indicator of goodness of fit:

$$EF = 1 - \left[\sum_{i=1}^{n} \left(c_i^{obs} - c_i^{sim} \right)^2 \Big/ \sum_{i=1}^{n} \left(c_i^{obs} - \bar{c}_m^{obs} \right)^2 \right] = 1 - \left(\frac{RMSE}{STD_{obs}} \right)^2 \tag{4.1}$$

where c_i^{obs} is the observed chloride concentration, c_i^{sim} is the corresponding simulated value, n is the number of values compared, and c_m^{obs} is the mean of the observed data. EF compares the root mean square error (RMSE) with the standard deviation of the observed data (STD_{obs}). A negative EF indicates that the model is worse than simply using the observed mean. An EF value close to one indicates a “near-perfect” model. (Loague and Green, 1991; Mayer and Butler, 1993)

By using a two-dimensional hydrodynamic model some effects has to be neglected, e.g. stratification in summer and ice cover in winter. These effects play a minor role in the horizontal circulation in Lake Tegel compared to the large-scale wind/river interchange dynamics (Section 2.3.1). Additionally, the utility of the two-dimensional approach will be proven by validation results in Section 4.3.2.

4.2.4 Scenarios

The aim of the scenario simulation is to evaluate different lake pipeline operation strategies regarding their ability to decrease the concentrations of the two target compounds—phosphorus and pharmaceuticals—in Lake Tegel. Therefore, we marked the water at the inflows with two virtual tracers. The 1st tracer represents phosphorus, and its concentration is constantly set to one at inflow #1 and zero at inflow #2. The 2nd tracer represents pharmaceuticals, and its concentration is constantly set to zero at inflow #1. The concentration at inflow #2 is calculated according to the mixing ratio of water from the lake pipeline (its concentration is calculated by the model at the pumping station on the other end of the pipeline) and water from the stream and canal (both concentrations constantly set to one).

The hydrodynamic model calculates the concentrations of both tracers with high spatial and temporal resolution depending on transient wind forcing, inflows and bathymetry. Finally, to facilitate comparison between the scenarios, we assembled the calculated data by averaging the tracer concentrations of all grid cells of the main basin for the whole simulation period, resulting in only two values per scenario, one for each tracer.

Seven scenarios were implemented (Table 4.1): actual (A) and previous (B) pipeline operations and five hypothetical operations (C–F). The hypothetical scenarios were designed to be as realistic as possible, using real discharge data and wind forcing from 1995 until 2010. The daily throughput of the pipeline and the PEP is calculated with respect to the maximum capacities of the lake pipeline (2.4 $m^3 s^{-1}$) and PEP (4.5 $m^3 s^{-1}$) and the minimum throughput of the PEP (0.8 $m^3 s^{-1}$).

For evaluation, Table 4.1 contains expected energy consumption and cost for each scenario. These values consider only pumping energy, which is most cost effective. Other operational costs, e.g. for flocculation chemicals or maintenance, and investment costs, e.g. for a new pipeline, are not included.

Table 4.1 Average operational conditions and energy consumption for each scenario

scenario		pipeline [a] throughput ($m^3\ s^{-1}$)	PEP [b] throughput ($m^3\ s^{-1}$)	pumping energy [c] ($GWh\ a^{-1}$)	total energy cost [d] and difference to reference scenario (10^3 € a^{-1})	
A	reference scenario (2002–2010)	+0.77 −0.20	2.4	7.7	930	
B	without lake pipeline (1997–2001)	+0.01 −0.03	1.44	3.4	410	(−520)
C	maximum pumping from Havel to PEP[b]	+2.3 −0.003	4.0	14.5	1740	(+810)
D_1	bypassing PEP[b] and Lake Tegel	+0.0 −1.63	0.0	3.7	450	(−480)
D_2	bypassing Lake Tegel	+0.0 −1.63	1.7	7.7	920	(−10)
E	simultaneous pumping in both directions	+1.2 −1.2	1.7	9.4	1130	(+200)
F	additional pipeline	+2.3 −0.003 1.6 [e]	4.0	18.2	2180	(+1250)

a pumping from inflow #1 (River Havel) to PEP (positive number), pumping from PEP to inflow #1 (negative number)
b PEP: phosphorus elimination plant situated at inflow #2
c specific energy consumption 0.073 kWh m^{-3}
d local energy price 0.12 € kWh^{-1}
e throughput of additional pipeline

4.2.4.1 A reference scenario (2002–2010)

Scenario A represents the actual operation of the pipeline/PEP since 2002. In summer, the PEP's throughput is increased to approximately 3.1 $m^3\ s^{-1}$ by pumping water from River Havel to the PEP. In winter, the PEP's throughput is decreased to approx. 1.9 $m^3\ s^{-1}$. The averaged annual values are listed in Table 4.1.

4.2.4.2 B without lake pipeline (1997–2001)

Scenario B is the "no pipeline" scenario, corresponding to the actual situation in 1997–2001 when the lake pipeline was not in operation, initially due to reconstruction and then to save energy costs. The lake responded with increasing phosphorus concentrations (maximum of 200 µg L^{-1} in 2001). Consequently, the local authorities decided to turn the pipeline on again, after which the phosphorus level declined to its present value.

4.2.4.3 C maximum pumping from River Havel to the PEP

In scenario C, the pharmaceuticals in Lake Tegel are diluted as much as possible with water from River Havel. Therefore, the pipeline's throughput is set to the maximum with respect to the capacity of the pipeline and the PEP.

4.2.4.4 D bypassing Lake Tegel

In scenarios D_1 and D_2, the concentrations of pharmaceuticals in Lake Tegel are reduced by diverting water from the stream and canal through the lake pipeline to the River Havel outflow. Because the pipeline-PEP conjunction is currently situated at the PEP influent, PEP operation would only make sense if the discharge of the stream and canal exceed the capacity of the pipeline. This occurs on an average of 57 days per year, with a mean flow rate of 0.7 $m^3 s^{-1}$, which is too rare and too low to keep the PEP in operation. Therefore, in scenario D_1, the spillover water is released untreated into Lake Tegel at inflow #2, with a mean phosphorus concentration of 266 $\mu g L^{-1}$.

In contrast, scenario D_2 assumes reconstruction of the pipeline-PEP conjunction by moving it to the PEP's effluent. The PEP thereby continues its operation to prevent further eutrophication of the River Havel reach downstream.

It is obvious, that in both D scenarios, the 1st tracer (phosphorus) will increase to an unacceptable level because of the high fraction of P-loaded River Havel water in the main basin. However, scenario D_2 can be used to calculate how low the phosphorus content of River Havel would have be to achieve the target P concentration in Lake Tegel.

Additionally, the D scenarios answer a question, related to the 2nd tracer (pharmaceuticals): How great is the influence of spillover water discharge and the backmixing of released bypass water? The latter is of special interest because the release point of the pipeline is not directly at the main outflow (c.f. Fig. 4.1); therefore, bypassed water could be mixed back into the main basin.

Both D scenarios are calculated from the same hydrodynamic model run because they only differ in the phosphorus concentration of inflow #2 (c.f. Section 4.2.6).

4.2.4.5 E simultaneous pumping in both directions

Scenario E is designed as a combination of dilution and bypassing. The lake pipeline was constructed with two parallel tubes, which can be operated separately (maximum flow rate 1.2 $m^3 s^{-1}$ for each tube). This makes it possible to use one tube to pump River Havel water to the upstream of PEP to promote the dilution of pharmaceuticals and to simultaneously pump water from the upstream of PEP to River Havel to benefit from bypassing the lake.

The efficiency of simultaneous pumping would be partly reduced by recirculation because at both ends of the pipeline it is possible that part of the water released from one tube gets into the other tube and is pumped back. These effects are taken into account in the hydrodynamic model.

4.2.4.6 F additional pipeline

Scenario F is a further development of scenario E that lacks the drawbacks of re-circulation and limited flow rates. In scenario F, the throughput of the lake pipeline is set to its maximum as in scenario C. However, the treated water from the PEP effluent is now split. The majority is released into the lake with a maximum flow rate of 2.4 $m^3 s^{-1}$, and the overspill water is pumped through a new pipeline into the River Havel downstream of Lake Tegel. In this configuration, inflow #2 would have the same mean annual flow rate as in scenario A, thereby ensuring that the phosphorus level in Lake Tegel would stay below the target concentration. The concentrations of pharmaceuticals in inflow #2 would be lower than in scenario A because of higher dilution with River Havel water. Additionally, part of the pharmaceuticals would bypass Lake Tegel. Drawbacks of scenario F include the high operational (Table 4.1) and investment costs of the new pipeline.

4.2.5 Target concentrations of pharmaceuticals and phosphorus

Currently, there are no regulations governing pharmaceuticals in surface waters in the European Union, although the environmental law provides two mechanisms of regulation: a community-wide definition of environmental quality standards (EQS) and a national setting of EQS by Member States (Kern, 2011). The European Parliament proposed several times to add pharmaceuticals (e.g., carbamazepine and diclofenac) to the list of priority substances, including the setting of EQS (EP, 2007; EP, 2008). However, no pharmaceuticals are included in the final Directive (2008/105/EC). The same happened on the national level in 2011. EQS for three pharmaceuticals (carbamazepine 0.5 $\mu g L^{-1}$, diclofenac 0.1 $\mu g L^{-1}$ and sulfamethoxazole 0.1 $\mu g L^{-1}$) were proposed for German surface waters, but none of them were included in the final law (OgewV, 2011) because uncertainties due to missing toxicity test data are too great.

Nevertheless, we expect EQS will be set in the near future at least for the three above-mentioned pharmaceuticals. Therefore, we used the proposed German EQS as target concentrations for the assessment procedure in this study.

In the case of phosphorus, we defined a target in-lake total P concentration of 45 $\mu g L^{-1}$ as the upper limit. This value equals the threshold value between mesotrophic and eutrophic defined by the German Working Group on water issues (LAWA, 1998). A value of 45 $\mu g L^{-1}$ total P corresponds to the numerical trophic state index (TSI) of 59 according to

Carlson (1977), which is also between mesotrophic and eutrophic. Heinzmann and Chorus (1994) presumed a threshold for transition of Lake Tegel's trophic state in the vicinity of 40–60 µg L^{-1} total P, which was later specified by Chorus and Schauser (2011), who documented a P-threshold of ~50 µg L^{-1} for Lake Tegel, explained by a switch from light limitation to P limitation and by the resilient dominance of cyanobacterial species.

4.2.6 Assessment procedure

To evaluate the different scenarios, the calculated mean concentrations of both virtual tracers must be compared with the target concentrations defined above. Therefore, a procedure for converting between the virtual tracers and pharmaceutical and phosphorus concentrations is needed.

In the case of pharmaceuticals, the boundary value of the 2nd tracer, which represents all three pharmaceuticals, was held constant at one in the canal and stream. This is a strong simplification because, in reality, the concentrations vary not only between each substance but also from month to month and between canal and stream. However, in view of the lack of data necessary to calculate a time-variable boundary value for each substance, the current simplification is the best possible option. Consequently, the procedure for converting between the 2nd tracer and each pharmaceutical is derived from reference scenario A and the measured in-lake concentrations: (i) from the measured and corresponding target concentrations, we calculate a normative reduction factor f_r for each substance (f_r = annual mean concentration divided by target concentration), and (ii) based on reference scenario A, the reduction factors are used to calculate normative concentrations of the 2nd tracer, which all scenarios are compared with (assessment norm = tracer concentration of scenario A divided by f_r). It is assumed that the conversion procedure derived from scenario A would be the same for each scenario.

In the case of phosphorus, we were able to implement a more precise conversion procedure. From the hydrodynamic model, we derived the annual mean concentration of the 1st tracer in the main basin t_1 in a range between zero and one. Likewise, t_1 is the mean fraction of River Havel water in the main basin; consequently, $1-t_1$ is the mean fraction of water from inflow #2 in the main basin. Accordingly, we are able to calculate the mean phosphorus concentration in the main basin assuming that phosphorus behaves like a conservative tracer: $P_t = t_1 \cdot P_1 + (1-t_1) \cdot P_2$, where P_1 and P_2 are the mean annual phosphorus concentrations in inflows #1 and #2, respectively. Assuming that there are no other sources of phosphorus (i.e., neglecting precipitation and storm water overflows), the ratio between P_t and the real lake-internal phosphorus concentration P_{real} depends only on lake-specific internal processes. We applied the widely used empirical and statistically verified approach from Vollenweider (1976), in which the ratio between the conservative

phosphorus concentration and the real phosphorus concentration at spring overturn is a function of water residence time τ_w: $P_t / P_{real} = 1+\tau_w^{0.5}$, where τ_w is given in years. τ_w varies for each scenario and is calculated from the measured flow rates and hydrodynamic model results: τ_w = volume of main basin (V) divided by sum of mean flow rate of inflow #2 (Q_2) and intrusion flow rate of River Havel (Q_1). Data regarding Q_2 is easily accessible from the measured PEP effluent flow rate, whereas a reliable derivation of Q_1 is hampered by the complex currents at the multi-connection between River Havel and the main basin of Lake Tegel, which causes recirculation and partial by-passing, as investigated in detail in the previous study (Chapter 2). The best way to derive a meaningful value for the water residence time is to again use the simulated concentration of the 1st tracer, which equals the mean fraction of River Havel water in the main basin. Consequently, $Q_1 = Q_2 \cdot t_1 / (1-t_1)$ and $\tau_w = (1-t_1) \cdot V / Q_2$, which results in the conversion equation between the 1st tracer and phosphorus:

$$P_{real} = \frac{t_1 P_1 + (1-t_1) P_2}{1 + \sqrt{\frac{V(1-t_1)}{Q_2} \Big/ 1\ year}} . \tag{4.2}$$

Equation (4.2) cannot be used to calculate intra-annual fluctuations because the Vollenweider approach assumes that the lake-internal processes of phosphorus retention and external phosphorus loading are in static equilibrium. Supplementary, the Vollenweider approach implicate that there is no net phosphorus release from sediment.

4.3 Results

4.3.1 Pollution level

The measured concentrations of the three pharmaceuticals under investigation show similar patterns (Fig. 4.2a-c). The values at inflow #1 are low, near the limit of quantification, whereas at inflow #2, the concentrations are high, up to 1.5 µg L^{-1}. The concentrations of total phosphorus show an inverse pattern (Fig. 4.2d). In the epilimnion of Lake Tegel, the mean values of all three pharmaceuticals are above the proposed environmental quality standards. However, the mean phosphorus concentration of the epilimnion, 43.6 µg L^{-1}, is slightly below the target of 45 µg L^{-1}.

The reduction factor f_r required to lower the epilimnion concentration below the target concentrations is 1.24 for carbamazepine, 2.41 for diclofenac and 3.25 for sulfamethoxazole.

The mean annual phosphorus concentrations in inflows #1 and #2 are $P_1 = 122$ µg L^{-1} and $P_2 = 21$ µg L^{-1}, respectively. These values are used to convert simulated tracer concentrations to phosphorus concentrations as described in Section 4.2.6.

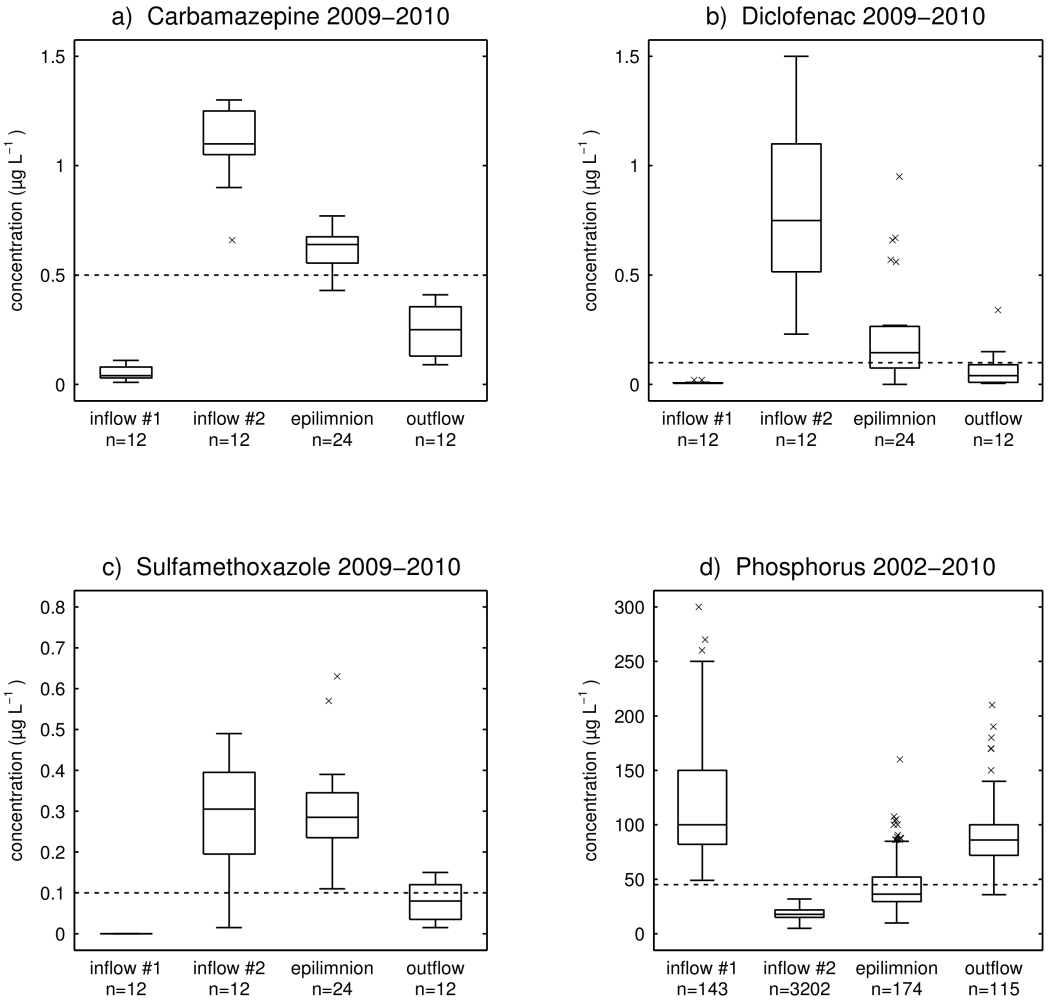

Fig. 4.2 Measured concentrations of pharmaceuticals and total phosphorus in Lake Tegel and in its in- and outflows; n, number of samples; dashed lines indicate target concentrations; outliers (x) are plotted individually

4.3.2 Model validation

The evolution of chloride concentrations in the main basin of Lake Tegel is well reproduced by the hydrodynamic model (Fig. 4.3). The modeling efficiency (indicator of goodness of fit) for the period 1995–2010 is EF = 0.48, which is comparable to that of the empirical box model by Schauser and Chorus (2009), EF = 0.51 for the validation period 1986–1990). For a better comparison, we calculated the EF values of both models for the overlapping period 1995–2002 and obtained values of 0.59 (this study) and 0.63 (Schauser and Chorus, 2009). The slightly higher modeling efficiency of the simpler box model can

be attributed to the fact that the box model was fitted to the chloride data for the period 1991–2002. In turn, our deterministic hydrodynamic model was neither fitted to nor calibrated with any data. The hydrodynamic model calculates the chloride concentration in the main basin from the transient two-dimensional flow field based on bathymetry and boundary conditions (wind forcing, inflow discharge and inflow concentration) only. Generally, a deterministic model able to resolve processes at sub-lake scales is more suitable for prognostic scenarios than a bulk empirical model, which is merely calibrated to the current situation. However, the higher reliability of the deterministic approach is achieved at higher computational costs. The model is still not perfect (EF < 1): the remaining differences between model and data arise mainly from neglecting ice cover in winter, neglecting stratification in summer and insufficiencies of boundary condition data.

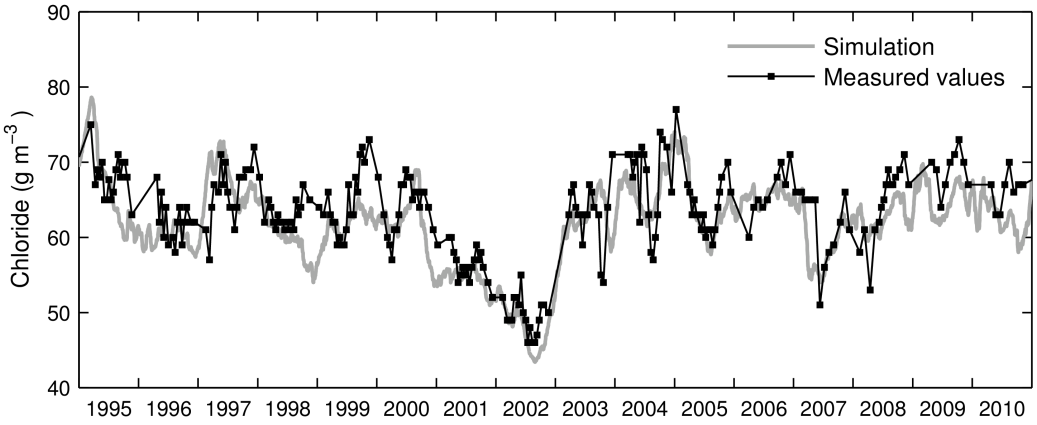

Fig. 4.3 Measured and simulated chloride concentrations in the main basin of Lake Tegel

4.3.3 Real scenarios A–B

Both real scenarios A and B are calculated within one simulation run (Fig. 4.4). The concentration of the 1st tracer in the main basin ranges from 20 to 70% with mean values of 41% for scenario A (2002–2010) and 58% for scenario B (1997–2001). Thus, the fraction of phosphorus-laden River Havel water in the main basin increases substantially if the lake pipeline stops operation, which explains the increasing phosphorus concentrations in the epilimnion of Lake Tegel (up to 200 µg L^{-1}) between 1997 and 2001, c.f. Fig. 4 in (Schauser and Chorus, 2009).

The concentration of the 2nd tracer (pharmaceuticals) differs only slightly between scenario A (42%) and scenario B (41%) (Fig. 4.4b). This contradicts the expectation that both tracers behave symmetrically and that a higher pipeline flow rate would result in the same dilution factor for both tracers. In fact, the tracers are not diluted symmetrically for two

reasons: (i) The pipeline pumping station takes the water not from River Havel before it enters the lake, but from a location near the outflow of Lake Tegel. Therefore, part of the water that is pumped to the PEP is recycled lake water. The recycling rate for the scenario A period can be calculated from the mass flow of the 2nd tracer, and it equals 4% (annual mean; maximum in summer up to 25%). This affects only the pharmaceuticals because phosphorus is reduced in the PEP in either case. (ii) Increased discharge from inflow #2 reduces the river's intrusion between the islands (c.f. Q_1 in Table 4.2), which affects the two tracers in different directions: lower phosphorus concentrations due to lower input from River Havel and higher pharmaceutical concentrations due to lower dilution with river water.

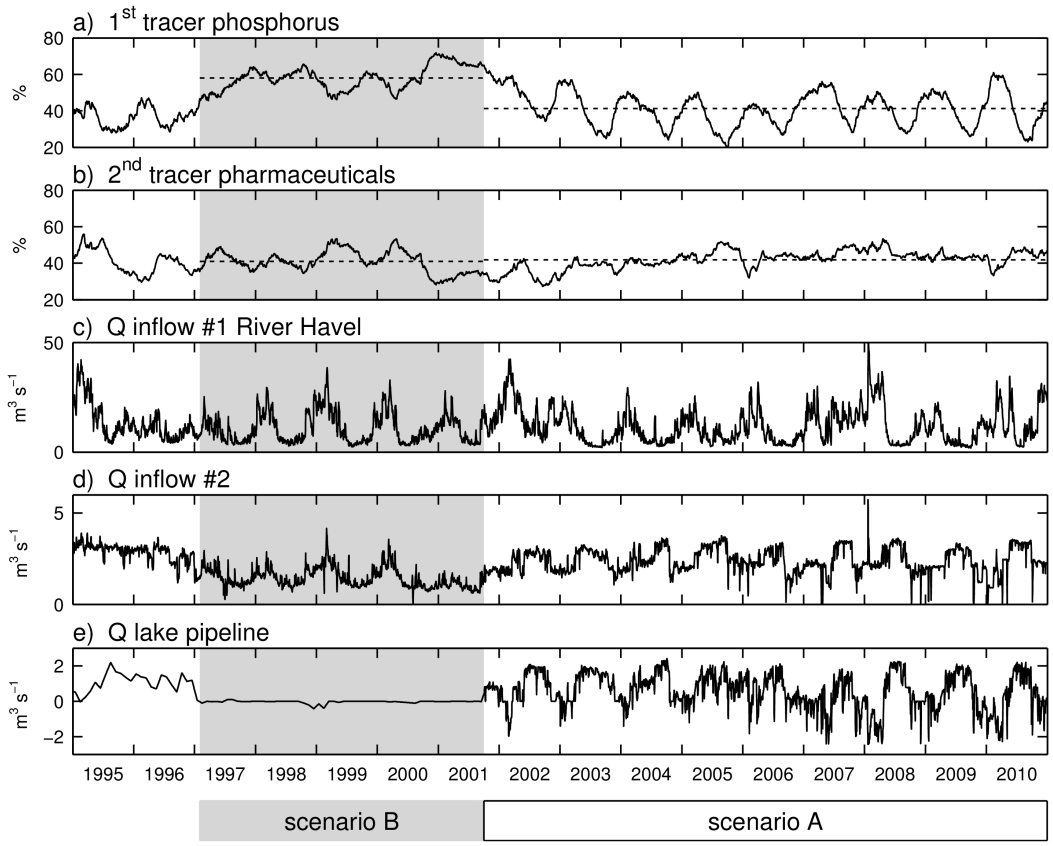

Fig. 4.4 Simulated concentrations of 1st and 2nd virtual tracers in the main basin of Lake Tegel (panel a and b), discharge of both inflows (panel c and d) and discharge of lake pipeline (panel e) used for scenarios A (2002–2010) and B (1997–2001). Dashed lines indicate averaged tracer concentrations.

The seasonal oscillations of the tracer concentrations are mainly caused by the variability of inflow #2 (52%), the wind (37%) and River Havel (8%). The remaining contributions of fluctuations in water level and water extraction rate from waterworks are marginal.

The assessment norms (tracer concentration from scenario A divided by reduction factor f_r), by which all scenarios will be compared, are 34% for carbamazepine, 17% for diclofenac and 13% for sulfamethoxazole. Table 4.2 shows the intermediate data for converting the 1st tracer concentrations into lake-internal phosphorus concentrations (P_{real}) for all six scenarios together with the corresponding measured values (P_{obs}) for both real scenarios.

Table 4.2 Data for conversion procedure between 1st virtual tracer and lake-internal phosphorus concentrations

scenario	t_1	P_t	Q_1	τ_w	P_{real}	P_{obs}
	%	µg L^{-1}	m^3 s^{-1}	days	µg L^{-1}	µg L^{-1}
A	41.3	62.9	1.67	64.6	44.3	43.6
B	58.0	79.7	1.99	76.1	54.7	63.2
C	21.9	43.3	1.12	51.3	31.5	-
D_1	94.9	129	1.42	175	76.5	-
D_2	94.9	117	1.42	175	69.2	-
E	53.9	75.6	1.98	71.0	52.5	-
F	40.5	62.1	1.63	64.8	43.7	-

t_1 mean annual concentration of the 1st virtual tracer in the main basin
P_t phosphorus concentration assuming phosphorus behaves like a conservative tracer (mean inflow concentrations are P_1=122 µg L^{-1}, P_2=21 µg L^{-1}, except scenario D_1: P_2=266 µg L^{-1} untreated spillover water and backmixed bypass water)
Q_1 intrusion flow rate of River Havel
τ_w water residence time
P_{real} lake-internal phosphorus concentration derived from P_t and τ_w with Vollenweider model
P_{obs} observed mean phosphorus concentration in the epilimnion
c.f. Section 4.2.6 for formulas

4.3.4 Hypothetical scenarios C–F

Scenario C provides the lowest phosphorus concentration (Table 4.2, Fig. 4.5) due to maximum pumping rates from River Havel to the PEP. However, the strategy of maximum dilution of inflow #2 with river water is not sufficient to achieve any of the three pharmaceutical assessment norms.

The strategy of exclusively bypassing the pharmaceutical-laden inflow #2 implemented in the D scenarios would suffice to achieve the assessment norms for all three pharmaceuticals, but it would fail to keep phosphorus at safe levels.

Strategies combining dilution with bypassing (scenarios E and F) would suffice to achieve the assessment norm for one pharmaceutical (carbamazepine) but not those for diclofenac

or sulfamethoxazole. Scenario F would also maintain the assessment norm for phosphorus, whereas scenario E would not. Consequently, scenario F is the only scenario that would reduce the content of at least one pharmaceutical to an acceptable level without exacerbating the current phosphorus level.

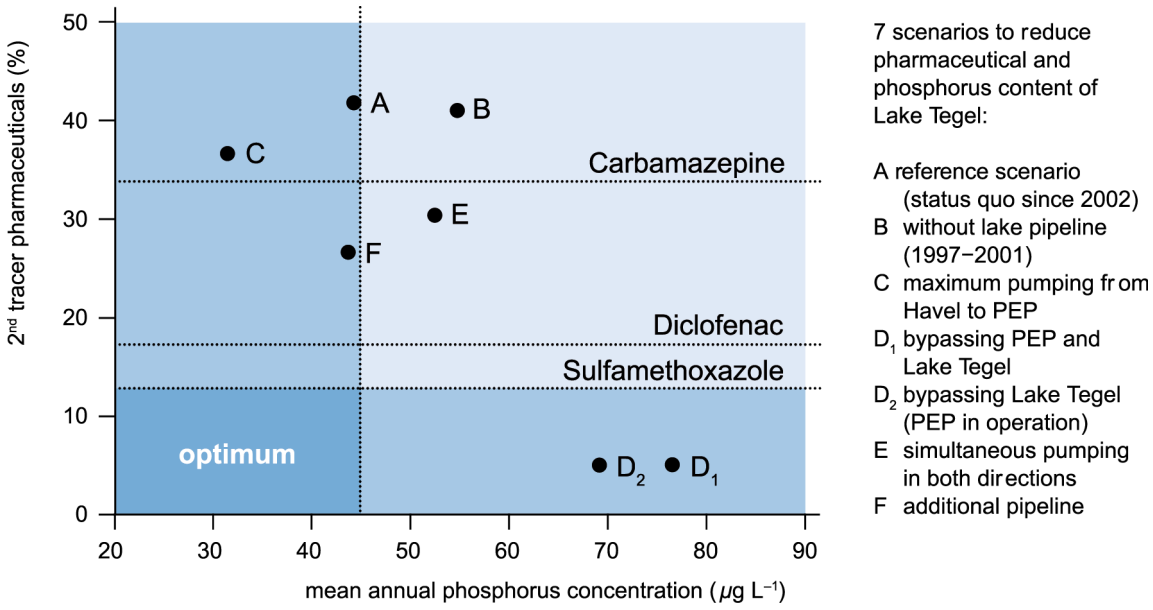

Fig. 4.5 Simulated concentration of phosphorus and 2nd virtual tracer in the main basin of Lake Tegel for all scenarios compared with assessment norms (dashed lines)

4.4 Discussion

4.4.1 Present pollution level

Currently, the water quality of Lake Tegel corresponds to the 'good surface water status' of the EU Water Framework Directive (2000/60/EC). However, the lake will lose this status if the phosphorus concentration increases or if any one of the three proposed pharmaceutical environmental quality standards becomes legally valid.

The fact that the mean pharmaceutical contents in the outflow are below the target concentrations demonstrates that dilution in the less polluted River Havel in principle suffices to achieve the proposed EQS. Nevertheless, in coming decades, the River Havel probably will not achieve 'good surface water status' because of its high phosphorus content.

4.4.2 Scenarios

In none of the investigated scenarios does Lake Tegel reach the assessment norms for all substances. However, the results from scenario D_2 indicate that diverting inflow #2 around

the lake might be a future solution if the phosphorus content of the River Havel were to decrease significantly. Assuming the same hydrological conditions as in scenario D_2, we were able to calculate the phosphorus concentration of River Havel (P_1) required to achieve the target of 45 µg L^{-1} total phosphorus in the main basin of Lake Tegel. We calculated a maximum P_1 values of 79 µg L^{-1} using the Vollenweider approach and 46 µg L^{-1} if phosphorus behaves like a conservative tracer. The second value represents the worst case if the lake does not behave like the Vollenweider model predicts. Linear extrapolation of the currently observed slowly decreasing trend in the mean annual phosphorus concentration of River Havel (−1.79 µg L^{-1} a^{-1}, 1994–2010, t-test $p = 0.036$) indicates that the above values will be reached in 2028 and 2046, respectively.

On the one hand, our model reproduces the hydrological, bathymetric and wind conditions in great detail with high temporal and spatial resolution, as proven by validation with measured chloride data. On the other hand, the concentrations of the target substances (phosphorus and pharmaceuticals) are implemented with very simple constant boundary values as conservative tracers. Nevertheless, the simulated and observed phosphorus values of scenario A are very similar (Table 4.2), which validates our modeling approach. In scenario B, the differences between simulated (54.7 µg L^{-1}) and observed (63.2 µg L^{-1}) phosphorus concentrations are higher. One explanation is that the Vollenweider approach is not valid for scenario B because the lake was not in equilibrium with regard to the phosphorus content in that period. After switching off the lake pipeline in 1997, the epilimnion phosphorus concentration in Lake Tegel increased every year until 2002, when the lake pipeline started operating again. The box model from Schauser and Chorus (2009) was able to reproduce the 1997–2001 re-eutrophication phase. The authors concluded that the phosphorus concentration increased mostly due to lake management measures (no pipeline operation), but it was also enhanced by climatic conditions.

In reality, the concentrations of pharmaceuticals in inflow #2 are not constant; instead, they vary frequently with a pronounced seasonal component that is characteristic of effluent from municipal wastewater treatment plants (Tixier et al., 2003). Some pharmaceuticals (e.g., diclofenac) are known to be degradable by UV light, and others (e.g., carbamazepine) are known to persist in the aquatic environment (Poiger et al., 2001; Tixier et al., 2003; Zhang et al., 2008). Thus, the representation of pharmaceuticals in the model as conservative tracers with steady-state sources is not strictly valid. To some extent, these substance-specific effects are indirectly taken into account in our model by assuming that the ratios between the measured in-lake concentrations of the different pharmaceuticals and the simulated tracer concentration of scenario A will be similar for all other scenarios. The assumption implies a local balance between the advection and degradation in the point measurements of concentrations, which is generally not true. The real concentrations for

degradable pollutants may differ from that achieved with the model. Technically, scenarios can be refined by including degradation in the model that requires, however, more detailed observational information.

4.5 Conclusion

Our calculations indicate that under current conditions, dilution, bypassing or a combination of both operation strategies will not be able to reduce the content of pharmaceuticals in Lake Tegel to an acceptable level without deteriorating the current phosphorus level, which is crucial to preventing renewed eutrophication. Consequently, if pharmaceutical concentrations in Lake Tegel need to be reduced, they must be eliminated from inflow #2 before entering the lake, e.g., by advanced wastewater treatment.

Diverting the pharmaceutical-laden inflow around the lake (as in scenario D_2) is only a potential solution if the mean annual phosphorus concentration of River Havel decreases from its current level of 122 µg L^{-1} to 46–79 µg L^{-1}.

These results can be used to evaluate water management options for improving water quality in Lake Tegel, and they can serve as the basis for future analyses of the benefits of advanced wastewater treatment for pharmaceutical removal, e.g., by LCA.

5 General conclusions and key findings

In the previous three chapters, the main topics of this thesis – hydrodynamics, pharmaceutical micro-pollutants, and management strategies – were discussed. This chapter summarizes the general conclusions and key findings from these discussions, followed by an outlook on future research, management options, and trends.

5.1 Benefits and shortcomings of the two-dimensional modeling approach

The application of a free-surface circulation model on Lake Tegel in two- instead of three-dimensional mode implied neglecting stratification in summer and ice cover in winter. In two-dimensional mode, each grid cell features only vertically integrated values of velocity and tracer concentrations. The 2D-POM model is therefore unable to reproduce vertical gradients of any quantity. Nevertheless, it serves as an adequate tool for representing the intrusion of River Havel and the mixing intensity of both inflows, as validated by vertically integrated measured data (electrical conductivity) and measured data from the epilimnion (chloride concentrations).

In contrast to empirical bulk models, the deterministic circulation model does not require fitting or calibrating with any site-specific data but is exclusively driven by information on transient boundary conditions (wind forcing, inflow discharge and inflow concentration) based on high-resolution bathymetry. This makes the 2D-POM model suitable for reproducing both epignostic (past) and prognostic scenarios. The 2D-POM model is better geared to simulate prognostic scenarios than empirical bulk models, which are calibrated solely to the status quo. It should, however, be noted that the superior reliability of the deterministic approach is achieved at higher computational cost.

5.2 River intrusion and mixing intensity as a result of wind and river discharge

The calculations based on archetypical scenarios indicated that the intrusion of River Havel into Lake Tegel fluctuates with river discharge and wind, both of which can amplify or neutralize the other. The simulated flow fields showed that the intensity of river intrusion depends strongly on wind direction. To quantify and compare the transfer rates of different wind situations, the intrusion flow rate Q_i was used as a rough estimator. However, calculation of currents alone proved insufficient to investigate water exchanges between rivers and lakes, especially when several islands create multiple pathways for river intrusion, as is the case in Lake Tegel. Therefore, simulated mass transport of a virtual tracer, combining the effects of advection, diffusion, and back-mixing on the river-lake exchange, provided an advanced overall estimator of the fraction of intruded river water in Lake Tegel (labeled f_H in Chapter 2 and t_1 in Chapter 4).

5.3 Pharmaceutical micro-pollutants in Lake Tegel

Compared to other surface waters (rivers, lakes, and reservoirs) also used as drinking water resources, Lake Tegel seams to feature the highest ever reported pharmaceutical concentrations worldwide. This was shown to be due to a combination of (i) the discharge of high total loads from WWTP effluent into the lake, (ii) a small lake volume, and (iii) a relatively high water residence time (low flushing).

The pharmaceutical pollution of Lake Tegel was exemplified by three substances, carbamazepine (CBZ), diclofenac (DCF) and sulfamethoxazole (SMX), whose concentration levels exceed proposed environmental quality standards (EQS). Spatial distribution, elimination rates, and seasonal patterns were discussed in detail. Further information on other micro-pollutants in Lake Tegel is provided in Appendix IV.

DCF showed the strongest elimination of all three pharmaceuticals and revealed significant seasonality with 50% elimination in winter and more than 95% in summer. Elimination of CBZ was 40%, while SMX did not degrade at determinable rates. In the case of DCF and CBZ, the observed elimination rates agreed well with results from other field and laboratory studies. By contrast, the missing elimination of SMX in Lake Tegel remains unsolved (Section 3.4.3).

The spatial distribution of CBZ and SMX in the lake was shown to be primarily affected by dilution with less contaminated water from River Havel (through river intrusion and operation of the lake pipeline) rather than by degradation within the lake. By contrast, concentrations of DCL are affected by both dilution and photodegradation, causing seasonal and spatial variation of DCL in the lake water.

5.4 Management strategies

This thesis examined two fundamentally simple management strategies for Lake Tegel: dilution and bypassing. However, considering the specific circumstances – challenging river-lake interactions, limited operational capacities, high current nutrient levels – and taking into account competing objectives such as the prevention of renewed eutrophication of the lake, the management task was found to be extremely complex.

Seven different management scenarios were tested to answer the question of whether the existing lake pipeline could be used to reduce the amount of pharmaceuticals in Lake Tegel without deteriorating the current phosphorus level. No scenario provided a strategy optimal for both pharmaceuticals and phosphorus. Diverting the pharmaceutical-laden inflow around the lake through the existing pipeline was shown to only be a potential solution if

the mean annual phosphorus concentration of River Havel decreases from its current level of 122 µg L^{-1} to 46–79 µg L^{-1} (Section 4.4.2).

Consequently, it was found that for the existing pipeline to be effectively used to reduce pharmaceutical concentrations in Lake Tegel, additional efforts need to be made, such as supplementary pharmaceutical treatment of the inflow originating from the WWTP prior to entering the lake, or phosphorus reduction in the River Havel catchment.

5.5 Outlook

This thesis leaves many open questions for further research, such as the findings on SMX elimination which deviate from previous studies, the fate of other micro-pollutants found in Lake Tegel (Appendix IV), or the interannual variability of pharmaceutical concentrations, especially in the hypolimnion. Against this background, one possible future task is the implementation of stratification and ice cover into the hydrodynamic model, supplemented by reactive mass transport of micro-pollutants and phosphorus – a very interesting challenge from a scientific point of view, even if the outcome is unlikely to significantly change the resulting management options.

The existing river-lake-PEP-pipeline system was shown to be ill-suited to meet the two competing objectives of preventing renewed eutrophication while at the same time reducing the current level of pharmaceutical micro-pollutants. Potential solutions must therefore be found externally or through expansion of the present system. Either practice will necessitate a modeling tool suitable for scenario prediction regarding an expanded surface water system, e.g. through inclusion of Stream Panke, and additional water treatment for the removal of organic micro-pollutants, e.g. through ozonation or activated carbon. Such modeling tool will need to be simplified for easy use without neglecting any relevant processes – a very interesting challenge from an engineering point of view.

Two observable trends are bound to change the future management of Lake Tegel: (i) The phosphorus load of River Havel is slowly decreasing (Section 4.4.2) while (ii) the loads of pharmaceutical micro-pollutants entering Lake Tegel are increasing. This second trend is caused by the rising usage of pharmaceuticals with potential environmental relevance – note the 20% increase between 2002 and 2012 (Ebert et al., 2014) – and is likely to be further amplified by the planned enlargement of the upstream WWTP, currently still at conception stage.

References

Alavian, V., Jirka, G.H., Denton, R.A., Johnson, M.C., Stefan, H.G., 1992. Density Currents Entering Lakes and Reservoirs. Journal of Hydraulic Engineering-Asce 118(11), 1464-1489

Andreozzi, R., Raffaele, M., Nicklas, P., 2003. Pharmaceuticals in STP effluents and their solar photodegradation in aquatic environment. Chemosphere 50(10), 1319-1330

Bartels, P. and von Tumpling, W., 2007. Solar radiation influence on the decomposition process of diclofenac in surface waters. Science of the Total Environment 374(1), 143-155

Benotti, M.J. and Brownawell, B.J., 2007. Distributions of pharmaceuticals in an urban estuary during both dry-and wet-weather conditions. Environmental Science & Technology 41(16), 5795-5802

Benotti, M.J., Trenholm, R.A., Vanderford, B.J., Holady, J.C., Stanford, B.D., Snyder, S.A., 2009. Pharmaceuticals and endocrine disrupting compounds in US drinking water. Environmental Science & Technology 43(3), 597-603

Blair, B.D., Crago, J.P., Hedman, C.J., Klaper, R.D., 2013. Pharmaceuticals and personal care products found in the Great Lakes above concentrations of environmental concern. Chemosphere 93(9), 2116-2123

Blumberg, A.F. and Mellor, G.L., 1987. A description of a three-dimensional coastal ocean circulation model. In: Heaps, N.S. (ed) Three-Dimensional Coastal Ocean Models. American Geophysical Union, Washington, DC, pp 1-16

Boehrer, B. and Schultze, M., 2008. Stratification of lakes. Reviews of Geophysics 46, RG2005

Bonvin, F., Omlin, J., Rutler, R., Schweizer, W.B., Alaimo, P.J., Strathmann, T.J., McNeill, K., Kohn, T., 2013. Direct photolysis of human metabolites of the antibiotic sulfamethoxazole: evidence for abiotic back-transformation. Environmental Science & Technology 47(13), 6746-6755

Bonvin, F., Rutler, R., Chèvre, N., Halder, J., Kohn, T., 2011. Spatial and temporal presence of a wastewater-derived micropollutant plume in Lake Geneva. Environmental Science & Technology 45(11), 4702-4709

Bührer, H. and Ambühl, H., 1975. Die Einleitung von gereinigtem Abwasser in Seen. Schweiz.Z.Hydrol. 37(2), 347-368

Buser, H.R., Poiger, T., Muller, M.D., 1998. Occurrence and fate of the pharmaceutical drug diclofenac in surface waters: Rapid photodegradation in a lake. Environmental Science & Technology 32(22), 3449-3456

Carlson, R.E., 1977. Trophic State Index for Lakes. Limnology and Oceanography 22(2), 361-369

Carmack, E.C., Gray, C.B.J., Pharo, C.H., Daley, R.J., 1979. Importance of Lake-River Interaction on Seasonal Patterns in the General-Circulation of Kamloops Lake, British-Columbia. Limnology and Oceanography 24(4), 634-644

Carmack, E.C., Wiegand, R.C., Daley, R.J., Gray, C.B.J., Jasper, S., Pharo, C.H., 1986. Mechanisms Influencing the Circulation and Distribution of Water Mass in A Medium Residence-Time Lake. Limnology and Oceanography 31(2), 249-265

Chorus, I. and Schauser, I. Oligotrophication of Lake Tegel and Schlachtensee, Berlin: Analysis of system components, causalities and response thresholds compared to responses of other waterbodies. 2011 Federal Environment Agency (Umweltbundesamt). http://www.umweltbundesamt.de/uba-info-medien/4144.html

Chu, P.C. and Fan, C.W., 1997. Sixth-order difference scheme for sigma coordinate ocean models. Journal of Physical Oceanography 27(9), 2064-2071

Corcoran, J., Winter, M.J., Tyler, C.R., 2010. Pharmaceuticals in the aquatic environment: A critical review of the evidence for health effects in fish. Critical Reviews in Toxicology 40(4), 287-304

Dijkstra, E.W., 1959. A Note on Two Problems in Connexion with Graphs. Numerische Mathematik 1, 269-271

DIN 38407-35 German standard methods for the examination of water, waste water and sludge - Jointly determinable substances (group F) - Part 35: Determination of selected phenoxyalkyl carbonic acids and further acid plant treatment agents - Method using high performance liquid chromatography and mass spectrometric detection (HPLC-MS/MS) (F 35).

DVWK. Ermittlung der Verdunstung von Land- uns Wasserflächen. 1996 Bonn, Deutscher Verband für Wasserwirtschaft und Kulturbau e.V. (DVWK). Mekblatt Nr. 238

Ebert, I., Conradi, S., Hein, A., Amato, R. Arzneimittel in der Umwelt - vermeiden, reduzieren, überwachen. 2014 Federal Environment Agency (Umweltbundesamt), Fachgebiet IV 2.2 Arzneimittel, Wasch- und Reinigungsmittel. http://www.umweltbundesamt.de/publikationen/arzneimittel-in-der-umwelt-vermeiden-reduzieren

EMEA. Guideline on the environmental risk assessment of medicinal products for human use. Doc. Ref. EMEA/CHMP/SWP/4447/00 2006 European Agency for the Evaluation of Medicinal Products. London.

Englert, J.P. and Stewart, K.M., 1983. Natural Short-Circuiting of Inflow to Outflow Through Silver Lake, New-York. Water Resources Research 19(2), 529-537

EP. Position of the European Parliament adopted at first reading on 22 May 2007 with a view to the adoption of Directive 2007/.../EC of the European Parliament and of the Council on environmental quality standards in the field of water policy and amending Directive 2000/60/EC (EP-PE_TC1-COD(2006)0129). 22-5-2007

EP. Proposal for a directive of the European Parliament and of the Council on environmental quality standards in the field of water policy and amending Directive 2000/60/EC, recommendation for second reading, (C6 0055/2008 2006/0129(COD)). 20-5-2008

Ezer, T., Arango, H., Shchepetkin, A.F., 2002. Developments in terrain-following ocean models: intercomparisons of numerical aspects. Ocean Modelling 4(3-4), 249-267

Ferguson, P.J., Bernot, M.J., Doll, J.C., Lauer, T.E., 2013. Detection of pharmaceuticals and personal care products (PPCPs) in near-shore habitats of southern Lake Michigan. Science of the Total Environment 458-460(0), 187-196

Franke, P. Wasseraustausch zwischen Oberhavel und Tegeler See. 1998 Hydro-Consult GmbH im Auftrag der Berliner Wasser Betriebe. Abschlussbericht

Gross, E.S., Koseff, J.R., Monismith, S.G., 1999. Three-dimensional salinity simulations of south San Francisco Bay. Journal of Hydraulic Engineering-Asce 125(11), 1199-1209

Heberer, T., 2002. Tracking persistent pharmaceutical residues from municipal sewage to drinking water. Journal of Hydrology 266(3), 175-189

Heinzmann, B. and Chorus, I., 1994. Restoration Concept for Lake Tegel, A Major Drinking and Bathing Water-Resource in A Densely Populated Area. Environmental Science & Technology 28(8), 1410-1416

Heinzmann, B., Sarfert, F., Stengel, A., 1991. Die Phosphateliminationsanlage Tegel in Berlin. gwf Wasser/Abwasser 132(12), 674-685

Hodges, B.R., Imberger, J., Saggio, A., Winters, K.B., 2000. Modeling basin-scale internal waves in a stratified lake. Limnology and Oceanography 45(7), 1603-1620

Hoerger, C.C., Akhtman, Y., Martelletti, L., Rutler, R., Bonvin, F., Grange, A., Arey, J.S., Kohn, T., 2014. Spatial extent and ecotoxicological risk assessment of a micropollutant-contaminated wastewater plume in Lake Geneva. Aquatic Sciences 76(1), 7-19

Huang, Q., Yu, Y., Tang, C., Zhang, K., Cui, J., Peng, X., 2011. Occurrence and behavior of non-steroidal anti-inflammatory drugs and lipid regulators in wastewater and urban river water of the Pearl River Delta, South China. Journal of Environmental Monitoring 13(4), 855-863

Imberger, J. and Hamblin, P.F., 1982. Dynamics of Lakes, Reservoirs, and Cooling Ponds. Annual Review of Fluid Mechanics 14, 153-187

Jacob, D. and Gerstengarbe, F.-W., 2005. Klimaszenarien für den deutschen Teil des Elbe-Einzugsgebietes. In: Wechsung, F., Becker, A., Gräfe, P. (eds) Auswirkungen des globalen Wandels auf Wasser, Umwelt und Gesellschaft im Elbegebiet. Weissenseeverlag, Berlin, pp 85-118

Jekel, M., Dott, W., Bergmann, A., Dünnbier, U., Gnirss, R., Haist-Gulde, B., Hamscher, G., Letzel, M., Licha, T. et al, 2015. Selection of organic process and source indicator substances for the anthropogenically influenced water cycle. Chemosphere 125, 155-167

Jekel, M., Ruhl, A.S., Meinel, F., Zietzschmann, F., Lima, S.P., Baur, N., Wenzel, M., Gnirss, R., Sperlich, A. et al, 2013. Anthropogenic organic micro-pollutants and pathogens in the urban water cycle: assessment, barriers and risk communication (ASKURIS). Environmental Sciences Europe 25(1), 1-8

Jones, O.A.H., Voulvoulis, N., Lester, J.N., 2001. Human Pharmaceuticals in the Aquatic Environment a Review. Environmental Technology 22(12), 1383-1394

Kern, K., 2011. Pharmaceuticals in the Water Cycle - Mechanisms for the Regulation of Environmentally Harmful Pharmaceutical Substances. Journal for European Environmental & Planning Law 8(1), 3-22

Kleywegt, S., Pileggi, V., Yang, P., Hao, C., Zhao, X., Rocks, C., Thach, S., Cheung, P., Whitehead, B., 2011. Pharmaceuticals, hormones and bisphenol A in untreated

source and finished drinking water in Ontario, Canada — Occurrence and treatment efficiency. Science of the Total Environment 409(8), 1481-1488

Kümmerer, K., 2009. The presence of pharmaceuticals in the environment due to human use - present knowledge and future challenges. Journal of Environmental Management 90(8), 2354-2366

Kunkel, U. and Radke, M., 2012. Fate of pharmaceuticals in rivers: Deriving a benchmark dataset at favorable attenuation conditions. Water Research 46(17), 5551-5565

Laborde, S., Antenucci, J.P., Copetti, D., Imberger, J., 2010. Inflow intrusions at multiple scales in a large temperate lake. Limnology and Oceanography 55(3), 1301-1312

Lam, M.W. and Mabury, S.A., 2005. Photodegradation of the pharmaceuticals atorvastatin, carbamazepine, levofloxacin, and sulfamethoxazole in natural waters. Aquatic Sciences 67(2), 177-188

Lam, M.W., Young, C.J., Brain, R.A., Johnson, D.J., Hanson, M.A., Wilson, C.J., Richards, S.M., Solomon, K.R., Mabury, S.A., 2004. Aquatic persistence of eight pharmaceuticals in a microcosm study. Environmental Toxicology and Chemistry 23(6), 1431-1440

LAWA, 1998. Gewässerbewertung stehender Gewässer. Kulturbuch-Verlag, Berlin. ISBN 3-88961-225-3

Lewandowski, J., Putschew, A., Schwesig, D., Neumann, C., Radke, M., 2011. Fate of organic micropollutants in the hyporheic zone of a eutrophic lowland stream: Results of a preliminary field study. Science of the Total Environment 409(10), 1824-1835

Lin, A.Y.-C., Plumlee, M.H., Reinhard, M., 2006. Natural attenuation of pharmaceuticals and alkylphenol polyethoxylate metabolites during river transport: photochemical and biological transformation. Environmental Toxicology and Chemistry 25(6), 1458-1464

Lindenschmidt, K.-E. and Fröhlich, M., 2000. Modelling the reciprocal water exchange between a river and a lake using a 2-D finite volume k-epsilon turbulence computer model. Lakes and Reservoirs: Research and Management 5(3), 137-143

Loague, K. and Green, R.E., 1991. Statistical and graphical methods for evaluating solute transport models: Overview and application. Journal of Contaminant Hydrology 7(1), 51-73

Löffler, D., Rombke, J., Meller, M., Ternes, T.A., 2005. Environmental fate of pharmaceuticals in water/sediment systems. Environmental Science & Technology 39(14), 5209-5218

Marsden, M.W., 1989. Lake restoration by reducing external phosphorus loading: the influence of sediment phosphorus release. Freshwater Biology 21(2), 139-162

Mayer, D.G. and Butler, D.G., 1993. Statistical Validation. Ecological Modelling 68(1-2), 21-32

Miehe, U., 2010 Wirksamkeit technischer Barrieren zur Entfernung von anthropogenen Spurenstoffen - Kläranlagen und Raumfilter. Dissertation, Technische Universität Berlin http://nbn-resolving.de/urn:nbn:de:kobv:83-opus-27775

Möller, K. and Burgschweiger, J. Wasserversorgungskonzept für Berlin und für das von den BWB versorgte Umland (Entwicklung bis 2040). 2008 Berliner Wasserbetriebe.

Morasch, B., Bonvin, F., Reiser, H., Grandjean, D., De Alencastro, L.F., Perazzolo, C., Chèvre, N., Kohn, T., 2010. Occurrence and fate of micropollutants in the Vidy Bay of Lake Geneva, Switzerland. Part II: Micropollutant removal between wastewater and raw drinking water. Environmental Toxicology and Chemistry 29(8), 1658-1668

Morillo, S., Imberger, J., Antenucci, J.P., Copetti, D., 2009. Using Impellers to Distribute Local Nutrient Loadings in a Stratified Lake: Lake Como, Italy. Journal of Hydraulic Engineering-Asce 135(7), 564-574

Morillo, S., Imberger, J., Antenucci, J.P., Woods, P.F., 2008. Influence of Wind and Lake Morphometry on the Interaction between Two Rivers Entering a Stratified Lake. Journal of Hydraulic Engineering-Asce 134(11), 1579-1589

Moschet, C., Götz, C., Longree, P., Hollender, J., Singer, H., 2013. Multi-level approach for the integrated assessment of polar organic micropollutants in an international lake catchment: The example of Lake Constance. Environmental Science & Technology 47(13), 7028-7036

Nikuradse, J., 1933. Strömungsgesetze in rauhen Rohren. VDI-Forschungsheft 361

Nützmann, G., Wiegand, C., Contardo-Jara, V., Hamann, E., Burmester, V., Gerstenberg, K., 2011. Contamination of Urban Surface and Ground Water Resources and Impact on Aquatic Species. In: Endlicher, W. (ed) Perspectives in Urban Ecology. Springer, Berlin Heidelberg, pp 43-88

OgewV , 20-7-2011. Verordnung zum Schutz der Oberflächengewässer vom 20. Juli 2011.Bundesgesetzblatt Jahrgang 2011 Teil I Nr. 37, 1429-1469.

Okely, P., Imberger, J., Antenucci, J.P., 2010. Processes affecting horizontal mixing and dispersion in Winam Gulf, Lake Victoria. Limnology and Oceanography 55(5), 1865-1880

Oosterhuis, M., Sacher, F., ter Laak, T.L., 2013. Prediction of concentration levels of metformin and other high consumption pharmaceuticals in wastewater and regional surface water based on sales data. Science of the Total Environment 442(0), 380-388

Ort, C., Hollender, J., Schaerer, M., Siegrist, H., 2009. Model-Based Evaluation of Reduction Strategies for Micropollutants from Wastewater Treatment Plants in Complex River Networks. Environmental Science & Technology 43(9), 3214-3220

Ottesen Hansen, N.-E., 1978. Effects of boundary layers on mixing in small lakes. In: Graf, W.H. and Mortimer, C.H. (eds) Hydrodynamics of lakes. Elsevier Scientific Publishing Company, Amsterdam, Netherlands, pp 341-356

Packer, J.L., Werner, J.J., Latch, D.E., McNeill, K., Arnold, W.A., 2003. Photochemical fate of pharmaceuticals in the environment: Naproxen, diclofenac, clofibric acid, and ibuprofen. Aquatic Sciences 65(4), 342-351

Park, M., Reckhow, D., Lavine, M., Rosenfeldt, E., Stanford, B., Park, M.H., 2014. Multivariate Analyses for Monitoring EDCs and PPCPs in a Lake Water. Water Environment Research 86(11), 2233-2241

Poiger, T., Buser, H.R., Muller, M.D., 2001. Photodegradation of the pharmaceutical drug diclofenac in a lake: Pathway, field measurements, and mathematical modeling. Environmental Toxicology and Chemistry 20(2), 256-263

Radke, M., Ulrich, H., Wurm, C., Kunkel, U., 2010. Dynamics and attenuation of acidic pharmaceuticals along a river stretch. Environmental Science & Technology 44(8), 2968-2974

Reemtsma, T., Miehe, U., Dünnbier, U., Jekel, M., 2010. Polar pollutants in municipal wastewater and the water cycle: Occurrence and removal of benzotriazoles. Water Research 44(2), 596-604

Richter, D., Dünnbier, U., Massmann, G., Pekdeger, A., 2007. Quantitative determination of three sulfonamides in environmental water samples using liquid chromatography coupled to electrospray tandem mass spectrometry. Journal of Chromatography A 1157(1-2), 115-121

Ripl, W., Heller, S., Koppelmeyer, B., Markwitz, M., Wolter, K.-D. Limnologische Begleitstudie zur Entlastung des Tegeler Sees. 1993 Institut für Ökologie der TU-Berlin. Endbericht

Roig, B., 2010. Pharmaceuticals in the environment: current knowledge and need assessment to reduce presence and impact. IWA publishing. ISBN 184339314X

Rueda, F.J. and Schladow, S.G., 2003. Dynamics of large polymictic lake. II Numerical simulations. Journal of Hydraulic Engineering-Asce 129(2), 92-101

Rueda, F.J., Schladow, S.G., Monismith, S.G., Stacey, M.T., 2005. On the effects of topography on wind and the generation of currents in a large multi-basin lake. Hydrobiologia 532, 139-151

Rueda, F.J. and MacIntyre, S., 2010. Modelling the fate and transport of negatively buoyant storm–river water in small multi-basin lakes. Environmental Modelling & Software 25(1), 146-157

Schauser, I. and Chorus, I., 2009. Water and phosphorus mass balance of Lake Tegel and Schlachtensee - A modelling approach. Water Research 43(6), 1788-1800

Schwarzenbach, R.P., Escher, B.I., Fenner, K., Hofstetter, T.B., Johnson, C.A., von Gunten, U., Wehrli, B., 2006. The challenge of micropollutants in aquatic systems. Science 313(5790), 1072-1077

Shchepetkin, A.F. and McWilliams, J.C., 2003. A method for computing horizontal pressure-gradient force in an oceanic model with a nonaligned vertical coordinate. Journal of Geophysical Research-Oceans 108(C3), 3090

Smagorinsky, J., 1963. General circulation experiments with the primitive equations: I. The basic experiment. Monthly Weather Review 91, 99-164

Smolarkiewicz, P.K., 1984. A Fully Multidimensional Positive Definite Advection Transport Algorithm with Small Implicit Diffusion. Journal of Computational Physics 54(2), 325-362

Snyder, S. and Benotti, M., 2010. Endocrine disruptors and pharmaceuticals: implications for water sustainability. Water Science and Technology 61(1), 145-154

Stevens, C.L., Hamblin, P.F., Lawrence, G.A., Boyce, F.M., 1995. River-Induced Transport in Kootenay Lake. Journal of Environmental Engineering-Asce 121(11), 830-837

Tang, J., Shi, T., Wu, X., Cao, H., Li, X., Hua, R., Tang, F., Yue, Y., 2015. The occurrence and distribution of antibiotics in Lake Chaohu, China: Seasonal variation, potential source and risk assessment. Chemosphere 122(0), 154-161

Tchobanoglous, G., Burton, F.L., Stensel, H.D., 2003. Wastewater engineering : treatment and reuse / Metcalf & Eddy, Inc. McGraw-Hill, Boston. ISBN 0-07-041878-0

ter Laak, T.L., van der Aa, M., Houtman, C.J., Stoks, P.G., van Wezel, A.P., 2010. Relating environmental concentrations of pharmaceuticals to consumption: A mass balance approach for the river Rhine. Environment International 36, 403-409

Tixier, C., Singer, H.P., Oellers, S., Muller, S.R., 2003. Occurrence and fate of carbamazepine, clofibric acid, diclofenac, ibuprofen, ketoprofen, and naproxen in surface waters. Environmental Science & Technology 37(6), 1061-1068

van Ulden, A.P. and van Oldenborgh, G.J., 2006. Large-scale atmospheric circulation biases and changes in global climate model simulations and their importance for climate change in Central Europe. Atmospheric Chemistry and Physics 6, 863-881

Vieno, N. and Sillanpää, M., 2014. Fate of diclofenac in municipal wastewater treatment plant — A review. Environment International 69(0), 28-39

Vincent, W.F., Gibbs, M.M., Spigel, R.H., 1991. Eutrophication Processes Regulated by A Plunging River Inflow. Hydrobiologia 226(1), 51-63

Vollenweider, R.A., 1976. Advances in defining critical loading levels for phosphorus in lake eutrophication. Memorie dell' Istituto Italiano di Idrobiologia 33, 53-84

Wenzel, H., Larsen, H.F., Clauson-Kaas, J., Hoibye, L., Jacobsen, B.N., 2008. Weighing environmental advantages and disadvantages of advanced wastewater treatment of micro-pollutants using environmental life cycle assessment. Water Science and Technology 57(1), 27-32

Wiese, B., 2007 Spatially and temporally scaled inverse hydraulic modelling, multi tracer transport modelling and interaction with geochemical processes at a highly transient bank filtration site. Dissertation, Humboldt-Universität zu Berlin http://nbn-resolving.de/urn:nbn:de:kobv:11-10077396

Wiese, B. and Nützmann, G., 2009. Transient Leakance and Infiltration Characteristics during Lake Bank Filtration. Ground Water 47(1), 57-68

Zhang, Y., Geißen, S.-U., Cal, C., 2008. Carbamazepine and diclofenac: Removal in wastewater treatment plants and occurrence in water bodies. Chemosphere 73(8), 1151-1161

Ziegler, D.H., 2001 Untersuchungen zur nachhaltigen Wirkung der Uferfiltration im Wasserkreislauf Berlins. Dissertation, Technische Universität Berlin http://nbn-resolving.de/urn:nbn:de:kobv:83-opus-3218

Zühlke, S., Dünnbier, U., Heberer, T., 2004. Determination of polar drug residues in sewage and surface water applying liquid chromatography-tandem mass spectrometry. Analytical Chemistry 76(22), 6548-6554

List of figures

List of tables

Appendices

I. Application of the Princeton Ocean Model (POM) on Lake Tegel

Bathymetry data was provided by Senatsverwaltung für Stadtentwicklung Berlin.

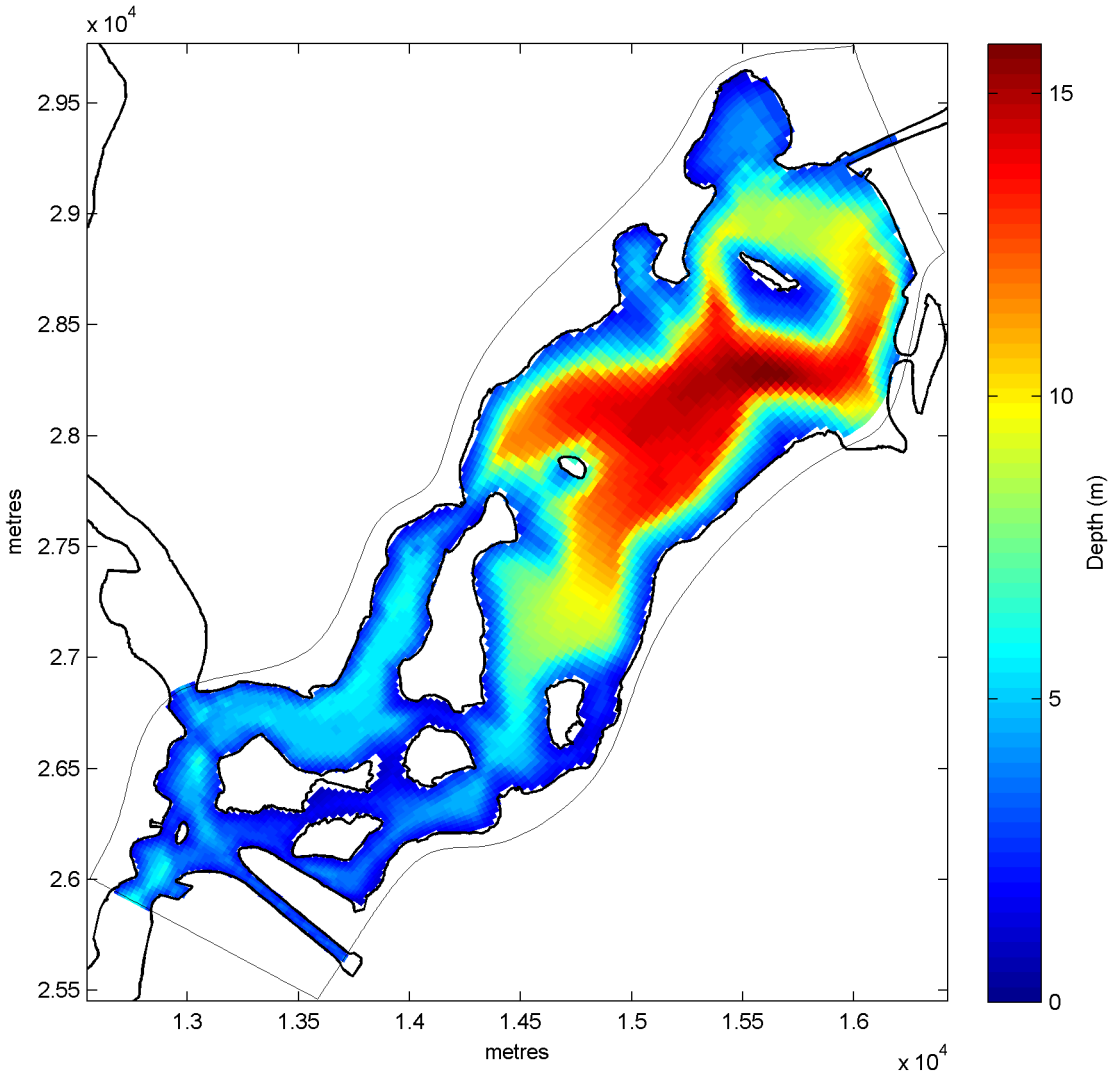

Fig. A 1 Horizontal curvilinear grid (200x60); color represents water depth of each grid cell; model boundaries (thin line); shore (bold line)

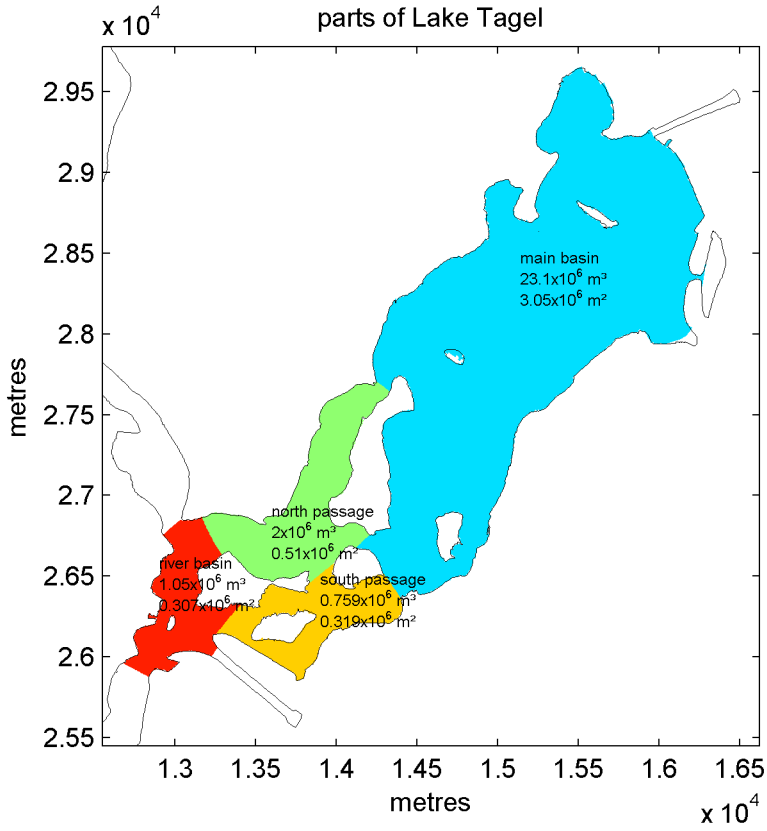

Fig. A 2 Volume and surface area of different parts of Lake Tegel

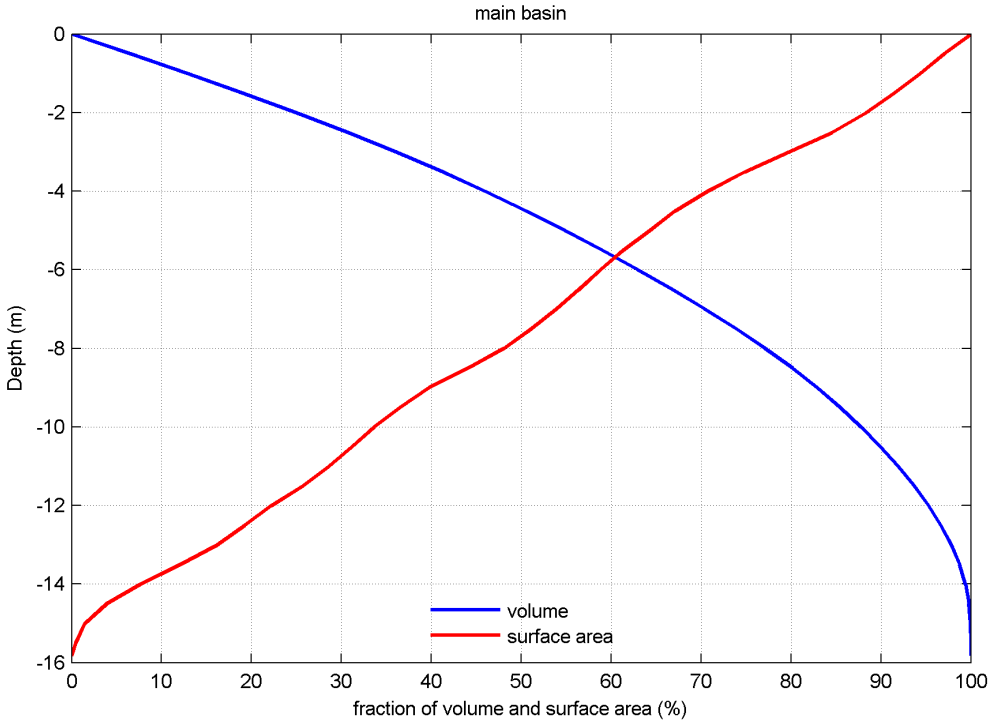

Fig. A 3 Hypsographic diagram of the main basin of Lake Tegel

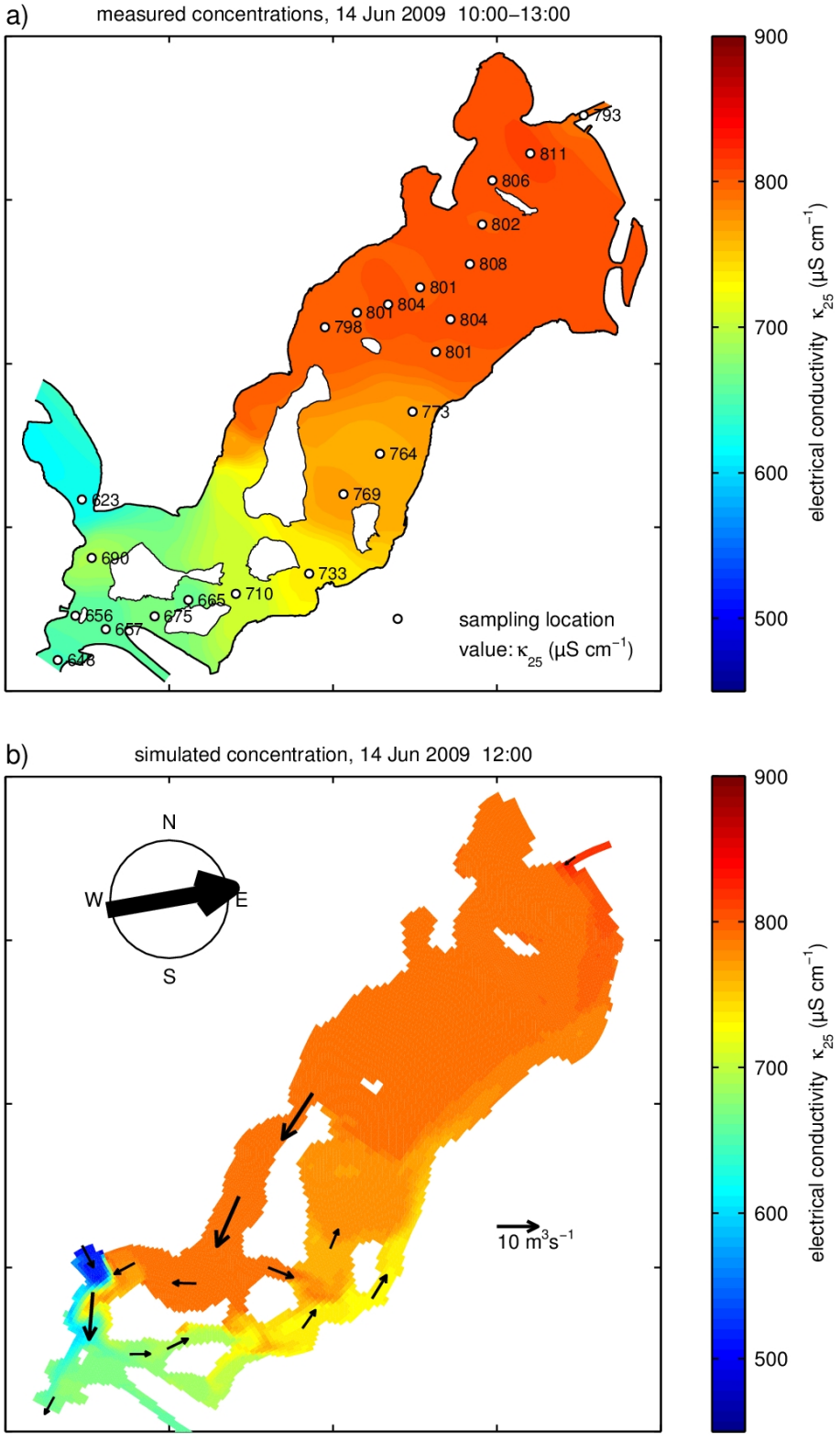

Fig. A 4 Measured a) and simulated b) electrical conductivity on 14 Jun 2009; the colored contour plot in panel a) is spatial interpolated from vertically integrated measured values (white circles) with a combination of Dijkstra's path-finding algorithm and inverse distance weighting

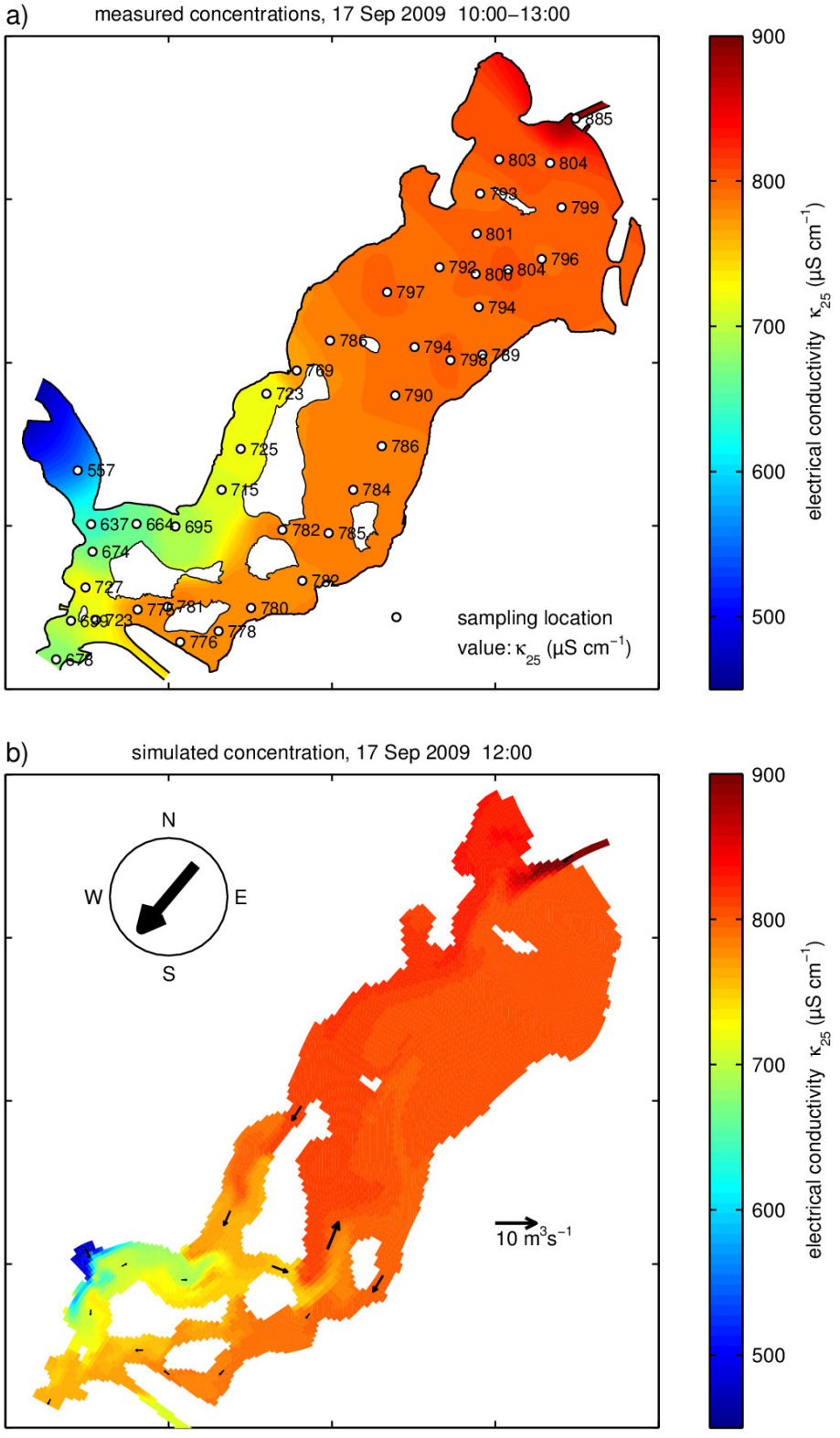

Fig. A 5 Measured a) and simulated b) electrical conductivity on 17 Sep 2009; the colored contour plot in panel a) is spatial interpolated from vertically integrated measured values (white circles) with a combination of Dijkstra's path-finding algorithm and inverse distance weighting

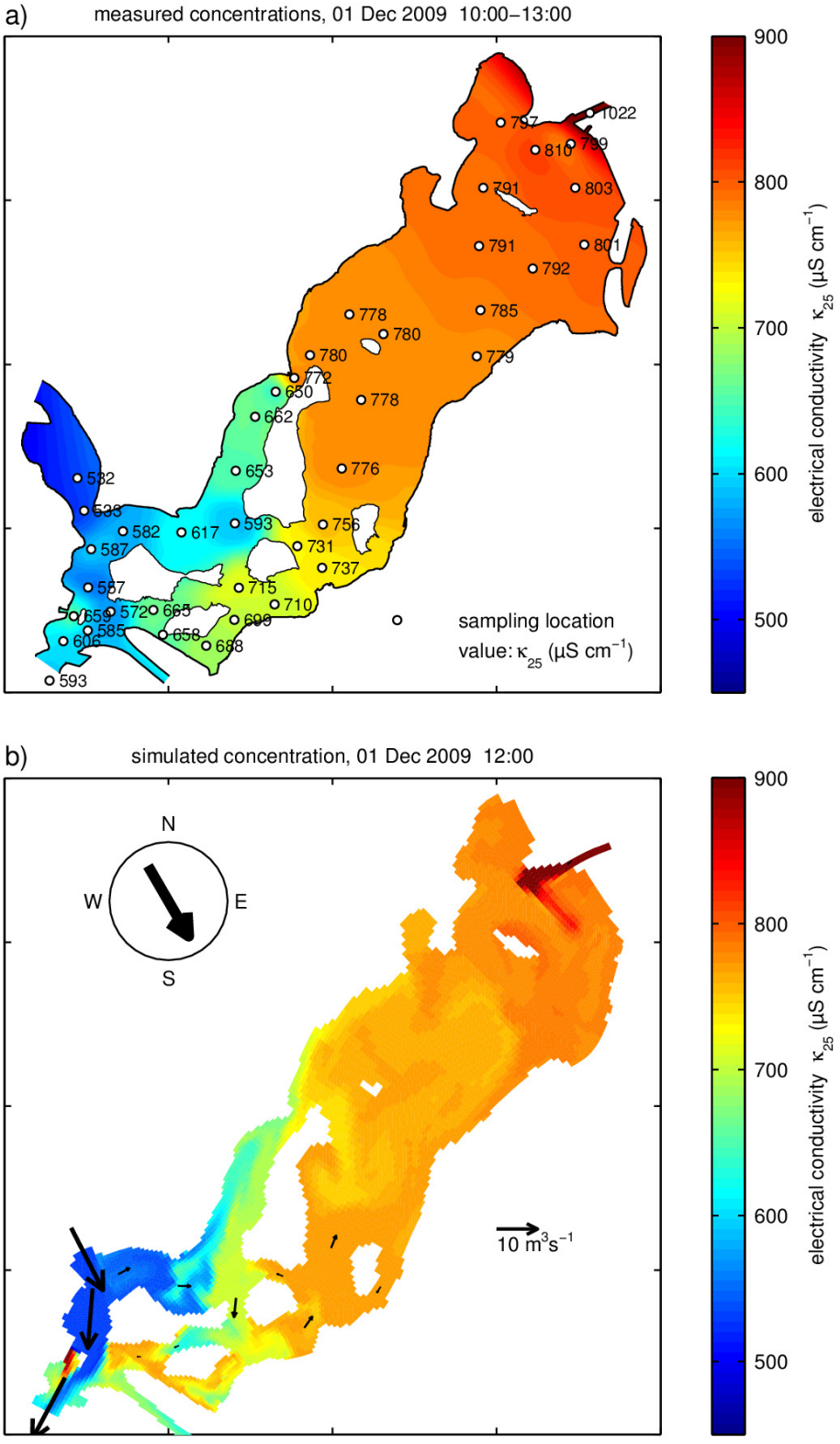

Fig. A 6 Measured a) and simulated b) electrical conductivity on 01 Dec 2009; the colored contour plot in panel a) is spatial interpolated from vertically integrated measured values (white circles) with a combination of Dijkstra's path-finding algorithm and inverse distance weighting

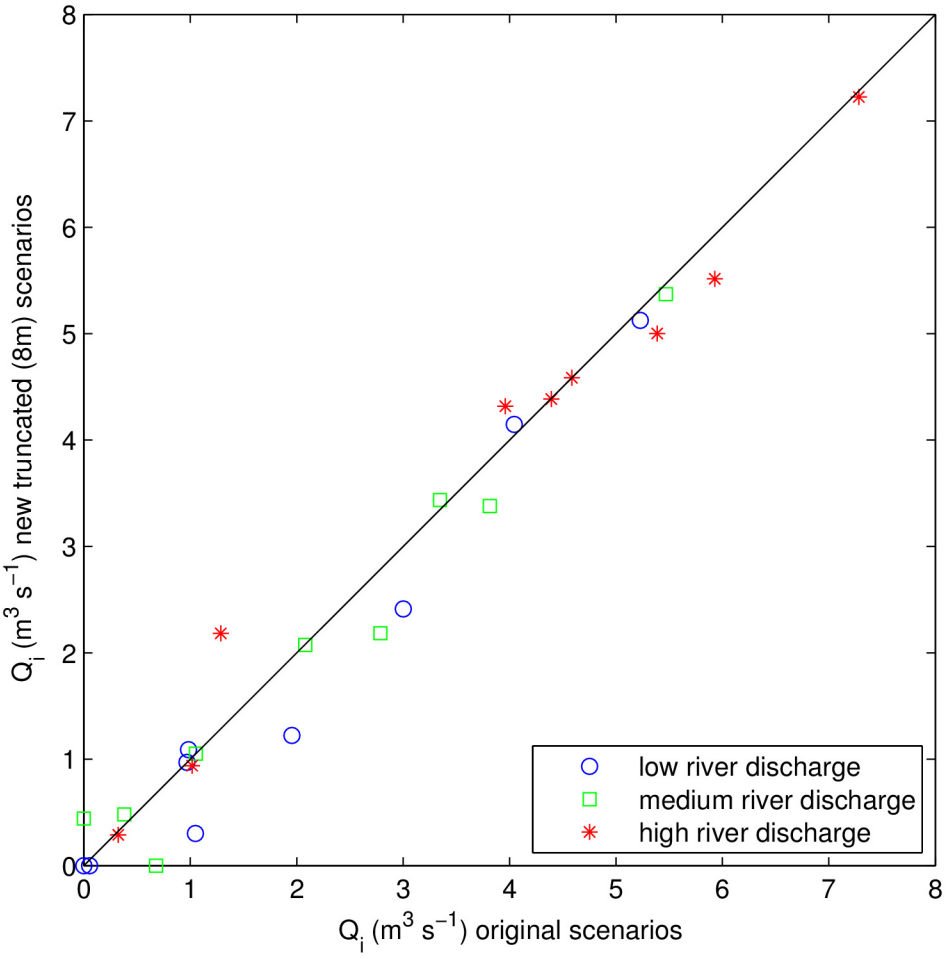

Fig. A 7 River intrusion flow rate Q_i of truncated vs. original scenarios; truncated bathymetry: max. depth 8 m, roughness length of truncated cells z_0 = 1 mm.

II. How pressure gradient error hampers the application of terrain-following three-dimensional circulation models on Lake Tegel

An important advantage of terrain-following (sigma coordinates) ocean models over other vertical discretization schemes, e.g. z-coordinates, is their ability to well simulate bottom boundary layer dynamics because of the smooth representation of bathymetry (Fig. A 8). On the other hand, this is accompanied by a not avoidable numerical error in the pressure gradient calculation (pressure gradient error, PGE) especially in the case of steep topography. (Ezer et al., 2002)

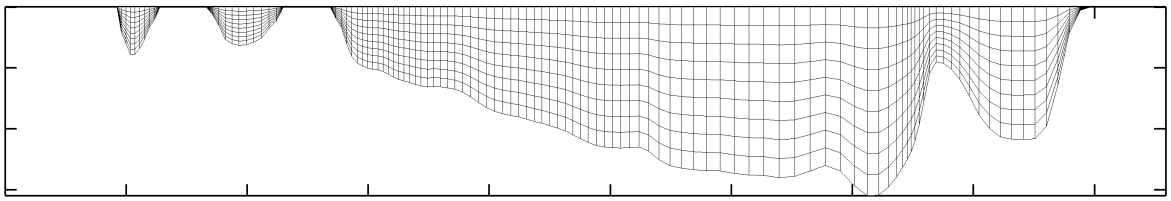

Fig. A 8 Terrain-following vertical discretization (sigma coordinates) of Lake Tegel's bathymetry

The pressure gradient error causes spurious currents, which at worst destroys stratification. The effects of PGE become apparent by simulation runs without any forcing (no wind, no inflows) and initial conditions of flat surface elevation and stable stratification.

Several methods are suggested to reduce this error to an acceptable level. In addition to the standard pressure gradient corrections of the Princeton Ocean Model (POM) and the Regional Ocean Modelling System (ROMS) (Fig. A 9), we tested a 6^{th}-order interpolation scheme (Chu and Fan, 1997), a parabolic reconstruction scheme (Shchepetkin and McWilliams, 2003) (Fig. A 10) and bathymetry smoothing (Fig. A 11).

In the case of Lake Tegel the Princeton Ocean Model (POM) demonstrates significant pressure gradient error. Neither the 6^{th}-order scheme nor smoothing of bathymetry reduces the error sufficiently (Fig. A 12). The Regional Ocean Modelling System (ROMS) produces less numerical errors. It is possible to reduce the errors by bathymetry smoothing, so that numerical mixing is slightly below the natural horizontal mixing. However, bathymetry smoothing is not a satisfying solution because of the decreased representation of Lake Tegel. Therefore, the application of three-dimensional terrain-following circulation models (POM as well as ROMS) failed due to the pressure gradient error.

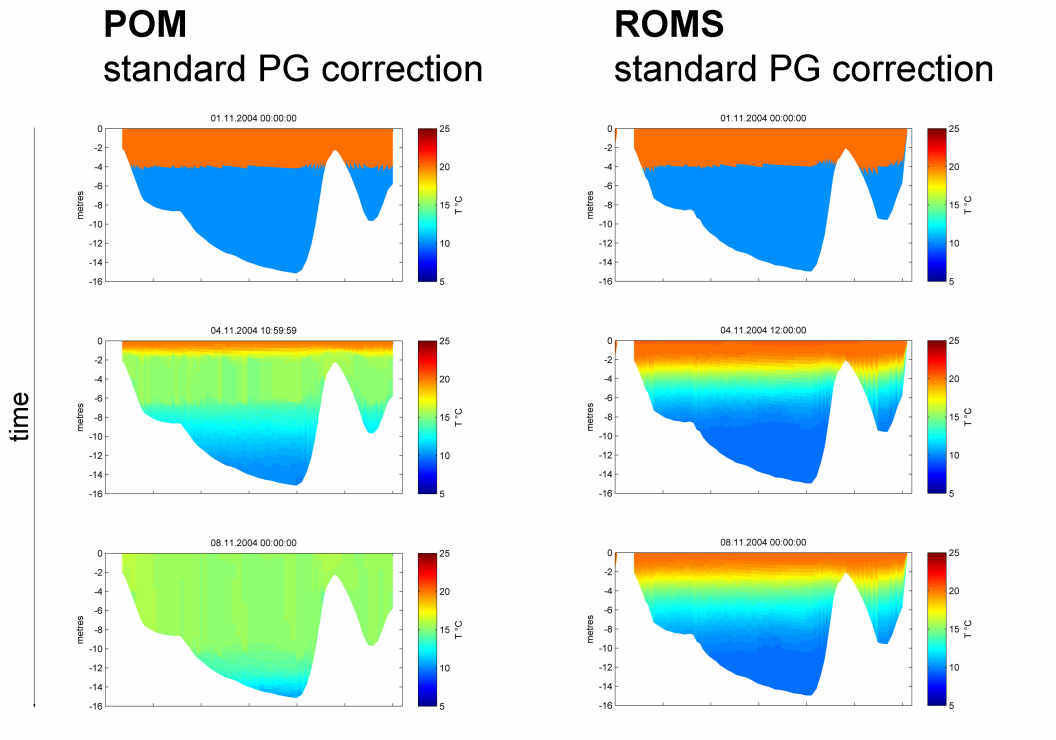

Fig. A 9 Effect of pressure gradient error on simulated temperature profiles for standard PG correction of different models after 0, 3 and 7 days (all runs with closed boundaries and no forcing); POM, Princeton Ocean Model; ROMS, Regional Ocean Modelling System; PG, pressure gradient

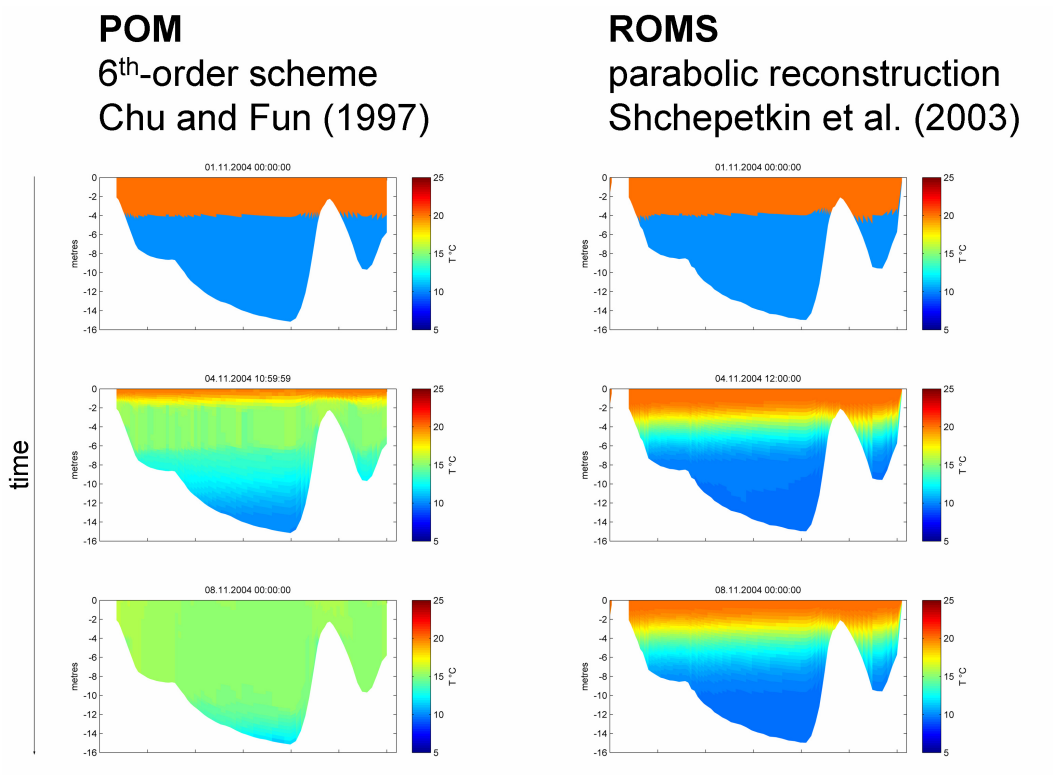

Fig. A 10 Effect of pressure gradient error on simulated temperature profiles for suggested PGE correction methods after 0, 3 and 7 days (all runs with closed boundaries and no forcing); POM, Princeton Ocean Model; ROMS, Regional Ocean Modelling System

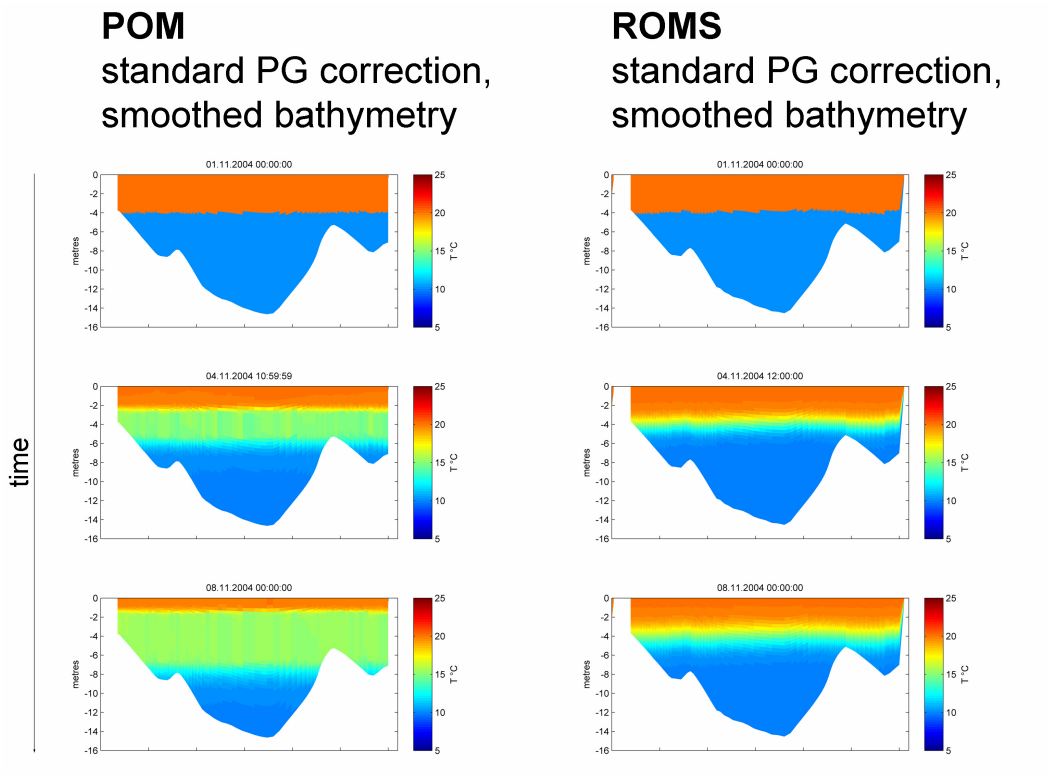

Fig. A 11 Effect of pressure gradient error on simulated temperature profiles with smoothed bathymetry for different models after 0, 3 and 7 days (all runs with closed boundaries and no forcing); POM, Princeton Ocean Model; ROMS, Regional Ocean Modelling System; PG, pressure gradient

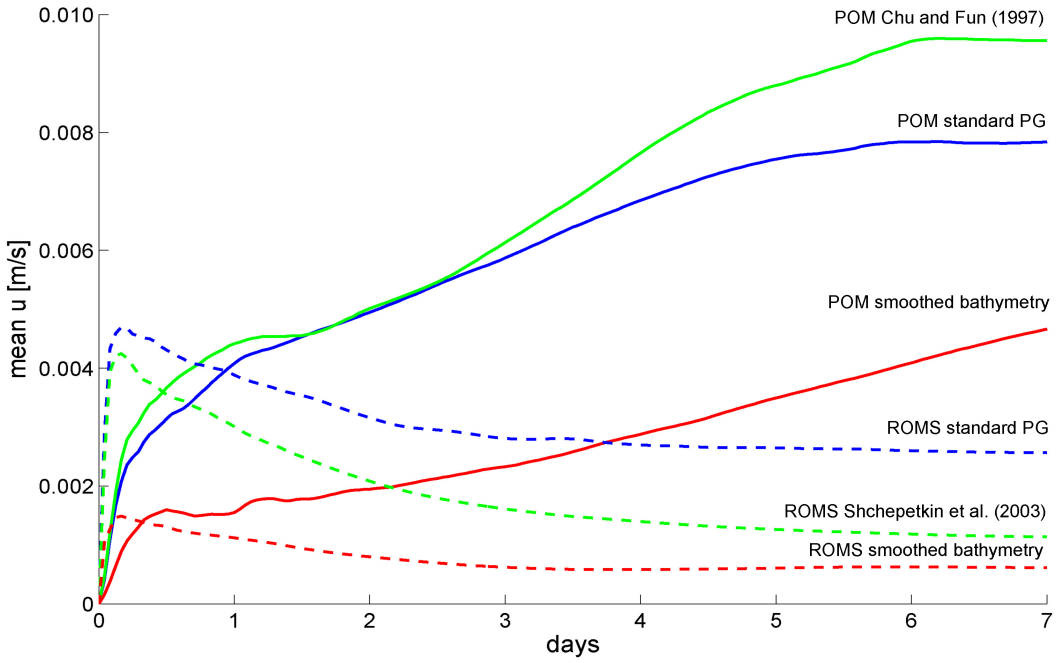

Fig. A 12 Mean error velocities of spurious currents caused by pressure gradient error for different model configurations (all runs with closed boundaries and no forcing); POM, Princeton Ocean Model; ROMS, Regional Ocean Modelling System; PG, pressure gradient correction

III. 2D spatial interpolation of measured data with attention of islands by implementation of Dijkstra's path-finding algorithm

Ordinary 2D spatial interpolation methods, e.g. inverse distance weighting (IDW), Barnes or Kriging interpolation, are not suitable in the case of multiple islands and sparse sampling data, because they do not consider that the linear distance between the interpolated and the measured position is sometimes an unsuitable estimator of value weighting. The following scheme (Fig. A 13) visualizes the difference between the linear distance and the shortest path "around the islands". With the help of Dijkstra's path-finding algorithm (Dijkstra, 1959) on a graph which was obtained from a POM grid with reduced resolution (50x20), the lengths of the shortest paths were calculated and subsequently used for spatial interpolation with IDW. A Comparison with ordinary interpolation methods is shown in Fig. A 14.

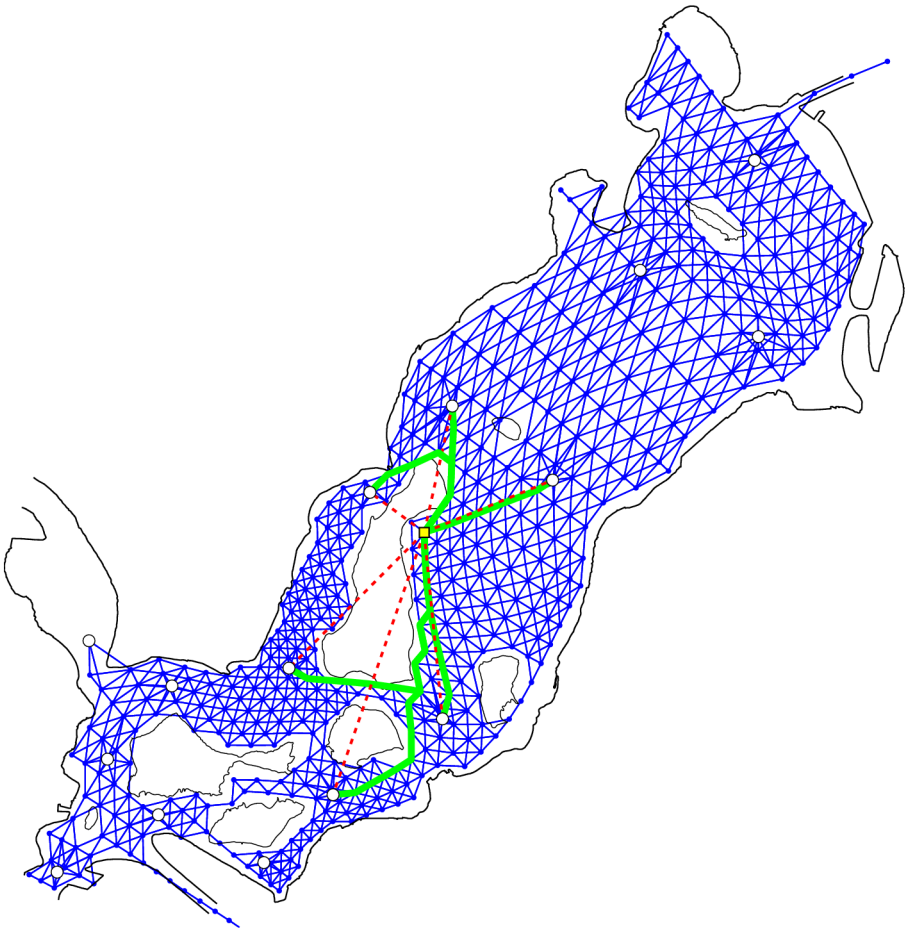

Fig. A 13 Implementation of Dijkstra's path-finding algorithm to evaluate the lengths of the shortest paths "around the islands" (green lines) from any arbitrary position (yellow square) to the surrounding sampling points (white circles) on a graph which approximates a network of all possible water flow paths (blue lines); cf. the shorter linear distances (dashed red lines) which are used by ordinary spatial interpolation methods

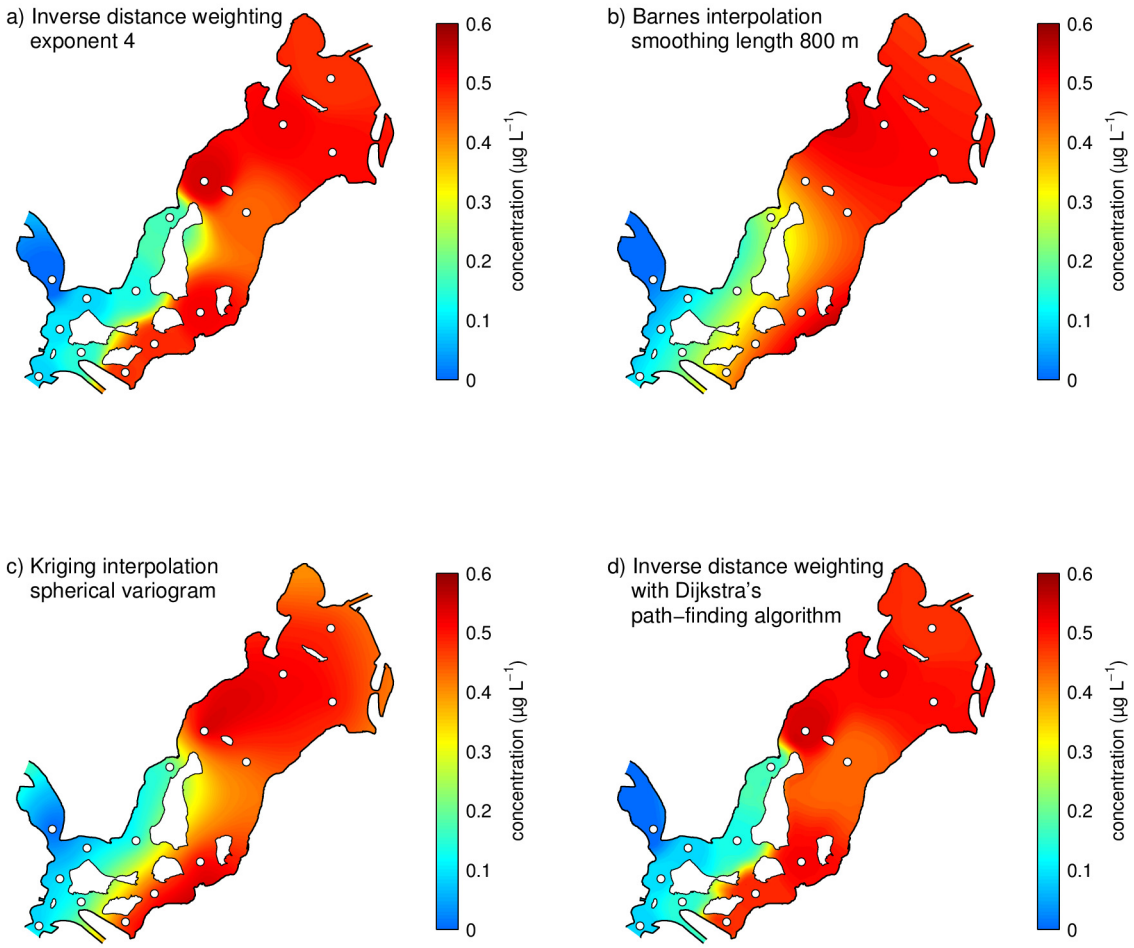

Fig. A 14 Comparison of three widely used spatial interpolation methods (a–c) with a combination of Dijkstra's path-finding algorithm and inverse distance weighting (d); measured values (white circles) are concentration of bezafibrate on 01 Apr 2010

IV. Measurement data of micro-pollutants in Lake Tegel

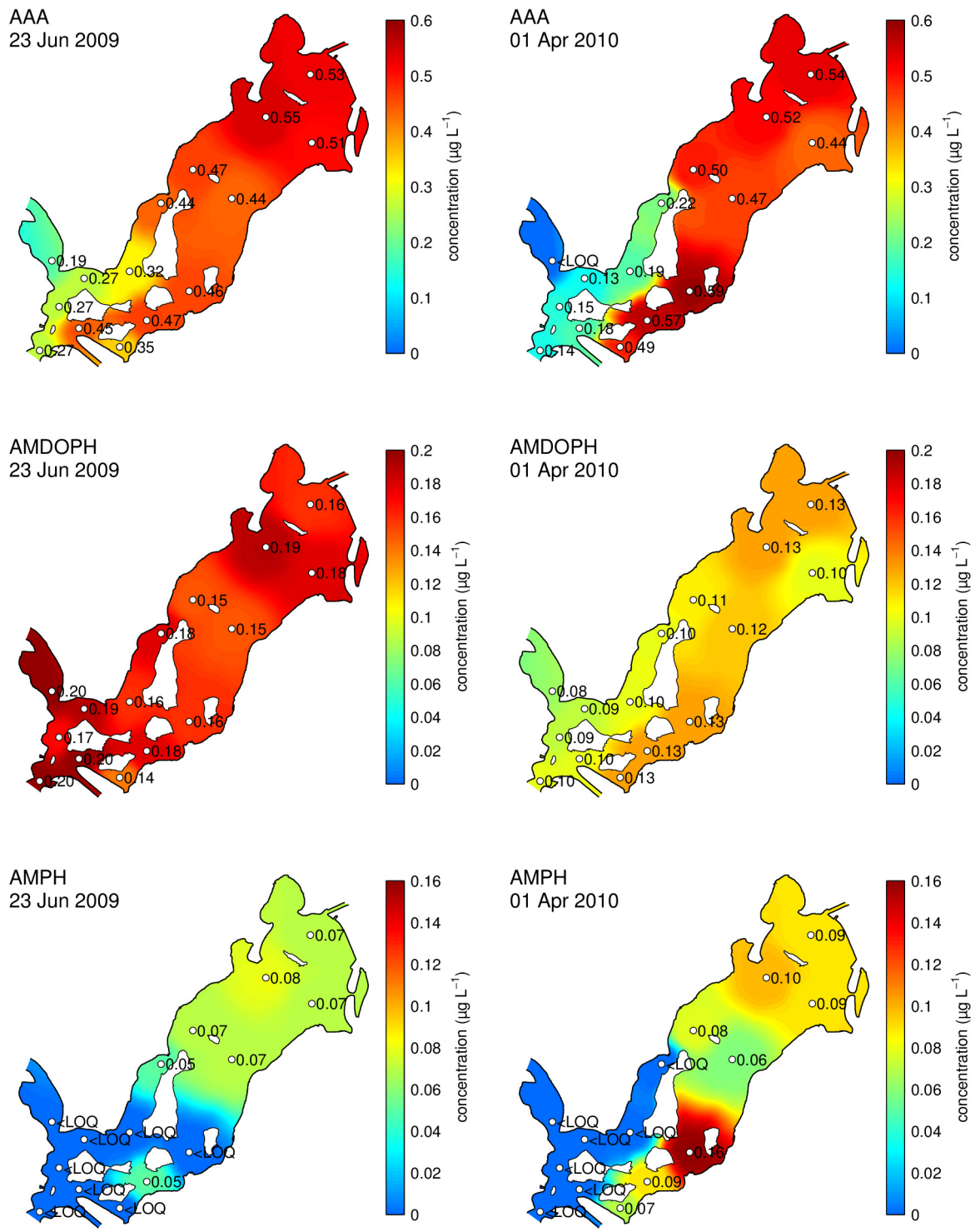

Fig. A 15 Horizontal distribution of AAA (CAS number 83-15-8), AMDOPH (CAS number 519-65-3) and AMPH (CAS number 38604-70-5) in Lake Tegel, sampling depth 0.5 m, values below level of quantification (LOQ) are displayed as zero

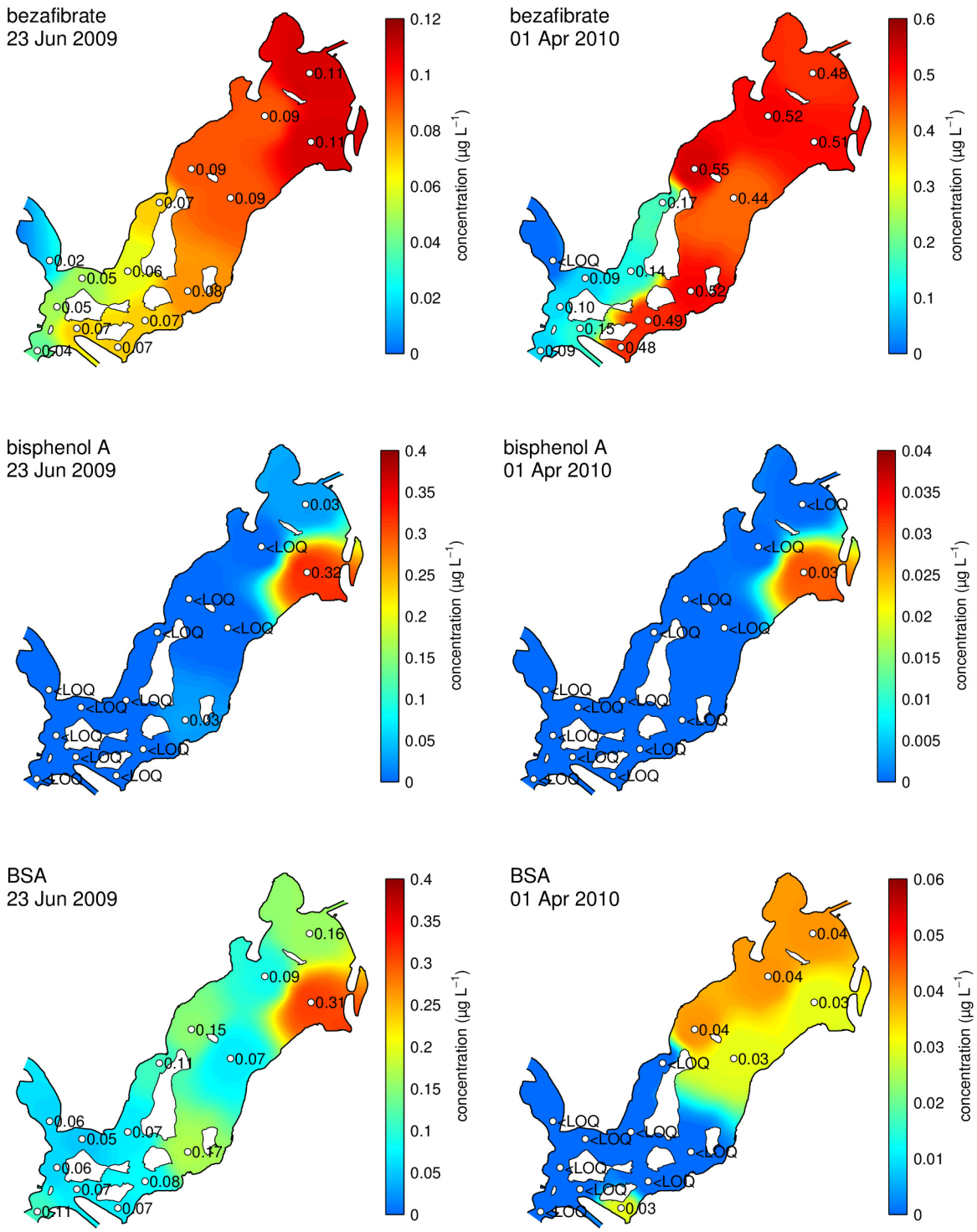

Fig. A 16 Horizontal distribution of bezafibrate (CAS number 41859-67-0), bisphenol A (CAS number 80-05-7) and BSA (benzenesulfonamide, CAS number 98-10-2) in Lake Tegel, sampling depth 0.5 m, values below level of quantification (LOQ) are displayed as zero

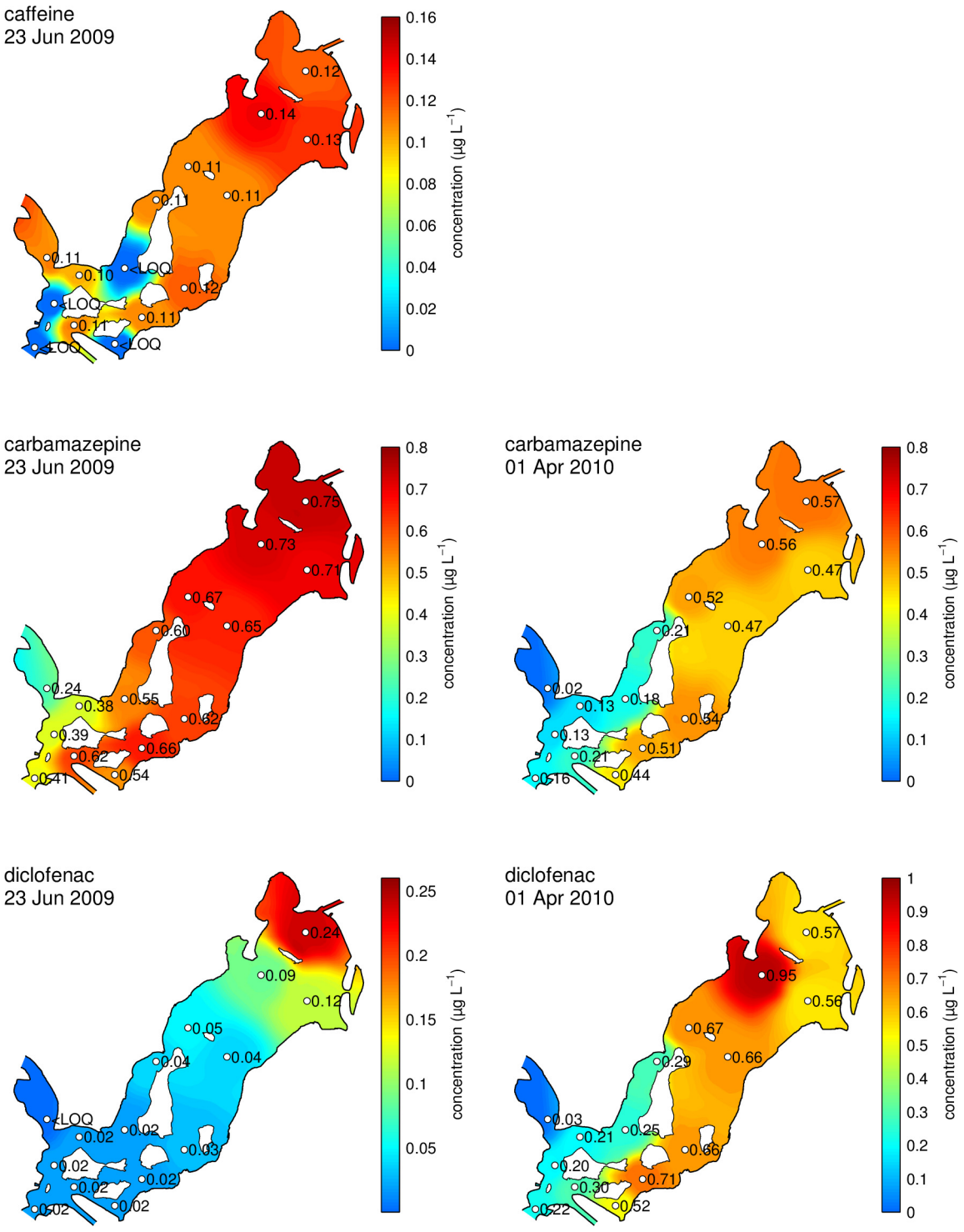

Fig. A 17 Horizontal distribution of caffeine (CAS number 58-08-2), carbamazepine (CAS number 298-46-4) and diclofenac (CAS number 15307-86-5) in Lake Tegel, sampling depth 0.5 m, values below level of quantification (LOQ) are displayed as zero

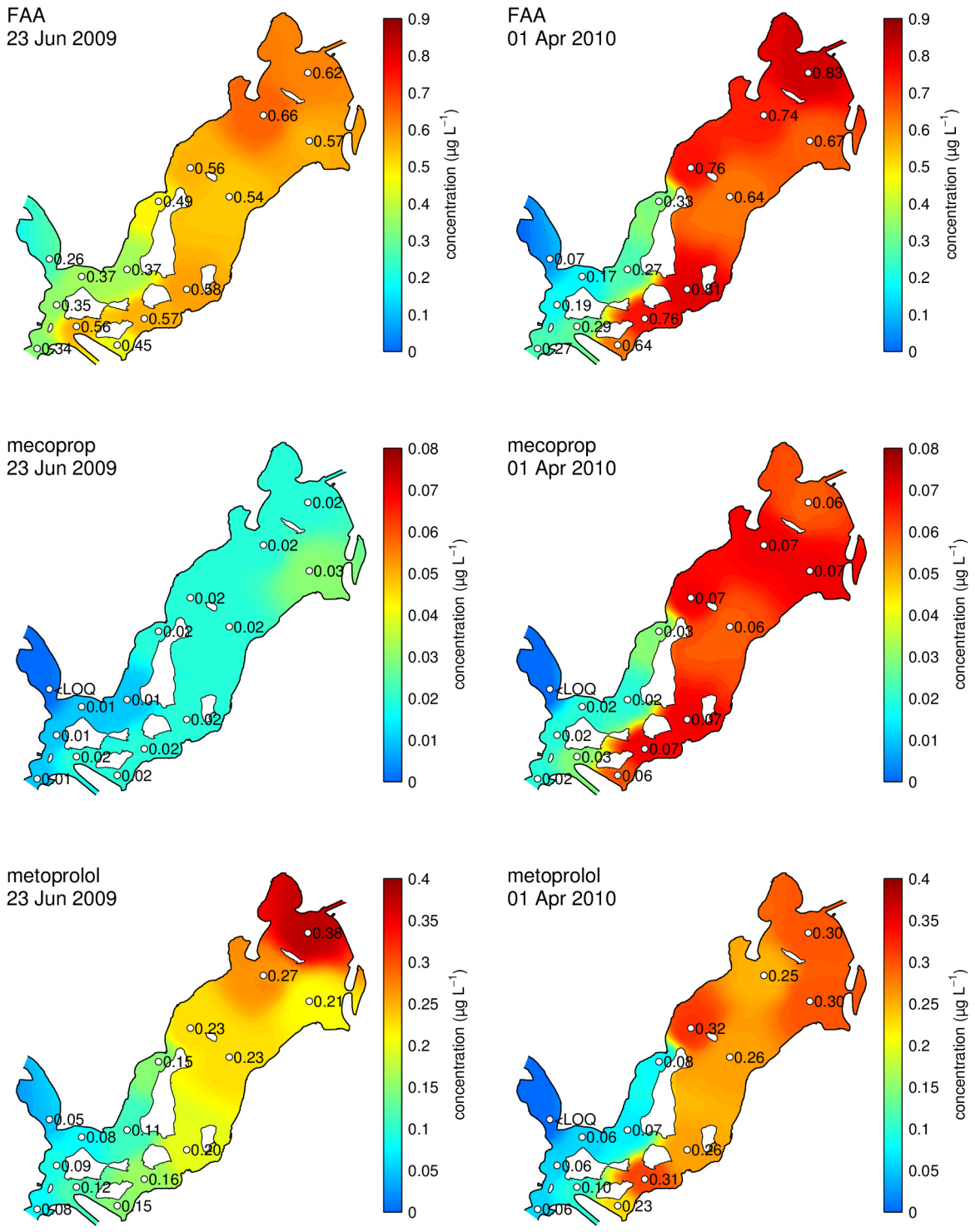

Fig. A 18 Horizontal distribution of FAA (CAS number 1672-58-8), mecoprop (CAS number 7085-19-0) and metoprolol (CAS number 37350-58-6) in Lake Tegel, sampling depth 0.5 m, values below level of quantification (LOQ) are displayed as zero

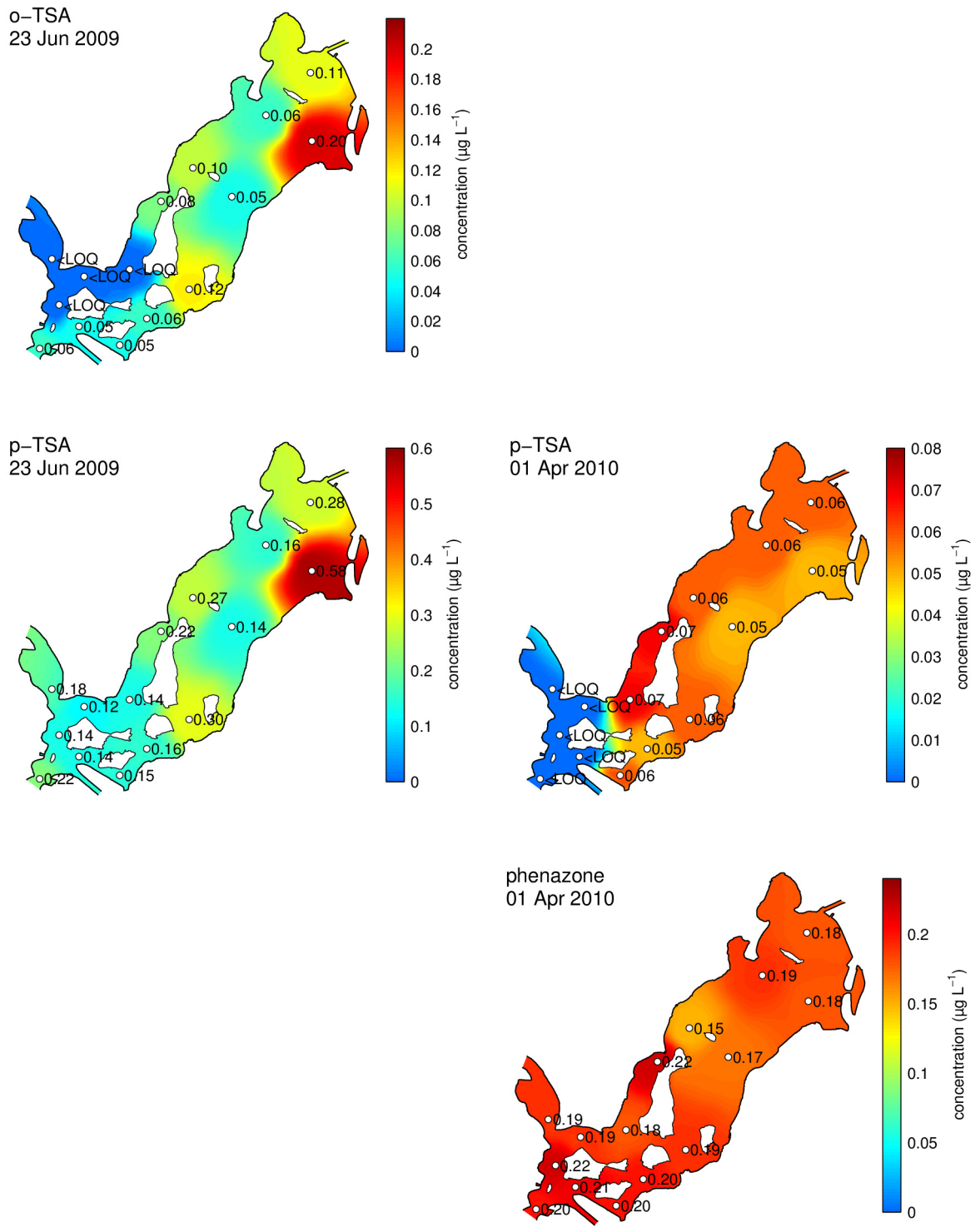

Fig. A 19 Horizontal distribution of o-TSA (CAS number 88-19-7), p-TSA (CAS number 70-55-3) and phenazone (CAS number 60-80-0) in Lake Tegel, sampling depth 0.5 m, values below level of quantification (LOQ) are displayed as zero

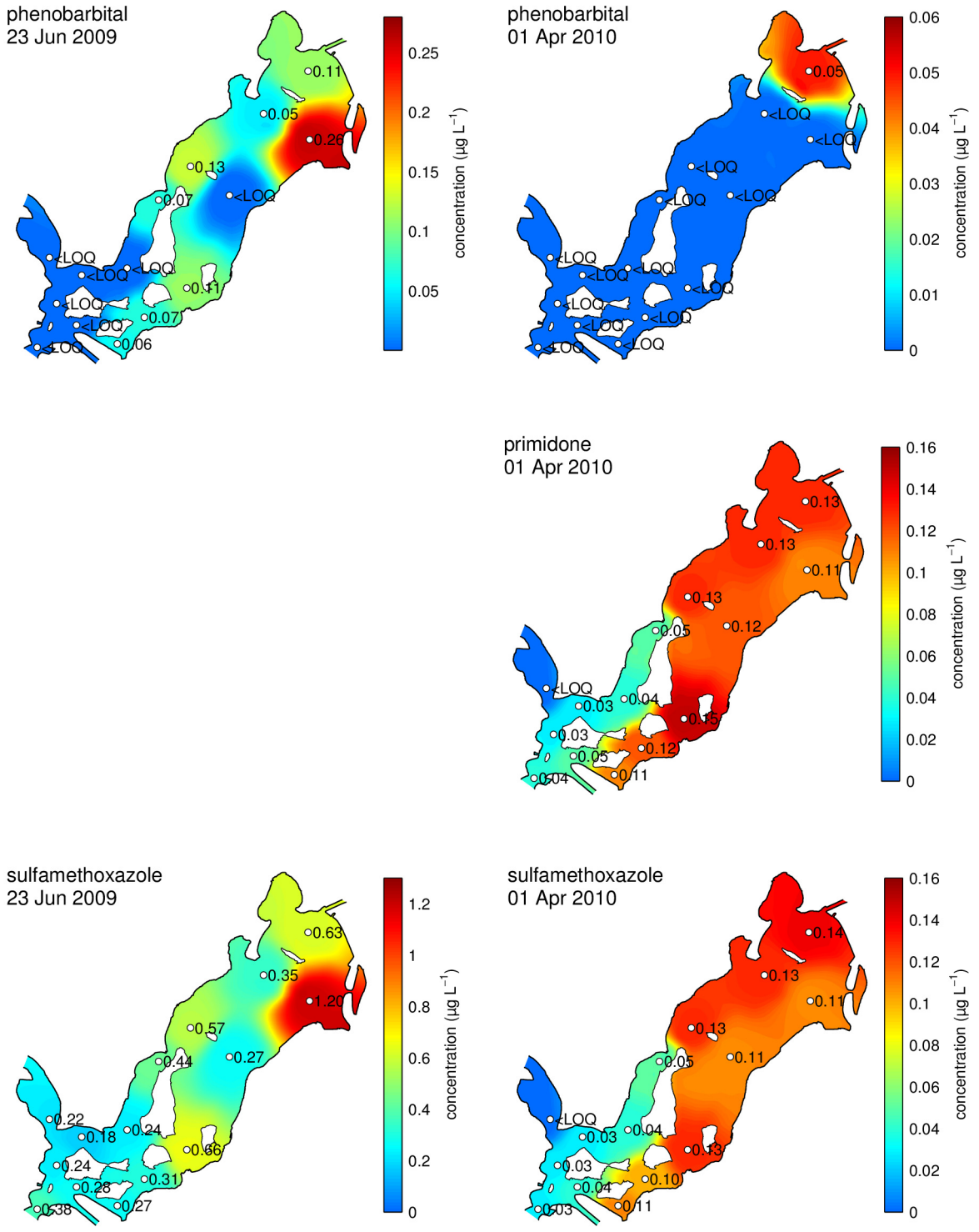

Fig. A 20 Horizontal distribution of phenobarbital (CAS number 50-06-6), primidone (CAS number 125-33-7) and sulfamethoxazole (CAS number 723-46-6) in Lake Tegel, sampling depth 0.5 m, values below level of quantification (LOQ) are displayed as zero

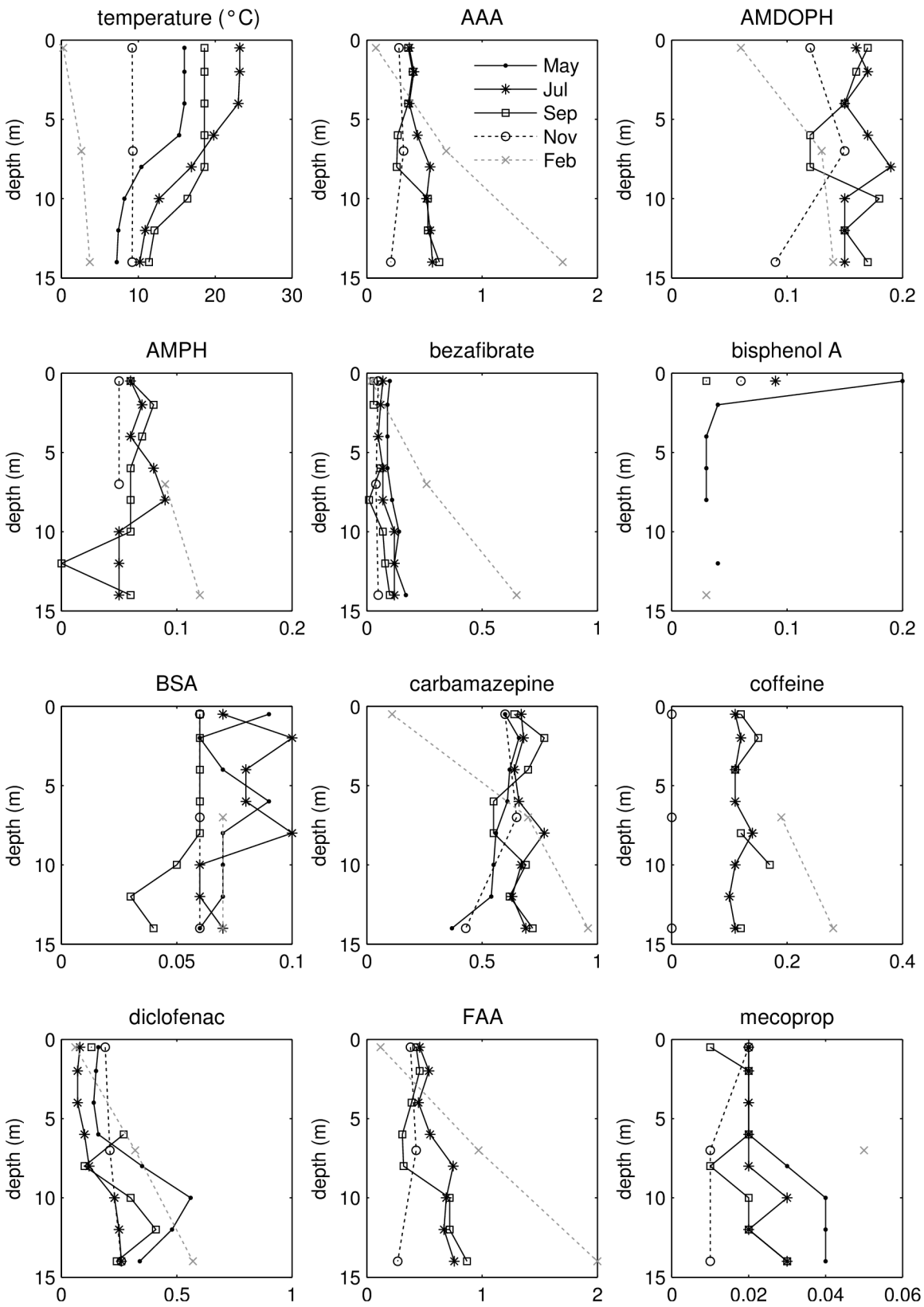

Fig. A 21 Vertical distribution of water temperature (°C) and micro-pollutants (µg L^{-1}) in Lake Tegel at the deepest point of the lake (Senatsboje), 2009–2010, sampling in February beneath 28 cm ice cover, values lower than level of quantification (LOQ) are displayed as zero

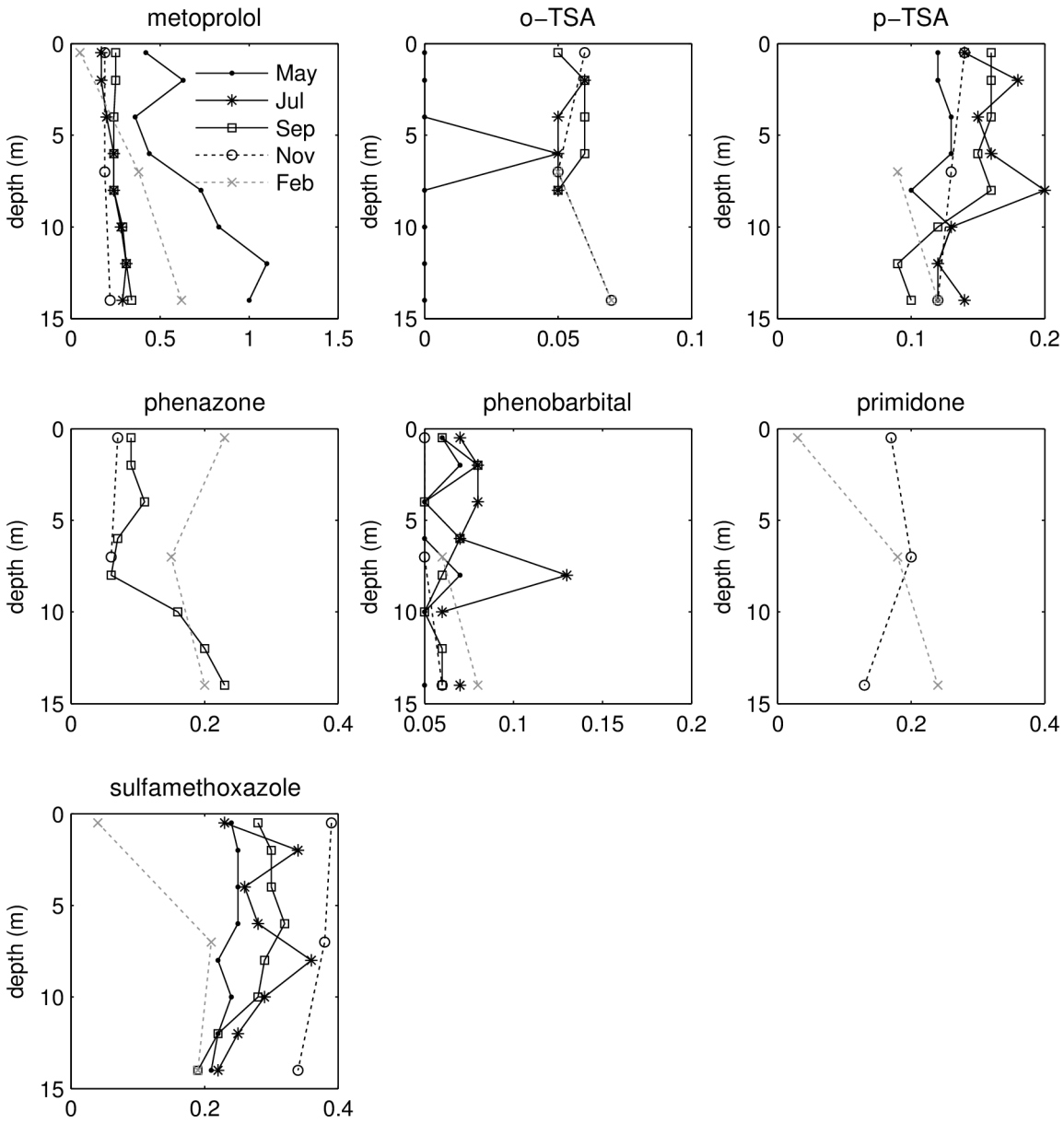

Fig. A 22 Vertical distribution of micro-pollutants (µg L^{-1}) in Lake Tegel at the deepest point of the lake (Senatsboje), 2009–2010, sampling in February beneath 28 cm ice cover, values lower than level of quantification (LOQ) are displayed as zero

V. Measurement data of electrical conductivity and temperature in Lake Tegel

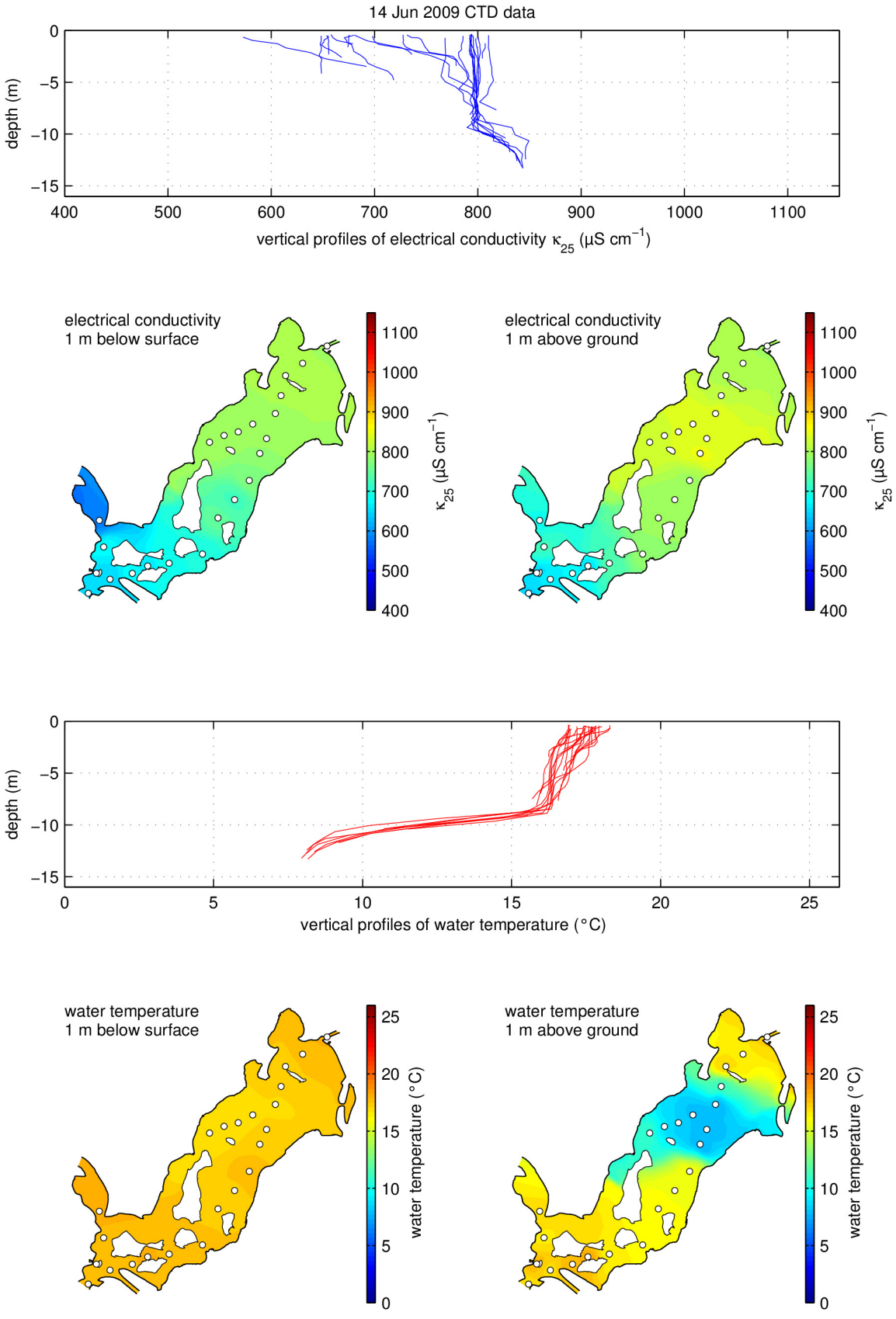

Fig. A 23 CTD data from different locations (white circles) on 14 Jun 2009

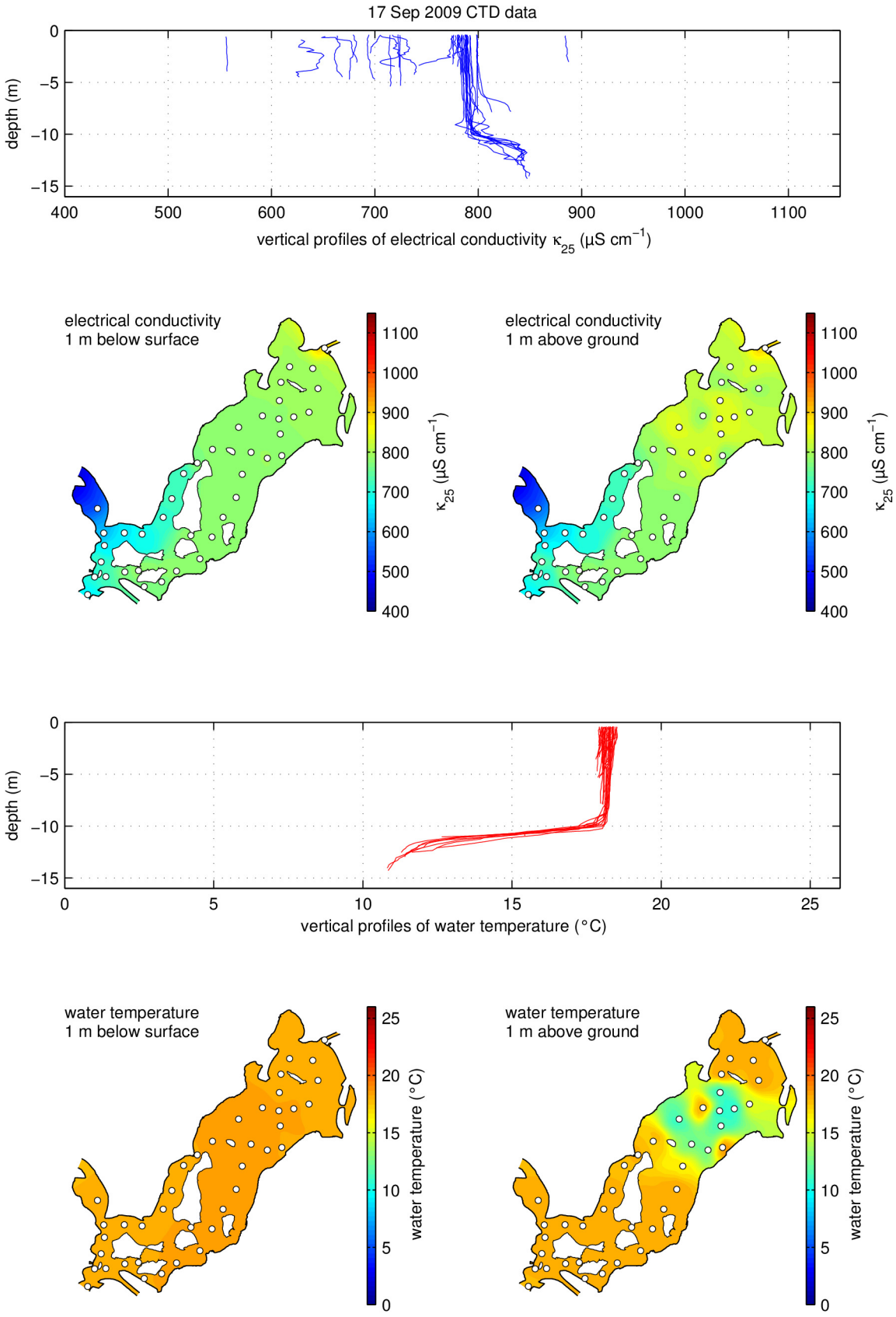

Fig. A 24 CTD data from different locations (white circles) on 17 Sep 2009

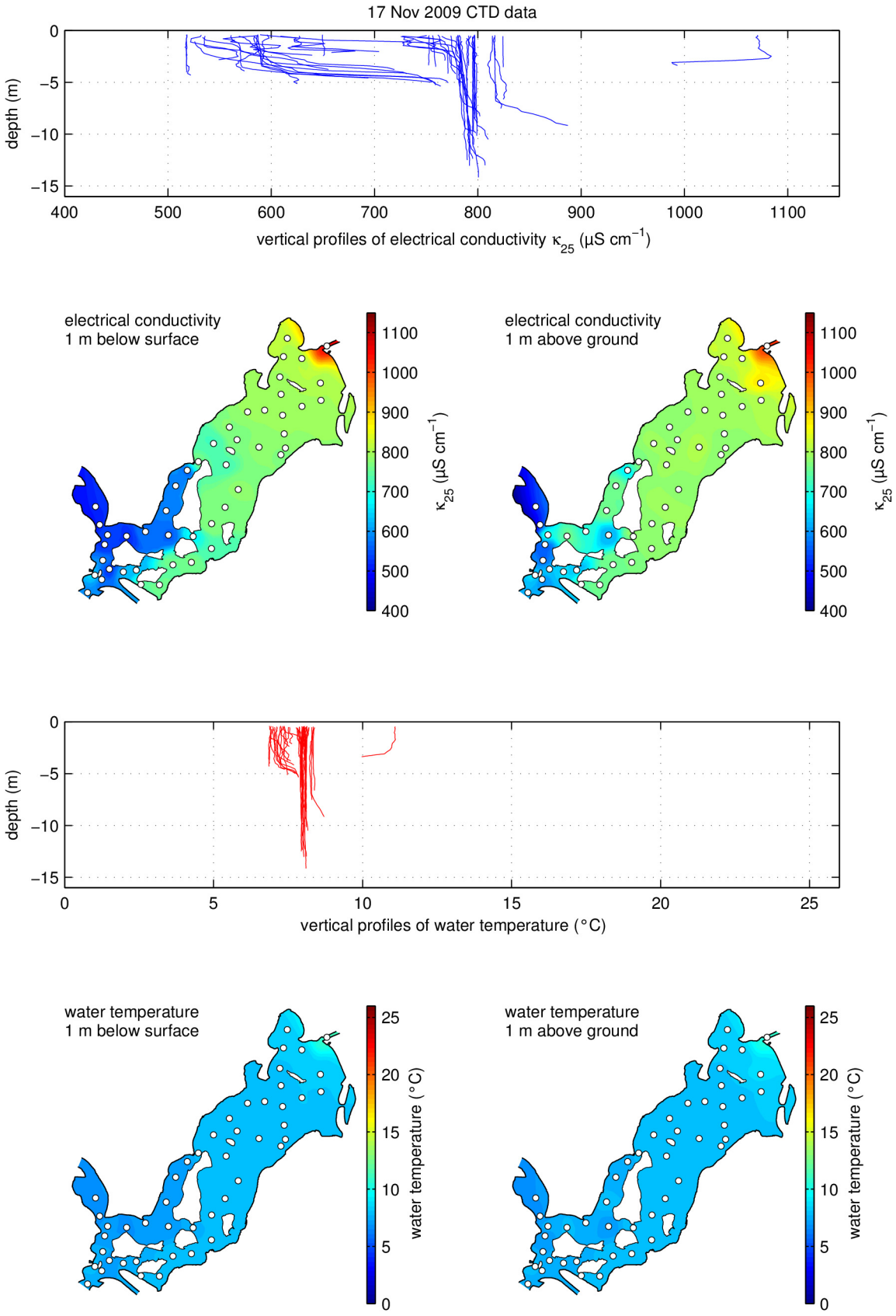

Fig. A 25 CTD data from different locations (white circles) on 17 Nov 2009

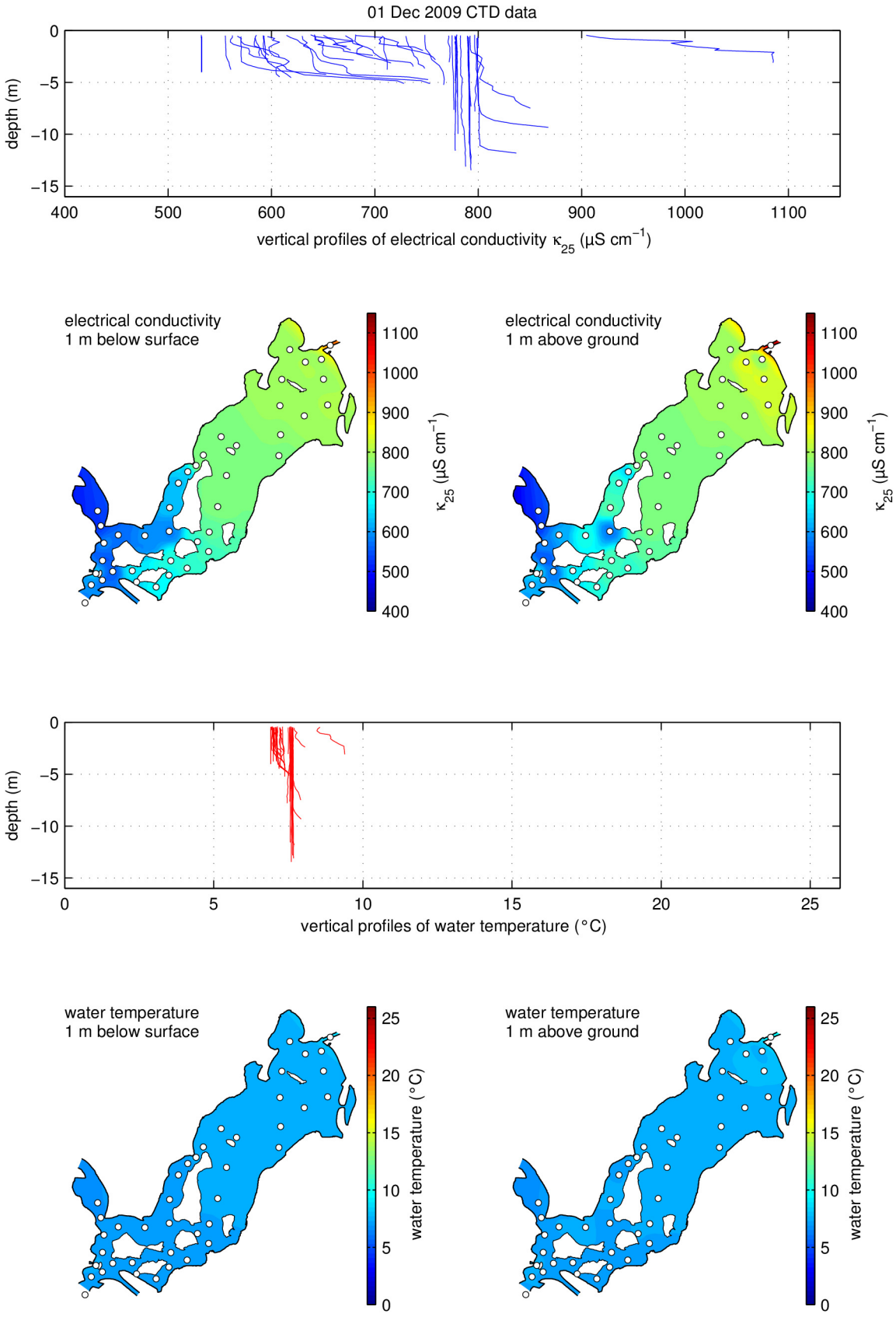

Fig. A 26 CTD data from different locations (white circles) on 01 Dec 2009

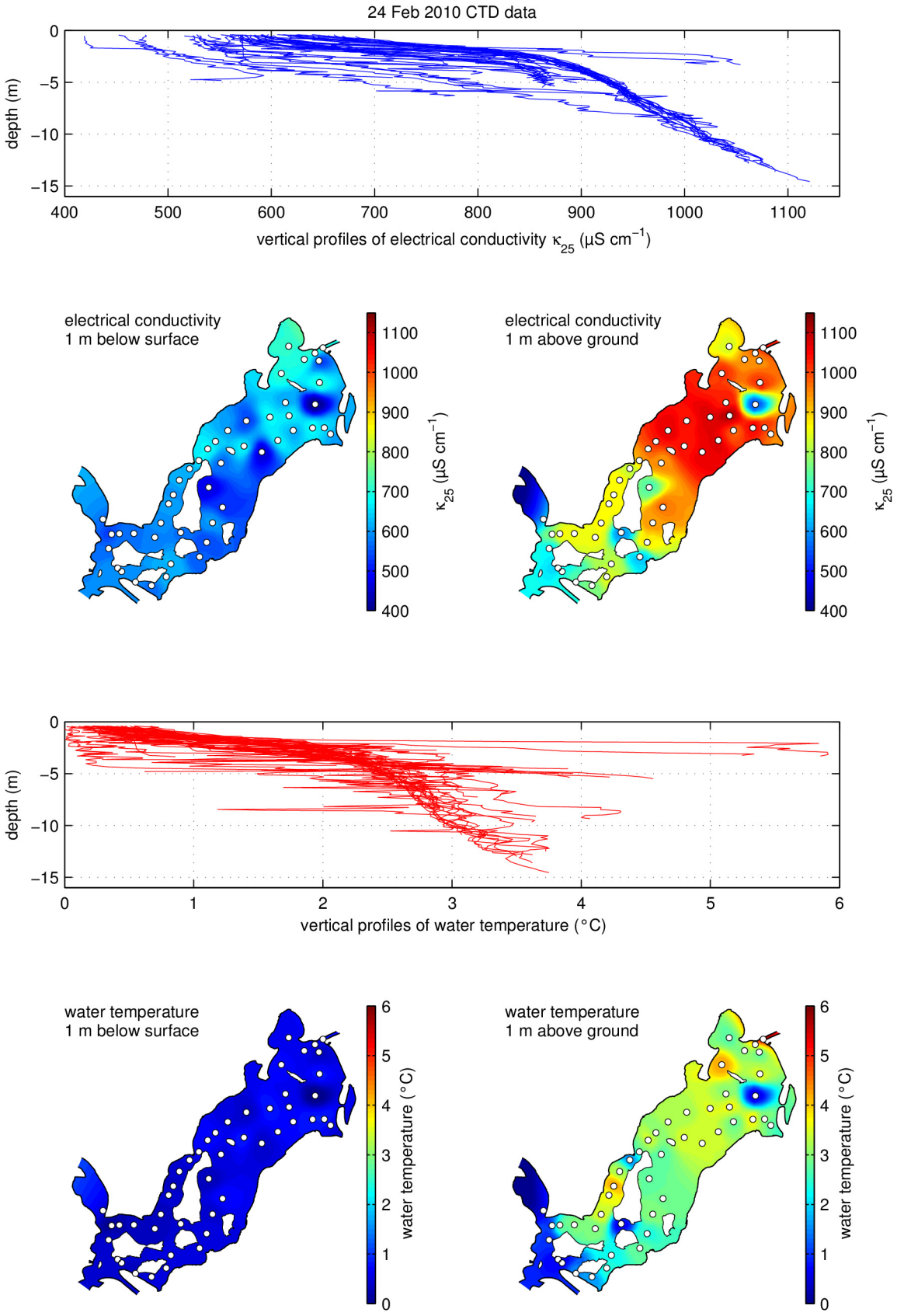

Fig. A 27 CTD data from different locations (white circles) on 24 Feb 2009; lake was ice-covered

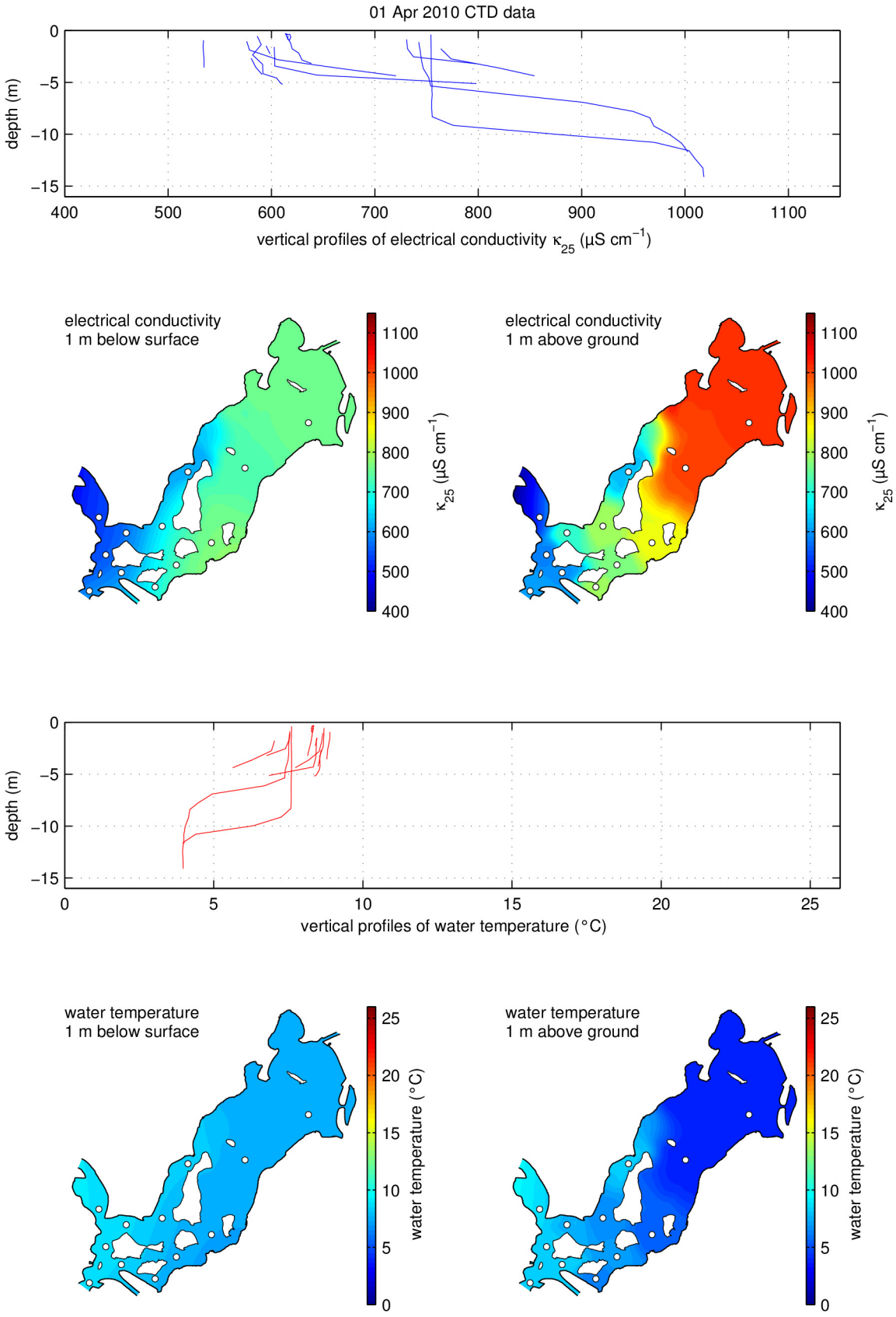

Fig. A 28 CTD data from different locations (white circles) on 01 Apr 2010

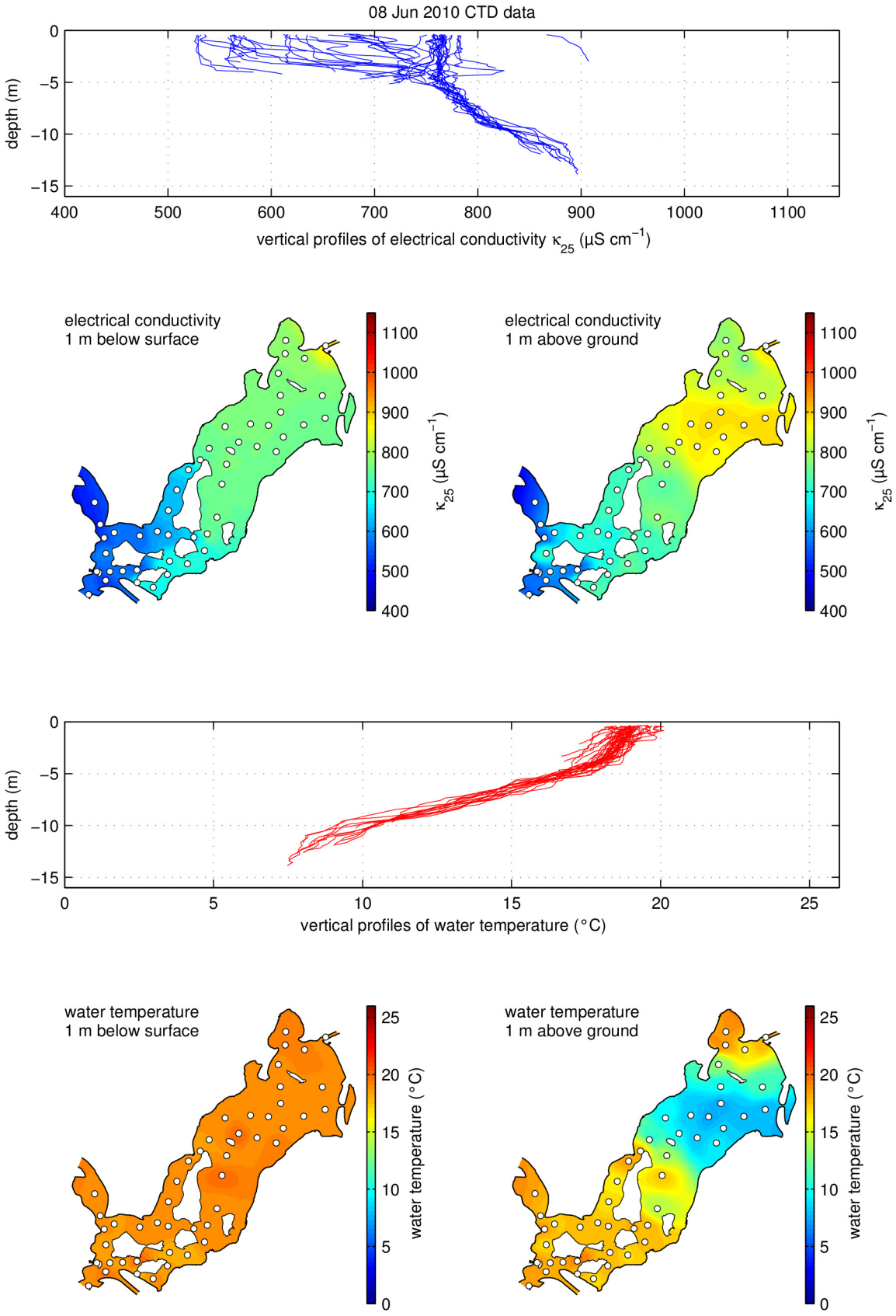

Fig. A 29 CTD data from different locations (white circles) on 08 Jun 2010

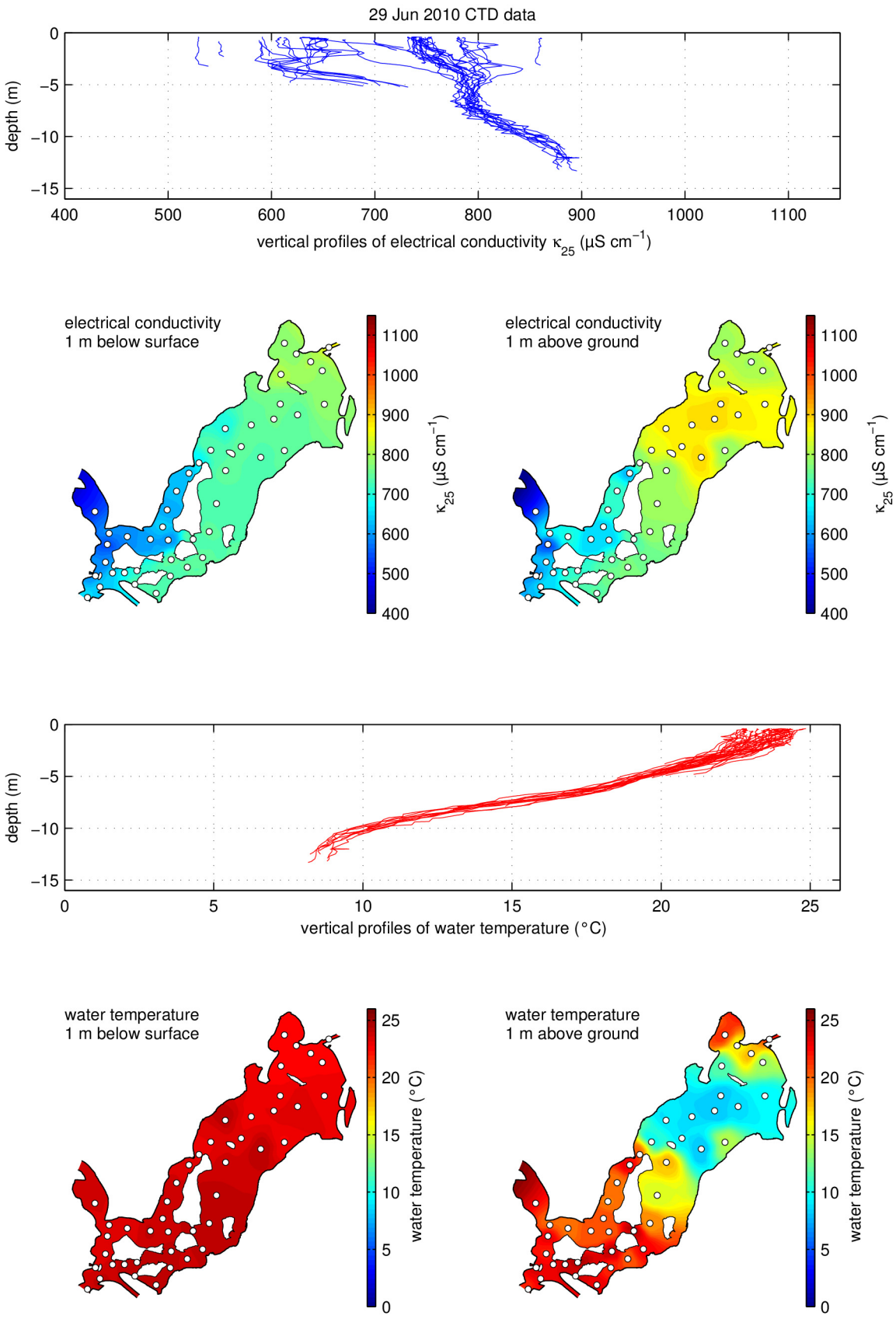

Fig. A 30 CTD data from different locations (white circles) on 29 Jun 2010

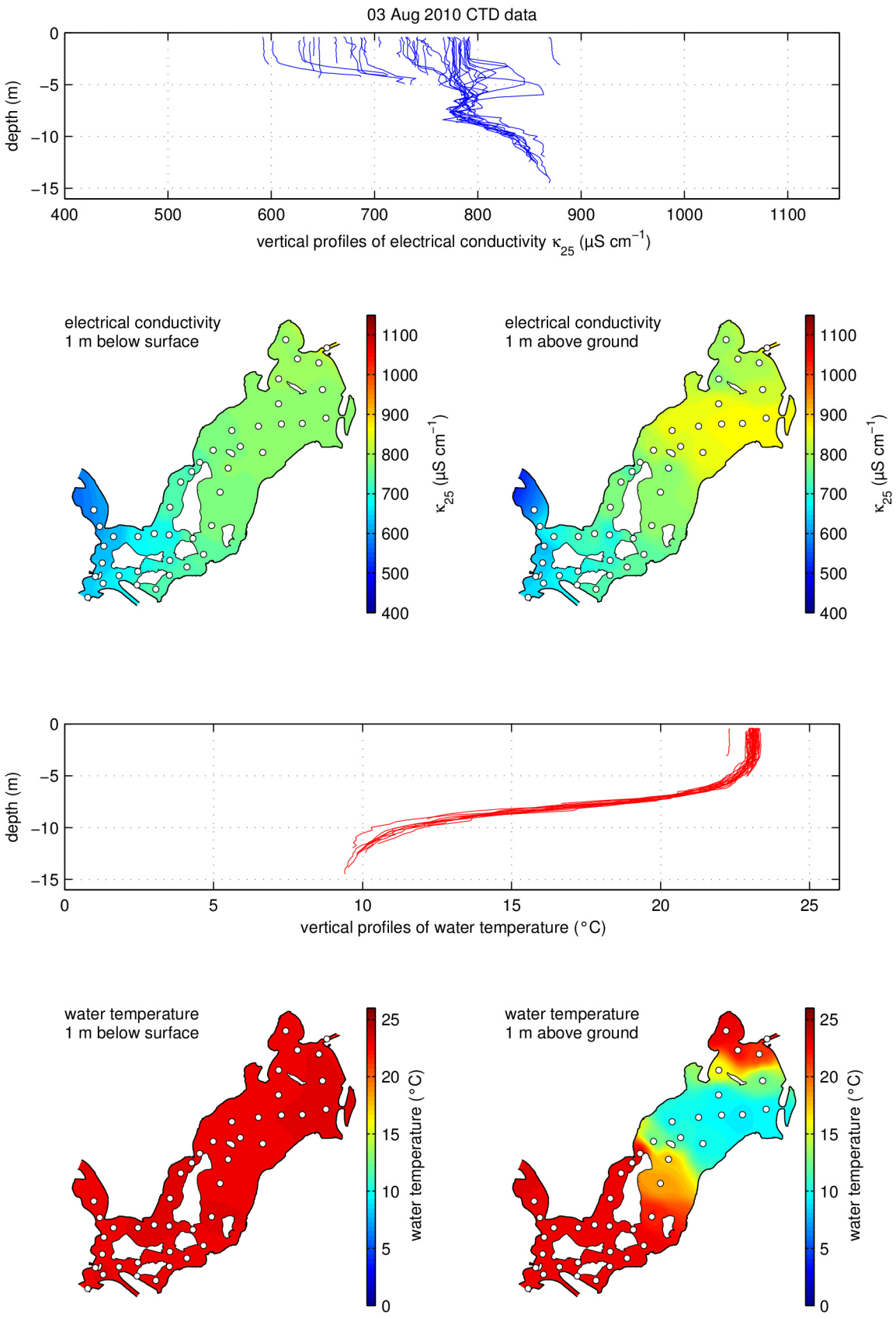

Fig. A 31 CTD data from different locations (white circles) on 03 Aug 2010

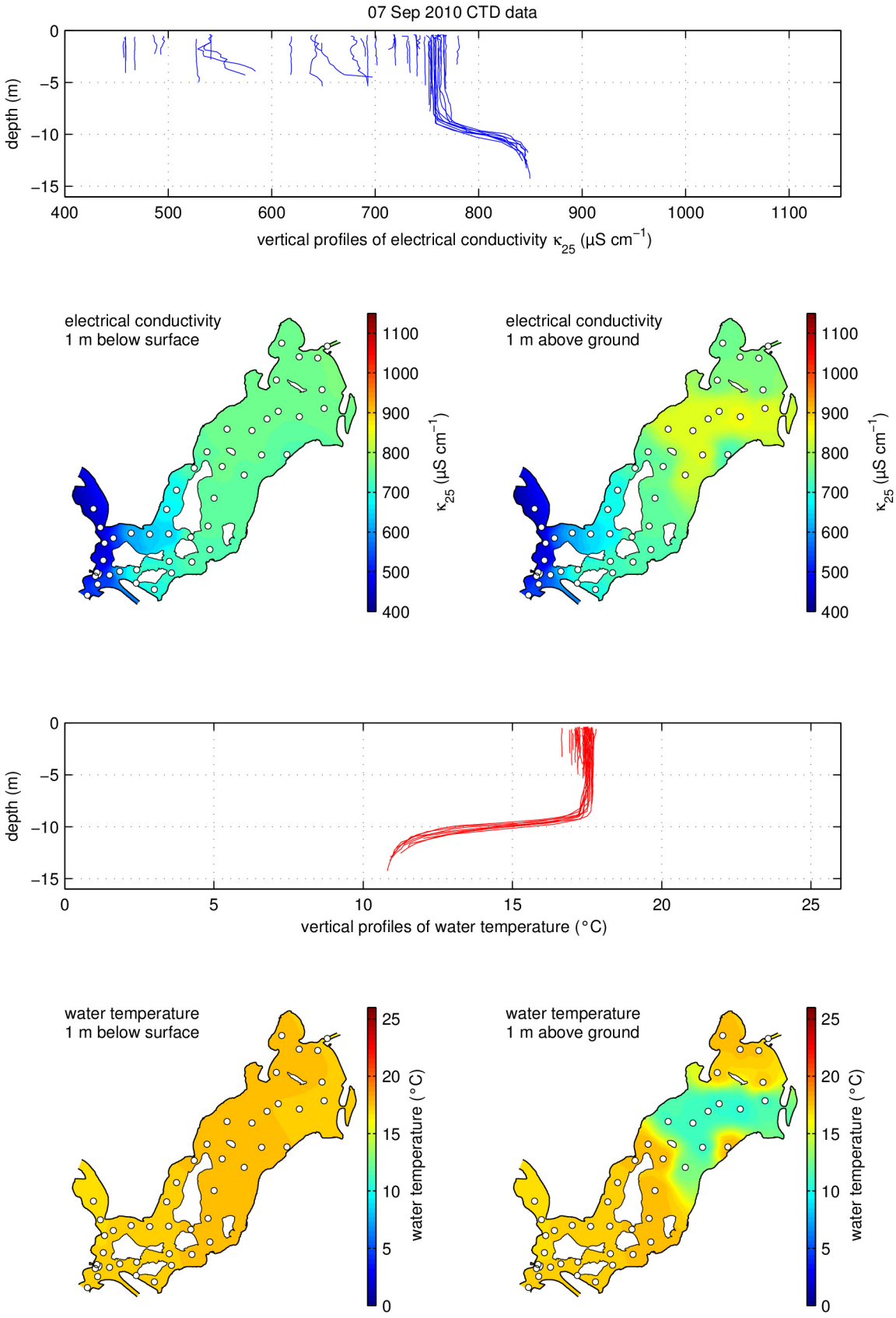

Fig. A 32 CTD data from different locations (white circles) on 07 Sep 2010

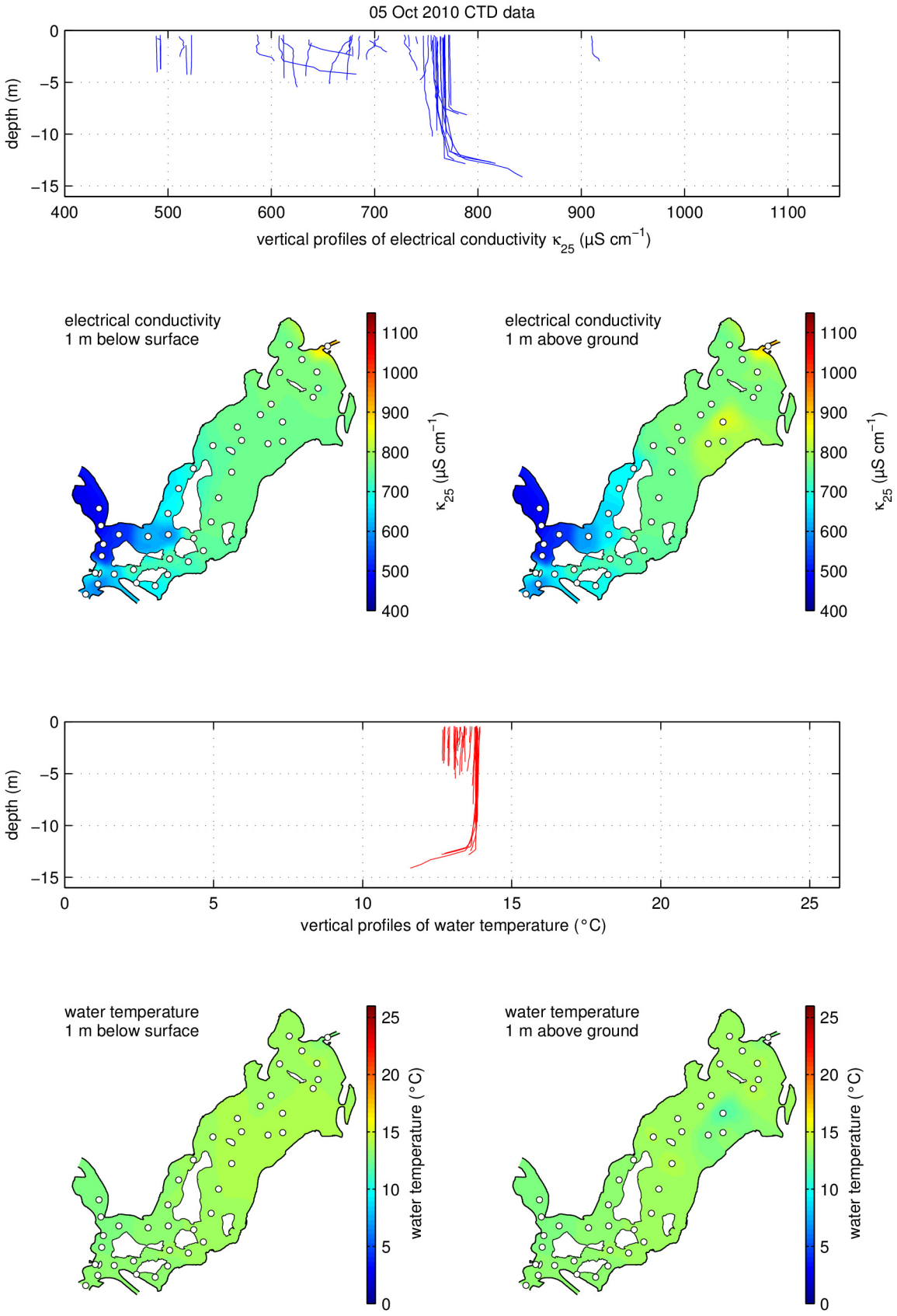

Fig. A 33 CTD data from different locations (white circles) on 05 Oct 2010

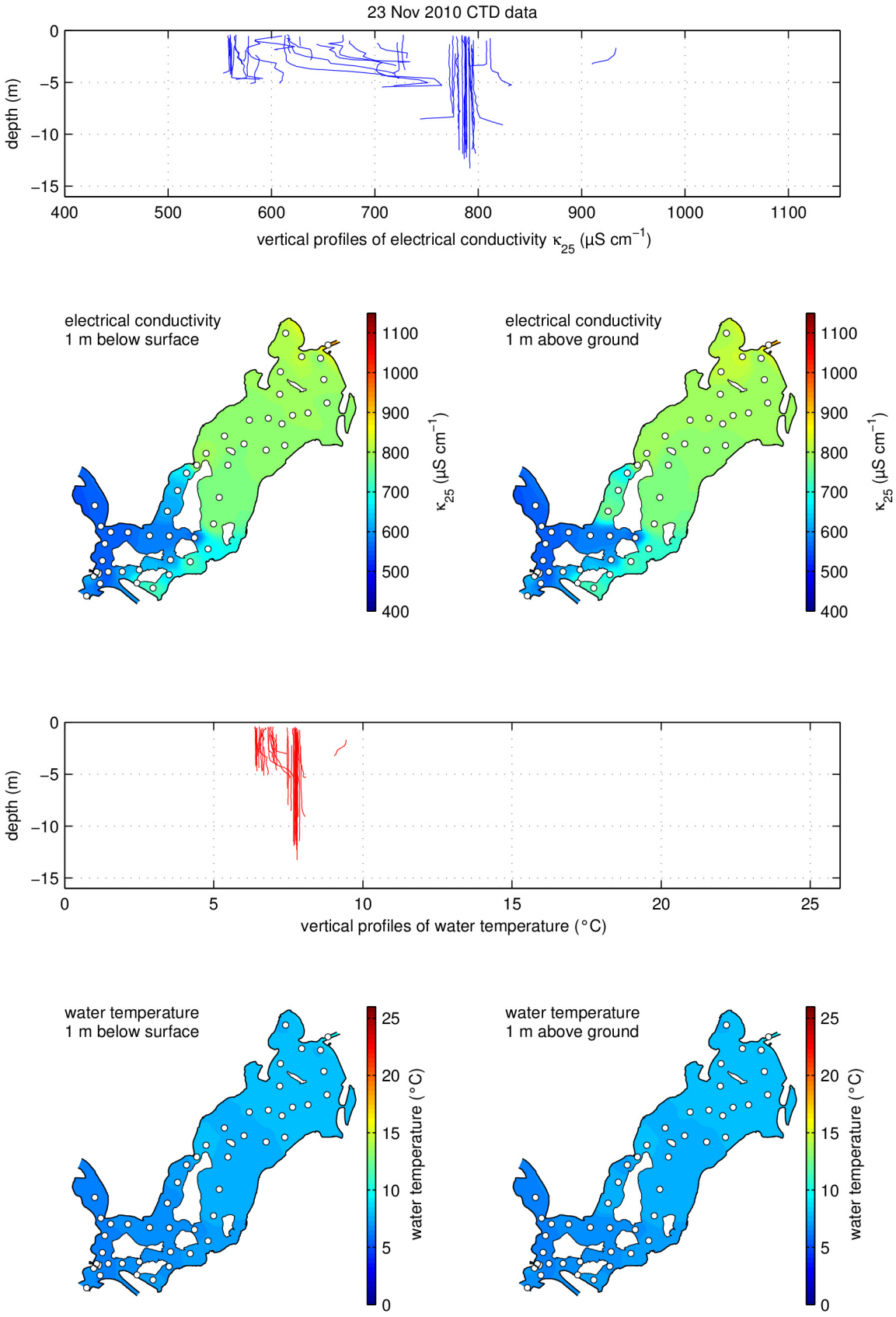

Fig. A 34 CTD data from different locations (white circles) on 23 Nov 2010

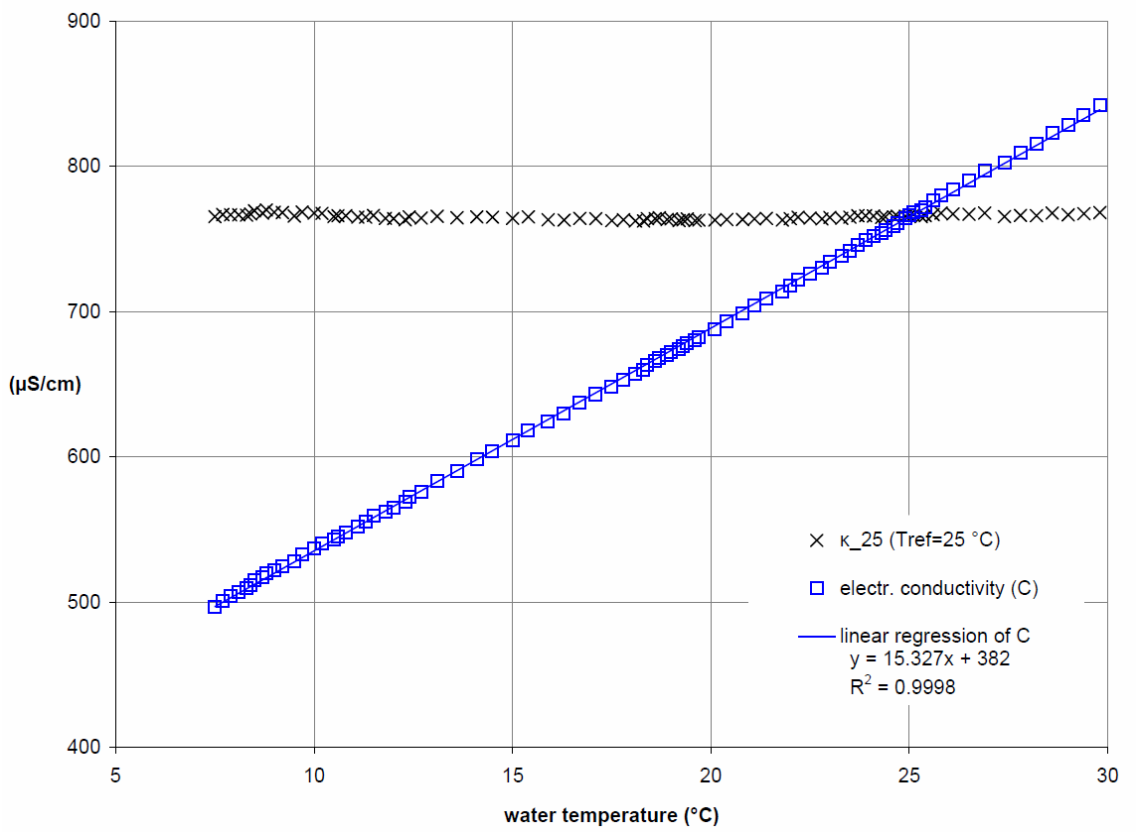

Fig. A 35 Temperature dependency of electrical conductivity in Lake Tegel (sampled on 09 Sep 2009)

According to Boehrer and Schultze (2008) the coefficient of temperature compensation α_{ref} of electrical conductivity C was derived from linear regression:

$C = a \cdot T + b$,

$\alpha_{ref} = [T_{ref} + (b/a)]^{-1}$, $a = 15.327$, $b = 382$,

$T_{ref} = 25°C$: $\alpha_{25} = 0.02003$

$T_{ref} = 20°C$: $\alpha_{20} = 0.02226$.

VI. Fitting data

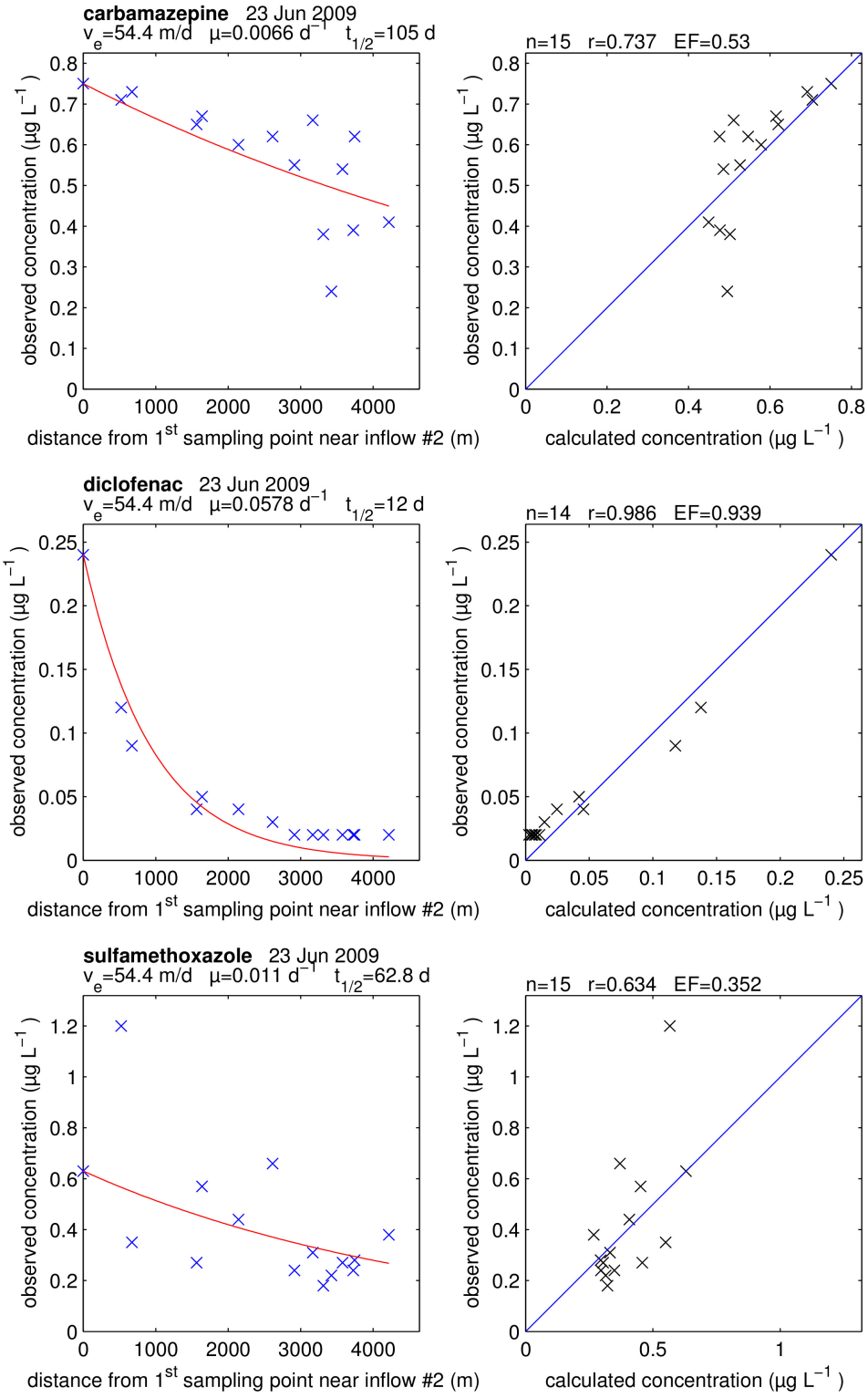

Fig. A 36 Calculation of elimination rates (μ) in summer by fitting observed concentrations to pseudo 1st-order decay (left); v_e, effective velocity; $t_{1/2}$, half-life. Goodness of fit scatter plot of observed vs. fitted concentration (right); n, number of data; r, Pearson's coefficient of correlations; EF, model efficiency.

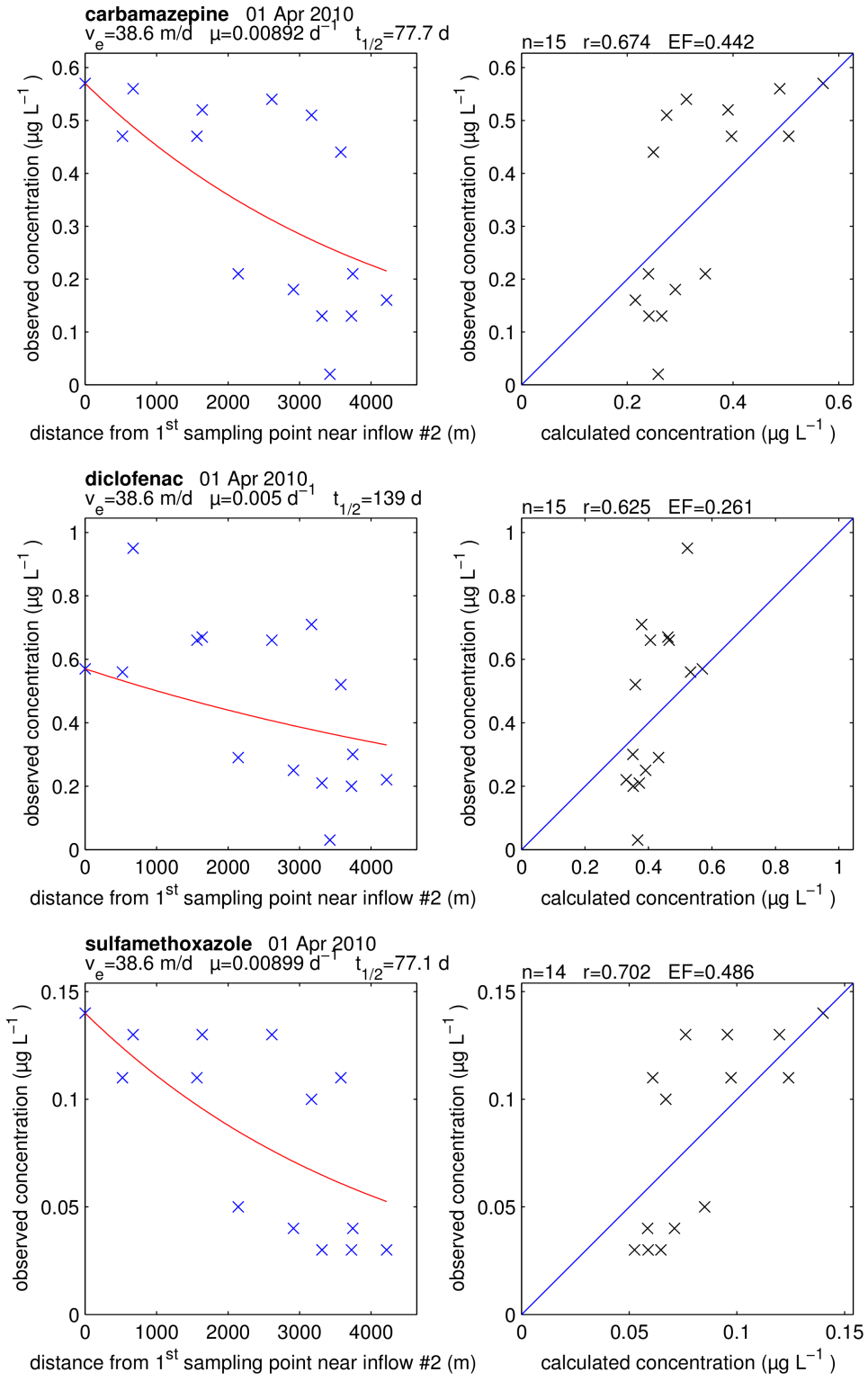

Fig. A 37 Calculation of elimination rates (μ) in spring by fitting observed concentrations to pseudo 1st-order decay (left side); v_e, effective velocity; $t_{1/2}$, half-life. Goodness of fit scatter plot of observed vs. fitted concentration (right side); n, number of data; r, Pearson's coefficient of correlations; EF, model efficiency; c.f. Section 3.3.2

VII. List of publications

Peer-reviewed publications

Schimmelpfennig, S., Kirillin, G., Engelhardt, C., Dünnbier, U., Nützmann, G., 2015. Fate of pharmaceutical micro-pollutants in Lake Tegel (Berlin, Germany): the impact of lake-specific mechanisms. Environmental Earth Sciences, submitted

Kirillin, G., Lorang, M.S., Lippmann, T.C., Gotschalk, C.C., Schimmelpfennig, S., 2015. Surface seiches in Flathead Lake. Hydrology and Earth System Sciences 19, 2605-2615

Schimmelpfennig, S., Kirillin, G., Engelhardt, C., Nützmann, G., Dünnbier, U., 2012. Seeking a compromise between pharmaceutical pollution and phosphorus load: Management strategies for Lake Tegel, Berlin. Water Research 46(13), 4153-4163

Schimmelpfennig, S., Kirillin, G., Engelhardt, C., Nützmann, G., 2012. Effects of wind-driven circulation on river intrusion in Lake Tegel: modeling study with projection on transport of pollutants. Environmental Fluid Mechanics 12, 321-339

Sperlich, A., Schimmelpfennig, S., Baumgarten, B., Genz, A., Amy, G., Worch, E., Jekel, M., 2008. Predicting anion breakthrough in granular ferric hydroxide (GFH) adsorption filters. Water Research 42(8), 2073-2082

Conference contributions

Schimmelpfennig, S., Kirillin, G., Engelhardt, C., Nützmann, G., June 2011. Application of hydrodynamic modelling for predicting the fate of inflows in Lake Tegel, Berlin. Second IWA symposium on Lake & Reservoir Management, Granada, Spain

Schimmelpfennig, S., Kirillin, G., Engelhardt, C., Nützmann, G., Sep 2009. Application of 3D circulation models to simulate the fate and behavior of pharmaceuticals in a shallow urban lake. 13th Workshop on Physical Processes in Natural Waters, Palermo, Italy

Schimmelpfennig, S., Sperlich, A., Jekel, M., May 2009. FAST - Fixed-bed Adsorption Simulation Tool. Wasser 2009 - Jahrestagung der Wasserchemischen Gesellschaft, Stralsund, Germany

Schimmelpfennig, S., Kirillin, G., Engelhardt, C., Nützmann, G., Sep 2008. Hydrodynamische 3D-Modellierung der Verteilung von Pharmaka im Tegeler See. Jahrestagung der Deutschen Gesellschaft für Limnologie, Koblenz, Germany

Software

Schimmelpfennig, S., Sperlich, A. (2009): Fixed-bed adsorption simulation tool (FAST), a software tool to assist in the design of fixed-bed adsorbers in water treatment. (http://www.fast-software.de)